

Assessment of hypoxoside and its derivatives as anti-cancer drugs

Bongiwe Ziphelele Xulu
BSc (UKZN) BSc Hons (UniZul)

Submitted in the fulfillment of the academic requirements for the degree of


MASTER OF SCIENCE IN BIOCHEMISTRY

Discipline of Biochemistry
School of Life Sciences
College of Agriculture, Engineering and Science
Pietermaritzburg
South Africa

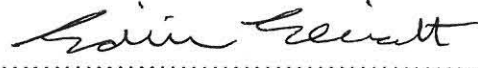
March 2013

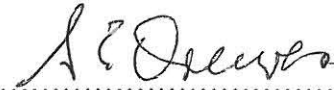
DECLARATION


I hereby certify that this research is a result of my own investigation, which has not been already been accepted in substance for any degree and is not being submitted in candidature for any other degree.

Signed: .....
Bongwiwe Ziphelele Xulu

We here by certify that this statement is correct

Signed: .....
Dr E. Elliott
Supervisor

Signed: .....
Professor S. E. Drewes
Co-supervisor

Signed: .....
Professor F.R. Van Heerden
Co-supervisor

DECLARATION

I hereby certify that this research is a result of my own investigation, which has not been already been accepted in substance for any degree and is not being submitted in candidature for any other degree.

Signed:

Bongiwe Ziphelele Xulu

We here by certify that this statement is correct

Signed.....

Dr E. Elliott

Supervisor

Signed.....

Professor S. E. Drewes

Co-supervisor

Signed.....

Professor F.R. Van Heerden

Co-supervisor

ABSTRACT

Extracts of the African potato have long been believed to have anti-cancer properties. The aim of the current research was to isolate hypoxoside (HYP) from *Hypoxis hemerocallidea* (African potato) and synthesize the dimethyl (DMH) and decaacetyl (DAH) derivatives and to test their selective cytotoxicity on a model consisting of a normal (MCF10A) and premalignant, invasive breast epithelial cells (MCF10A-NeoT).

Hypoxoside was extracted from the *H. hemerocallidea* corms using ethanol, purified using a C-18 reverse phase column and the compound examined by nuclear magnetic resonance (NMR) spectroscopy and high-resolution mass spectrometry and found to be of high purity. This was also the case for the synthesized compounds. To assess possible selective effects (cytotoxicity) of derivatized and underivatized hypoxoside, effects on the metabolism of premalignant and normal cells were assessed using the 3-(4,5-dimethylthiazol-2-yl)-5-(3-carboxymethoxyphenyl)-2-(4-sulfophenyl)-2H-tetrazolium (MTS) assay. Effects on cell number (total counts) and cell death [trypan blue and propidium iodide (PI) staining for dead cells versus a lack of staining for live cells] were, thereafter, assessed. Imaging of live adherent cells was also carried out using acridine orange (AO) and PI for live and dead cells (respectively). Propidium iodide staining of detached cells was carried out for flow cytometric determination of cell death (PI indicating early apoptotic or late apoptotic/necrotic cells).

After treatment of normal (MCF10A) breast epithelial cells and premalignant cHa-*ras*-transfected (MCF10A-NeoT) derivative breast epithelial cells with HYP, DMH and the DAH derivative, the MTS assay and the Duncan's multiple range, analysis of variance (ANOVA) post hoc analysis of the MTS results revealed that only the 150 and 300 μ M DAH derivative had a statistically significant effect on the metabolic activity of the abnormal cell line relative to the dimethyl sulfoxide (DMSO) and revealed no significant effect on the normal MCF-10A cell line after treatment with any of the test compounds. Supravital PI staining of adherent cells seemed to indicate a far higher rate of induction of cell death in abnormal cells than evident in the MTS assay and the PI-based flow cytometry or the trypan blue exclusion assays and need re-investigating, though result trends were similar.

Total cell counts, show that HYP and its derivatives appear to increase both cancer and normal cell proliferation significantly, except in the case of DAH at 150 and 300 μM in the MCF10A-NeoT, without affecting the MCF-10A cell line. The trypan blue method for detection of cell death, together with total cell counts, the Duncan's analysis of MTS results and a 24 hour exposure to test compounds, seems to constitute an optimal system for drug screening and indicates the statistically significant selective toxicity of the DAH compound at 150 and 300 μM in the MCF10A-NeoT, suggesting that the DAH derivative at 150 and 300 μM would have significant, selective therapeutic potential on Ras-related malignancies.

ACKNOWLEDGEMENTS

I would like to express my heartfelt thanks to the following people who have contributed to the success of this project:

Dr Edith Elliott, for her meticulous supervision, her professional guidance, encouragements and stimulation throughout the duration of my masters studies. Her patience with me and my many troubles is appreciated, and was not in vain, I learnt a lot from her. The human relationship established and constructive views shared were also very much appreciated. I could not have asked for a better supervisor. Thank you very much.

My co-supervisors, Prof S.E. Drewes and Prof F.R. Van Heerden, thank you very much for bringing light to the chemistry side of my project and for the useful discussions held.

A very special thanks goes to Mr Oliver and Mr Nhlahlazabantu Mthaba for their assistance with statistical analyses, as I did not study statistics in my undergraduate years. Their help is much appreciated.

Very special thanks to my colleagues, Dan Bohen and Dr C. Snyman for their academic support when I was new in the lab. They gave me strength and motivation during the dark days and their support is much appreciated.

I wish to express my deep gratitude to my family, my father Mr P. Z. Xulu, my mother Mrs N. R. Xulu, and my siblings for their unfailing support, love and kindness towards me. The patience they showed for me throughout my academic career. The trust and belief they have in my intellectual ability, really gave me strength and encouraged me to continue with my studies.

A special word of thanks goes to my husband, Mbongeni Mthembu, my pillar of strength and encouragement. He stood by me during difficult moments and throughout this study and has ensured the achievement of this goal.

I wish to thank the NRF and the Department of Chemistry for the financial support that met my personal financial needs during my MSc studies.

Last but not least, I am grateful to God almighty, my Father, the author and the furnisher of my faith, for giving me strength and courage to complete this project and also giving me the skills to unravel the wonders of our world through science. He deserves all credit.

DEDICATION

This research is dedicated to my father Mr Phindithemba Z. Xulu and my mother, Mrs Nokuthula R. Xulu, for their unconditional love and support throughout my studies, and childhood. I love them, and am especially grateful to them for encouraging me to further my studies. This is also in honor of my late second parents Mr Gwalizwe R. Mthembu and Mrs Vina Mthembu.

TABLE OF CONTENTS

Declaration	i
Abstract	ii
Acknowledgements	iv
Dedication	vi
Table of contents	vii
List of figures	viii
List of tables	ix
Abbreviation list	x
CHAPTER 1	1
INTRODUCTION	1
1.1 CANCER	1
1.1.1. Causes and prevention of cancer.....	3
1.1.2 Breast cancer.....	4
1.1.3 Treatment of breast cancer.....	5
1.2 TRADITIONAL MEDICINE	8
1.2.1 <i>Hypoxis hemerocallidea</i>	8
1.2.2 Uses of <i>Hypoxis hemerocallidea</i>	10
1.3 DRUGS EFFECTIVENESS	11
1.3.1 Cell death	12
1.3.2 Apoptosis	14
1.3.2.1 Intrinsic apoptotic pathway.....	15
1.3.2.2 Extrinsic pathway.....	17
1.3.2.3 Perforin/granzyme apoptotic pathway	18
1.3.3 What do the common executioner caspases do?	19
1.3.4 Regulators of apoptotic cell death.....	21
1.3.5 Methods of assessing cell death (apoptosis or necrosis).....	21
1.4 MCF10A	25
1.5 RESEARCH AIMS AND OBJECTIVES	27
CHAPTER 2	28
HYPOXOSIDE: EXTRACTION, ISOLATION AND SYNTHESIS OF TWO DERIVATIVES	28

2.1	OVERVIEW	28
2.2	COLLECTION AND IDENTIFICATION OF THE CONSTITUENTS IN <i>H. hemerocallidea</i>	30
2.3	EXTRACTION AND ISOLATION	31
2.3.1	Materials and equipment.....	31
2.3.2	Extraction and isolation procedures.....	32
2.3.3	Results.....	33
2.3.4	Elucidation of the hypoxoside structure by ¹ H and ¹³ C NMR spectroscopy.....	33
2.3.4.1	Procedure	34
2.3.4.2	Results.....	34
2.4	PREPARATION OF HYPOXOSIDE DERIVATIVES.....	35
2.4.1.	Methylating hypoxoside.....	36
2.4.1.1	Preparation of nitrosomethylurea (diazomethane precursor).....	36
2.4.1.2	Precursor preparation procedure	36
2.4.1.3	Methylation step of hypoxoside.....	37
2.4.1.5	Results.....	37
2.4.2	Acetylation of hypoxoside	38
2.4.2.1	Procedure	38
2.4.2.2	Results.....	39
CHAPTER 3	40
	ASSESSMENT OF ANTI-CANCER SELECTIVE CYTOTOXICITY OF THE HYPOXOSIDE AND TWO DERIVATIVES	40
3.1	INTRODUCTION.....	40
3.2	HYPOXOSIDE AND TWO DERIVATIVES AS POTENTIAL ANTI- CANCER DRUGS	41
3.3	EXPERIMENTAL.....	42
3.3.1	Materials and equipment.....	42
3.3.2	Preparation of the stock and working solutions of hypoxoside and hypoxoside derivatives	43
3.3.2.1	Reagents.....	44
3.3.2.2	Procedure	44
3.3.3.	Culturing MCF10A and MCF10A-NeoT cell lines.....	45
3.3.3.1	Reagents.....	46
3.3.3.2	Procedure	48

3.3.4.	MTS Assay optimization, compound exposure and data analysis.....	49
3.3.4.1	Reagents.....	54
3.3.4.2	Procedure.....	54
3.3.5.	Acridine orange/propidium iodide (PI) fluorescence microscopic assay.....	58
3.3.5.1	Reagents.....	60
3.3.5.2	Procedure.....	61
3.3.6.	Propidium iodide (PI) flow cytometric assay.....	62
3.3.6.1	Reagents.....	65
3.3.6.2	Procedure.....	66
3.3.7.	Trypan blue hemocytometric assay.....	66
3.3.7.1	Reagents.....	68
3.3.7.2	Procedure.....	68
3.4	RESULTS AND DISCUSSION.....	69
3.4.1	The effect of hypoxoside, dimethylhypoxoside and decaacetylhypoxoside effect on the metabolic activity of MCF-10A and MCF-10A-NeoT cell lines.....	69
3.4.2	The influence of hypoxoside and its derivatives on cell death of MCF-10A and MCF-10A-NeoT cell lines using AO/PI staining.....	82
3.4.2.1	Cell death assessment of MCF10A cell line through AO/PI staining.....	83
3.4.2.2	Cell death assessment of MCF10A-NeoT cell line through AO/PI staining.....	84
3.4.3	Cell death assessment of the MCF10A and MCF10A-NeoT cell lines by Flow Cytometry and PI staining.....	86
3.4.4	Trypan blue hemocytometric cell count.....	88
3.5	CONCLUSION.....	93
CHAPTER 4	94
GENERAL DISCUSSION, CONCLUSION AND FUTURE WORK	94
4.1	GENERAL DISCUSSION.....	95
4.2	CONCLUSION.....	101
4.3	FUTURE STUDIES.....	102
APPENDIX.....	115

LIST OF FIGURES

Figure 1.1:	Angiogenesis and metastatic stages	2
Figure 1.2:	Conversion of hypoxoside into rooperol	9
Figure 1.3:	Rooperol acting as antioxidant	11
Figure 1.4:	Differences between apoptosis and necrosis	12
Figure 1.5:	Different programmed cell death pathways	15
Figure 1.6:	Mechanism of the intrinsic apoptotic pathway	16
Figure 1.7:	Extrinsic apoptotic pathway mechanism	18
Figure 1.8:	Executioner caspases and their substrates recognition for completion of apoptosis	20
Figure 2.1:	Corn and flower of the collected <i>Hypoxis hemerocallidea</i>	31
Figure 2.2:	TLC plate showing fractions collected from a reverse phase chromatography column in the manifold assembly	33
Figure 2.3:	Numbering of carbons in the hypoxoside structure	34
Figure 2.4:	Numbering of carbons in the dimethylhypoxoside structure	37
Figure 2.5:	Numbering of carbons in the decaacetylhypoxoside	38
Figure 3.1:	The preparation of hypoxoside and derivatives	45
Figure 3.2:	The calibration curves for MCF10A (A) and MCF10-NeoT (B) optimization for the MTS Assay	55
Figure 3.3:	Residual plots of MCF10A (A) and MCF10A-NeoT (B) metabolic activity collected data after treatment with the three hypoxoside compounds	57
Figure 3.4:	Epi-fluorescence microscopy set up	59
Figure 3.5:	The layout of components in a flow cytometer	63
Figure 3.6:	Multiparameter flow cytometry analysis of blood cell populations	64
Figure 3.7:	Improved Neubauer Hemocytometer counting chamber gridlines	67
Figure 3.8:	MTS assay metabolic activity results of MCF10A and MCF10A-NeoT cells treated with three hypoxoside compounds	70
Figure 3.9:	Mean plot of the mean metabolic activity induced by various concentrations (μ M) test compounds on the MCF10A and MCF10A- NeoT cells	74
Figure 3.10:	Effect of hypoxoside and its derivatives on MCF-10A assessing using AO/PI staining	83

Figure 3.11: Effect of hypoxoside and its derivatives on MCF10A-NeoT assessing using AO/PI staining	84
Figure 3.12: Total cell counts and the percentage dead cells (trypan blue stained cells) after treatment with different hypoxoside compounds	89
Figure 3.13: Cell death after treatment with three hypoxoside compounds assessed using cell counts with trypan blue	90

LISTS OF TABLES

Table 2.1:	Collected masses of the hypoxoside and derivative weights.....	33
Table 2.2:	NMR Chemical shifts for hypoxoside in CD ₃ OD	34
Table 3.1:	An example of the ANOVA table from GenStat	52
Table 3.2:	Analysis of variance table from Genestat	71
Table 3.3:	Duncan's multiple range test results	80-81
Table 3.4:	Cell death indicated by PI staining in the two cell lines seen after treatment with hypoxoside and derivatives	82
Table 3.5:	Flow cytometric determination of % live and dead cells in the two cell lines post treatment	87
Table 3.6:	Comparison of the PI flow cytometric test with the trypan blue test results	92

ABBREVIATIONS LIST

1/2D	one/two dimensional
¹³ C NMR	carbon-13 nuclear magnetic resonance
¹ H NMR	proton nuclear magnetic resonance
7-AAD	7-amino-actinomycin D
AIF	apoptosis-inducing factor
ANOVA	analysis of variance
AO	acridine orange
AP	African potato
Apaf-1	apoptosis protease-activating factor-1
BAD	bcl-2-associated death promoter
BAK	bcl-2 homologous antagonist/killer
BAX	bcl-2-associated X protein
BID	BH3 interacting-domain death agonist
BMF	bcl-2 modifying factor
BSA	bovine serum albumin
CAD	caspase-activated deoxyribonuclease
CCE	counter-current extraction
COSY45	correlated spectroscopy
COX-1	cyclooxygenase-1
COX-2	cyclooxygenase-2
CPT	camptothecin
Cyt. C	cytochrome c
DAH	decaacetylhypoxoside
DEPT	distortionless enhancement polarization transfer
df	degrees of freedom
DISC	death-inducing signaling complex
DMH	dimethylhypoxoside
DMSO	dimethyl sulfoxide
DNA	deoxyribose nucleic acid
PK-DNA	DNA dependent protein kinases
DNase	deoxyribonuclease
DPBS	Dulbecco's phosphate-buffered saline

DRG	DNA repair genes
EB	ethidium bromide
EDTA	ethylenediaminetetraacetic acid
EGF	epidermal growth factor
ESS	explained (regression) sum of squares
F (or vr value)	variance ratio
FACS	fluorescence-activated cell-sorting
FADD	fas-associated death domain protein
FITC	fluorescein isothiocyanate-conjugated
FS	forward scatter
FWER	family wise error rate
GG	growth genes
HBSS	Hanks' balanced salt solution
HMBC	heteronuclear multiple bond correlation
HO	Hoechst dye
HPLC	high-performance liquid chromatography
HR-MS	high-resolution mass spectrometry
HSQC	heteronuclear single quantum coherence
HYP	hypoxoside
ICAD	inhibitor of caspase-activated deoxyribonuclease
KOH	potassium hydroxide
MCF10A-NeoT/NTs	Michigan Cancer Foundation 10-adherent, neomycin resistant and mutationally activated (Val-12) H- <i>ras</i> -transfected cells.
MCF10As/10As	Michigan Cancer Foundation 10-adherent cells
MeOH	methanol
MOMP	mitochondrial outer membrane permeability
ms	mean sum of squares,
MTS	3-(4,5-dimethylthiazol-2-yl)-5-(3-carboxymethoxyphenyl)-2-(4-sulfophenyl)-2H-tetrazolium
NADH	reduced nicotinamide adenine dinucleotide
NMR	nuclear magnetic resonance
OTC	over-the-counter
PARP	poly (ADP-ribose) polymerase
PBS	phosphate-buffered saline

PCD	programmed cell death
Pen/Strep	penicillin and streptomycin
PERP	p53 apoptosis effector related to PMP-22
PI	propidium iodide
PMS	phenazine methosulfate
PS	phosphatidylserine
PS	phosphatidylserine
PUMA	p53 upregulated modulator of apoptosis
RIKP	kinase receptor interacting proteins
RIP	receptor interacting protein
ROS	reactive oxygen species
RT	room temperature
SCGE	single cell gel electrophoresis
SDS	sodium dodecyl sulfate
SED	standard error of the difference
SS	side scatter
TLC	thin-layer chromatography
TNF	tumour necrosis factor
TRADD	tumour necrosis factor receptor-associated death domain
TSG	tumour suppressor genes
TUNEL	terminal dUTP nick end-labeling
VEGF	vascular endothelial growth factor

CHAPTER 1

INTRODUCTION

1.1 CANCER

Cancer is a disease in which cell growth becomes uncontrolled, and subsequently an imbalance between cell proliferation and apoptosis results (Cancer facts and figures, 2009). If proteases are upregulated and the cells are invasive, they also spread to other parts of the body through lymph or blood. The South African Medical Research Council reported that, in 2003, cancer was ranked as the fourth leading death-causing disease in South Africa (Bello *et al.*, 2011). This disease has been a leading cause of death worldwide and in 2008, around 12.7 million cancer cases were reported and 7.6 million deaths were due to cancer. The economic state of the country has a major impact on the seriousness of the cancer burden. The developed countries have more cases but fewer deaths as more advanced ways of detecting, treating and funding cancer treatment in such countries (Jemal *et al.*, 2011).

The complexity of the disease is reflected by the fact that more than 100 distinct types and subtypes of tumours within a specific organ have previously been identified (Hanahan and Weinberg, 2000). Cancers may be categorized into five different classes named according to the location in the body in which they develop. Carcinomas are derived from epithelial cells and include lung, breast, prostate and colon cancers, and about 90% of cancers belong to this class. Sarcomas are derived from muscle and connective tissues while germ line tumours are from totipotent cells which are found in testes and ovaries. Lymphomas and leukaemia are derived from the hematopoietic cells, while blastomas are derived from the immature embryonic tissue, most commonly in children (WHO, 2006). Blastomas arise from a single cell that is transformed from a normal to a cancer cell via multistage processes. The leading groups resulting in terminal cancers are cancers of the lung, stomach, and breast, liver and colon (WHO, 2006).

A tumour usually exhibits uncontrollable cell growth and can either be benign or malignant. Malignant metastatic tumours or “neoplasm” can invade normal tissues and spread to distant body sites, while the benign tumours remain confined in their original location (Cooper, 1993). The tumour formed by the malignant cells generally cannot grow beyond 2 mm in diameter without developing a new vasculature system so as to be nourished (Bluff *et al.*,

2008). This process is called “angiogenesis” and is very important for the growth of the tumour. Tumour cells with the capacity to migrate and metastasize may subsequently gain access to the bloodstream to migrate and form secondary tumours at distant sites (Bluff *et al.*, 2008) (Figure 1.1).

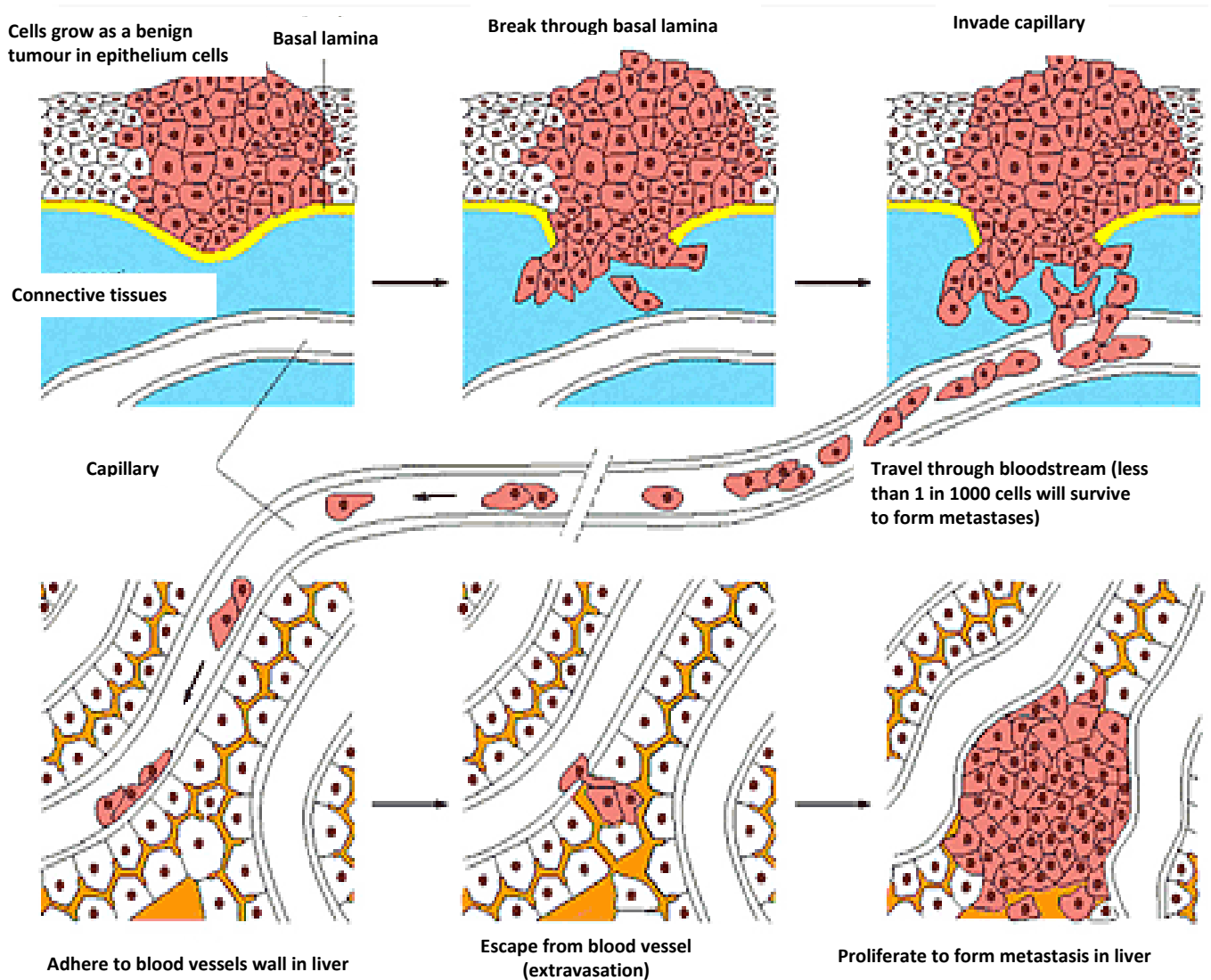


Figure 1.1: Angiogenesis and metastatic stages.

There is a cascade of events that the tumour cells go through before it can metastasize. When cells grow into benign tumours in the epithelium cells, genetic alterations permit cells to break through the basal lamina and invade into capillaries. Once they reach the capillaries they can travel to any distant site in the body. The tumour cells invade the distant tissues by adhering to the capillary walls and invading into the surrounding tissues, where they can proliferate and become transformed into many types of tumours due to environment and genetic mutation (Alberts *et al.*, 2002).

1.1.1. Causes and prevention of cancer

Cancer can be diagnosed in anyone at any time but the risks of developing cancer increases with age. About 77% of all cancers are diagnosed in people over the age of 55 years (Cancer facts and figures, 2009) and arise mainly due to the mutation in the genetic material resulting in transformation. Transformation usually arises due to mutations affecting three classes of genes: DNA repair genes (DRG), tumour suppressor genes (TSG) or genes involved in cell growth (GG). DRG usually prevent accumulation of genetic mistakes, TSG genes usually restraining cell growth and division, and the GG genes usually regulate cell growth and division (Hanahan and Weinberg, 2000). Together or in isolation, these contribute to a progression towards the malignant, invasive phenotype, the focus of the current study as the invasive tumours tend to cause the highest rate of mortality.

p53 is a commonly mutated tumour suppressor gene guarding the fidelity of replication of the genomic DNA upon cell division and regulating cell division. Random mutations eventually allow progression and select for cells of increased malignancy as increasing numbers of mutations escape removal (Spandidos *et al.*, 1999). One of the later mutations associated with invasion is the Val-12 mutation in the normal H-Ras signalling protein, a protein that controls the cell division, proliferation and phenotype, switching on a more migratory, invasive phenotype and switching off a polarized non-migratory, normal epithelial-type phenotype (Ota *et al.*, 2009). This specific combination of mutations facilitates invasion, increasing cell proliferation and uncontrolled replication (Bluff *et al.*, 2008) and hence forms a focus of the current study.

Mutations can initially be due to internal factors such as inherited mutations, hormones, immune conditions, and mutations that occur due to metabolic imbalances (Cancer facts and figures, 2009). External factors involve smoking cigarettes, alcohol consumption, asbestos-inhalation, ultraviolet light or ionizing radiation exposure, as well as exposure to drinking water contaminated with chemicals such as arsenic, and some infectious organisms (Ma and Yu, 2006). The infections associated with cancer development involve viruses such as human papilloma virus (HPV), for cervical cancer, human immune deficiency virus (HIV) for Kaposi sarcoma, hepatitis B for liver cancer; bacteria such as *Helicobacter pylori* for stomach cancer, and parasites such as schistosomiasis for bladder cancer (WHO, 2006).

For the current research reported in this dissertation the focus is cancer of the breast or mammary glands, a cancer common in women.

1.1.2 Breast cancer

Breast cancer is the leading cause of cancer deaths in women and was reported to account for 23% cancer cases and 14% cancer deaths in 2008 worldwide (Jemal *et al.*, 2011) . Risks of developing cancer have been investigated but no explanation for the international variation in frequency and prognosis in breast cancer is known. In South Africa, breast cancer has been more common in white women and less common in black and coloured women. Recently, however, there has been a tremendous increase in black and coloured women with breast cancer. This seems due to several factors including socio-economic factors and a change to westernized diet (Matatiele, 2008).

Cancer risk factors are almost the same for most cancers. Breast cancer risk factors in females include having breast tissues dependent on hormones like oestrogen for growth and a lack of child-bearing or child-bearing at an age above 35 years (Cooper, 1993). Longer breast feeding has also been claimed to protect women against developing breast cancer (Bray *et al.*, 2004) .

Breast cancer has been found to have 5 stages of progression, just like all other cancers. At Stage 0, the carcinoma present but no invasion has occurred. At Stage 1, a tumour growth (≤ 2 cm) is present but there is still no trace of invasion. At Stage II, either angiogenesis has occurred but the tumour is still small (≤ 2 cm), or a large tumour (over 5 cm) is present but no angiogenesis is evident, or a moderate sized tumour, with or without angiogenesis, is present. At Stage III, however, a large tumour with angiogenesis, or tumour of any size with extensive angiogenesis, or angiogenesis at the chest wall and skin is present. At Stage IV, the cancer has grown beyond the lymph nodes and grown at a distant site from the point of origin (Kols, 2002). It is the invasive stage that is the most dangerous and forms the target in the current study.

Breast cancers can originate from any tissue of the breast and are named according to location of origin or particular features of the disease. Breast cancers more commonly arise in the ducts of the breast and are referred to as ductal carcinomas. Fewer arise in the lobules and even fewer in other tissues (Cooper, 1993). Invasive ductal carcinomas account for about 70% of breast cancers and, though they originate inside the ducts, they usually invade into the fatty tissues and spread to other parts of the body (Danziger and Simonsen, 2011).

Invasive lobular carcinomas begin in the milk glands situated deep inside the breast and account for about 10% of the breast cancers. Inflammatory breast cancer is the least common kind of breast cancer and is usually found in the soft tissues of the breast, in the form of sheets and not in lumps (Stephan, 2009). Medullary carcinoma accounts for the least number of breast cancers (about 3-6%) and are more common in woman with a genetic predisposition to breast cancer (Danziger and Simonsen, 2011). Paget's disease is the rare kind of breast cancer and involves the nipple. As invasive cancers are responsible for the highest mortality, they remain the target of the current investigation, as treatment of the more advanced, refractory cancers remains a problem (Bray *et al.*, 2004) .

1.1.3 Treatment of breast cancer

A great deal of research has been focused on finding an improved treatment for cancer. Treatment methods that are mainly used are: surgery, radiotherapy, chemotherapy, hormone therapy, and antibody-based treatment (National Cancer Institute, 2006; Cooper, 1993). Choice of treatment method is based upon the stage of breast cancer progression, i.e. the primary tumour, region lymph node involvement, and distant metastasis (Kols, 2002). The success of treatment method varies with the type of cancer and how early the tumour was detected, more advanced cancers being less easily treated (Cooper, 1993).

All methods of cancer treatment used alone, or in combination, may vary depending on the type of cancer. The primary methods of treatment of early stage breast cancer are surgery and radiotherapy. This is because, at early stages, cancers are not invasive and will have not metastasized, so they can be completely eradicated by focused treatment or surgical removal (Pratt *et al.*, 1994).

Radiotherapy is usually used post-surgery and involves irradiation (with X-rays or gamma rays) of any remaining cancer cells with the aim of destroying the malignant cells. Normal cells are also killed, however. For this reason, recent research has focused on finding tumour-specific antibodies to which radiolabels may be attached to direct radiation specifically to tumour targets (Ghosh *et al.*, 2009).

Another method of treatment is chemotherapy. This involves the treatment of cancer cells with anti-cancer drugs. This method is very effective as it can prevent the spreading of cancer cells, decrease the size of the tumour and relieve symptoms such as pain (Ghosh *et al.*, 2009). To date, by far one of the most effective cancer therapeutics are the anti-angiogenesis drugs.

These keep tumours from providing their own blood supply and thereby stopping the supply of oxygen and nutrients to the cancerous cells leading them to starve to death (Bluff *et al.*, 2008). An example is a humanized anti-vascular endothelial growth factor antibody, bevacizumab, with the trade name of Avistan. Anti-vascular endothelial growth factor plays a critical role in tumour growth and invasion, and Avistan has been known to inhibit the VEGF activity and hence control tumour growth (Ranpura, 2011).

Chemotherapy, on the other hand, is thought to be the most universally effective method of treatment, especially for the invasive cancers (Bluff *et al.*, 2008). This is because this therapy can be supplied throughout the blood system. Plant-derived anti-cancer drugs are also believed to have great potential as anticancer drugs.

Anti-cancer chemotherapeutic drugs are classified according to their mode of action. There are alkylating agents like cisplatin and mitomycin, DNA cleavage agents like bleomycin, and DNA binders like dactinomycin (Ghosh *et al.*, 2009). Cisplatin is a metal-based anti-cancer drug and also an alkylating agent. About 50-70% of cancer patients are treated with platinum-based drugs. Their strength is illustrated by the fact that hardly any combination chemotherapy does not include platinum-based drugs (Hannon, 2007).

Natural products have played a critical role in prevention and treatment of diseases for over thousands of years (Chin *et al.*, 2006). Egypt, China, India and Greece have been using traditional medicines since ancient times and a number of very important drugs have been developed from plants (Shoeb, 2006). About 60% of the anticancer drugs are, in one way or the other, derived from plants and this suggests that traditionally used plant-derived compounds may be a good resource for further drug development. The search for anti-cancer drugs derived from plants started in the 1950's (Cragg and Newman, 2005; Newman and Cragg, 2012).

The success of the drug can be judged using four criteria, i.e. the rate of introduction of the drug onto the market, its potential for laboratory synthesis, the number of diseases treated using such a drug, and its level of use in the treatment of specific disease (Chin *et al.*, 2006).

The first plant-derived anti-cancer drugs to be introduced for clinical use were the Vinca alkaloids, vinblastin and vincristine, isolated from Madagascar periwinkle, *Catharanthus roseus*, which belongs to the Apocynaceae family (Shoeb, 2006). Vinblastine and vincristine

are primarily used for treatment of a variety of cancers including breast cancer and in combination with other chemotherapeutic drugs (Shoeb, 2006) .

In the 1970's camptothecin (CPT) isolated from the Chinese ornamental tree, *Camptotheca acuminata* from Cornaceae family was introduced for clinical trials (Cragg and Newman, 2003). This plant grows rapidly in areas like China and Tibet, where it is known as the happy tree and the camptothecin drug is usually isolated from the bark and stem (Ghosh *et al.*, 2009). This drug was also used as an anti-cancer drug, but because of severe bladder toxicity the use of the drug was discontinued (Shoeb, 2006) . To overcome the side effects of CPT, analogues were synthesized e.g. topotecan, exatecan, ironotecan and rubitecan. Exatecan derivative is more efficient in killing malignant tumors. It inhibit DNA topoisomerase I which plays a major role in various DNA functions like replication and transcription, and has a lower toxicity against normal cells (Nirmala *et al.*, 2011).

Paclitaxel, trade name Taxol[®], is isolated from the Pacific Yew, *Taxus brevifolia* of the Taxaceae family and has been reported for it's anti-tumour activity against rodent tumours (Ghosh *et al.*, 2009). Paclitaxel with other precursors actually occur in a number of *Taxus* species e.g. *T. canadensis*, *T. baccata*, *T. cuspidate* and *T. mairei leme* (Cragg and Newman, 2003). Initially paclitaxel was only sourced from the Pacific Yew, but recently this has been made semi-synthetically (Ghosh *et al.*, 2009).

Paclitaxel has been reported to be significantly active against ovarian cancer, advanced breast cancer and lung cancer (Shoeb, 2006) . However, it is poorly water-soluble and toxic, and, this led to the preparation of a semi-synthetic derivative, docetaxel which was found to be more effective. Both drugs are still in use as first and second line treatments. If the malignant tumour is resistant to paclitaxel, docetaxel is normally used in cases of breast cancer and ovarian cancer (Nirmala *et al.*, 2011).

Podophyllotoxin is a clinically used anticancer drug extracted from the roots of *Podophyllum* species i.e. *peltatum* and *emodi*. Epipodophyllotoxin is the podophyllotoxin isomer that has two semi-synthetic derivatives, i.e. etoposide and teniposide and their application has been reported in a number of cancer treatment regimens such as in lymphomas and bronchial and testicular cancers (Shoeb, 2006) .

Ellipticine is also a plant-derived anti-cancer drug isolated from a *Bleekeria vitensis* found on a Fijian island. This drug was derivatized to produce elliptinium which is now well known in France for treatment of breast cancer (Shoeb, 2006) .

The above-mentioned, plant-derived anti-cancer products are already in clinical use for cancer treatment. In 2002, paclitaxel and camptothecin were the most used compounds and were estimated to account for one-third of the worldwide anti-cancer drugs supplied to the market (Shoeb, 2006) . There are still a number of natural anti-cancer products in clinical trials (Albrecht *et al.*, 1995a). Few clinical trials have been carried out on the compound used in the current study i.e. hypoxoside, isolated from *Hypoxis hemerocallidea*. Natural products were used as traditional medicine in bygone times, and to this day traditional healers make use of them. For this reason, derivatives of a constituent of a locally-available traditional medicinal plant, *Hypoxis hemerocallidea*, were prepared and investigated for anti-cancer properties in this study.

1.2 TRADITIONAL MEDICINE

Traditional medicine is currently being used by about 80% of the developing world and there are as many as 100 000 traditional healers in South Africa alone (Owira and Ojewole, 2009) . South Africa is one of the richest centers in plant diversity in the world and that contributes to the high numbers of traditional healers who mainly use medicinal plants (Mulholland and Drewes, 2004). Traditional medicines go back a long time in history, especially in Africa. For treatment of many kinds of diseases and recently even for treatment of HIV/AIDS (Mills *et al.*, 2005). The interest in traditional medicines has increased recently and has drawn the attention of not only the government and research laboratories, but also pharmaceutical companies, in order to use the scientific knowledge and therapeutic properties of African traditional medicines (Owira and Ojewole, 2009) .

1.2.1 *Hypoxis hemerocallidea*

One of the most important traditional plants that has always been popular and is still largely used is *Hypoxis hemerocallidea* Fish. Mey. & Ave-Lall (Hypoxidaceae), previously known as *H. rooperi*. There are at least 100 other different *Hypoxis* species and at least 3 are used in traditional medicine, i.e. *Hypoxis colchicifolia* Baker, *Hypoxis gerrardii* Baker and *H. hemerocallidea*, (Hutchings *et al.*, 1996). It has a tuberous root (corm) which is commonly known as the African potato (AP) (inkomfe or ilabatheka in isiZulu) and can be easily

recognized by its bright yellow flowers and strap green leaves (Drewes *et al.*, 2008; Nair *et al.*, 2007) (Figure 2.1).

The AP extracts have been used as traditional medicine in treatment of many diseases like tuberculosis, common cold, flu, hypertension, diabetes mellitus, psoriasis, urinary infections, testicular tumours, prostate hypertrophy, internal cancer, cardiac diseases, HIV/AIDS and some central nervous disorders (Drewes *et al.*, 2008; Laporta *et al.*, 2007a; Zibula and Ojewole, 2000). The main component of the AP extract is a norlignan diglucoside, hypoxoside, which is a trivial name for (*E*)-1,5-bis(4'- β -D-glucopyranosyloxy-3-hydroxyphenyl)pent-4-en-1-yne, a pale yellow water soluble crystalline compound that is readily converted into a lipophilic aglucone, rooperol, in the presence of β -glucosidase (Figure 1.2). The pentenyne system connecting the two aromatic rings is rare in nature. It is significant that, with this arrangement the central CH₂ group, the compound becomes prochiral, an important stereochemical attribute for biological activity (Drewes and Khan, 2004).

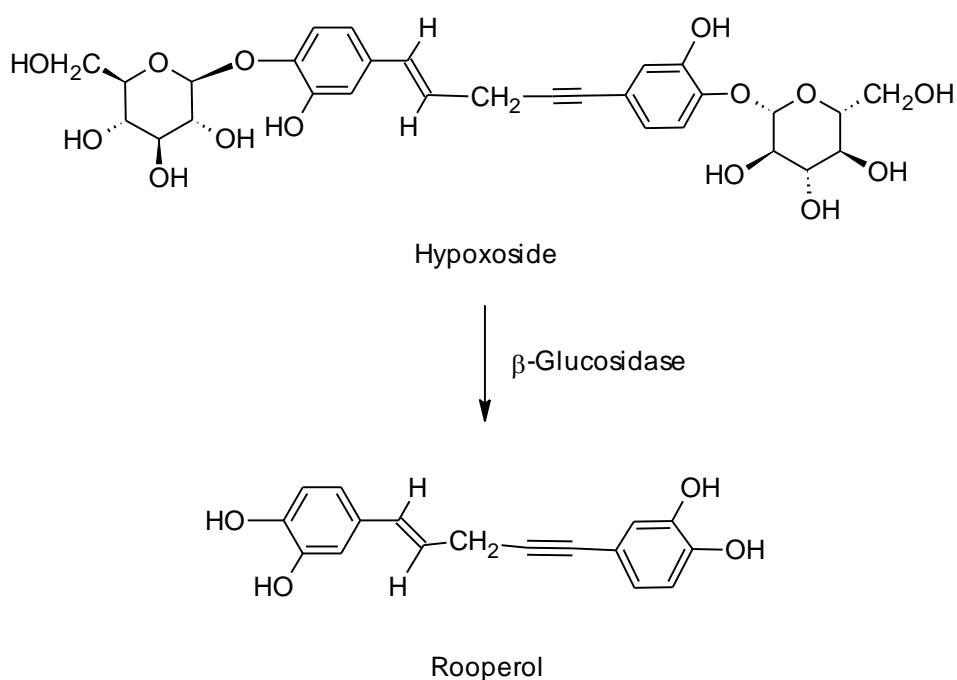


Figure 1.2: Conversion of hypoxoside into rooperol.

The hypoxoside molecule contains two β -glucose moieties. When the enzyme β -glucosidase reacts with hypoxoside, the two glucoside bonds are hydrolysed, the resultant compound, named rooperol, has exposed hydroxyl groups instead of glucosyloxy substituents and has very different properties to its parental structure (adapted from Albrecht *et al.*, 1995b).

Hypoxoside was initially isolated with a methanol/butanol extraction procedure and its structure was elucidated using NMR and UV spectroscopy (Bettolo *et al.*, 1982). Extraction with ethanol, however, gave a better percentage yield and was hence used in the current study. Hypoxoside is pharmacologically inactive but is transformed into its biologically active form rooperol, in the large intestines or by the liver cells of humans, by the enzyme β -glucosidase (Drewes *et al.*, 1984; Kruger *et al.*, 1994). *In vitro* hypoxoside is non-toxic to normal cells but becomes toxic to cancer cells as they produce the enzyme β -glucosidase that converts the hypoxoside into active rooperol (Albrecht *et al.*, 1995a).

1.2.2 Uses of *Hypoxis hemerocallidea*

Many scientific reports have reported that the AP extract is a possible remedy for a variety of pathophysiological disorders. Zibula and Ojewole (2000) reported that the methanol extract from the African potato induces hypoglycemic effects in both normal and hyperglycemic rats (Zibula and Ojewole, 2000). The anti-oxidative activity of prepared aqueous AP was found to be significantly higher than that of extracted hypoxoside, but lower than that of rooperol. This anti-oxidative activity is due to the dicatchol-like structure which hypoxoside assumes when converted to rooperol (Figure 1.3). It behaves in a similar fashion to the known antioxidant, nordihydroguaiaretic acid (Bettolo *et al.*, 1982; Drewes *et al.*, 1984; Nair *et al.*, 2007).

Cell membranes are lipophilic and since rooperol is more lipophilic than hypoxoside, this will allow rooperol to penetrate cells more readily than hypoxoside. Rooperol was found to have strong anti-microbial activity and was able to inhibit cyclooxygenase-1 (COX-1) and cyclooxygenase-2 (COX-2) which contributes to the anti-inflammatory and anti-noceptive activity of this compound (Laporta *et al.*, 2007a; Ojewole, 2006). Childhood convulsions and epilepsy may result in death, especially in rural areas, but treatment with AP has been shown to improve this ailment (Ojewole, 2008). The main focus of the current study was to test hypoxoside and two derivatives as anti-cancer pro-drugs and this activity was assessed on two different adherent cell lines i.e. a normal MCF10A and its premalignant derivative MCF10A-NeoT cell line.

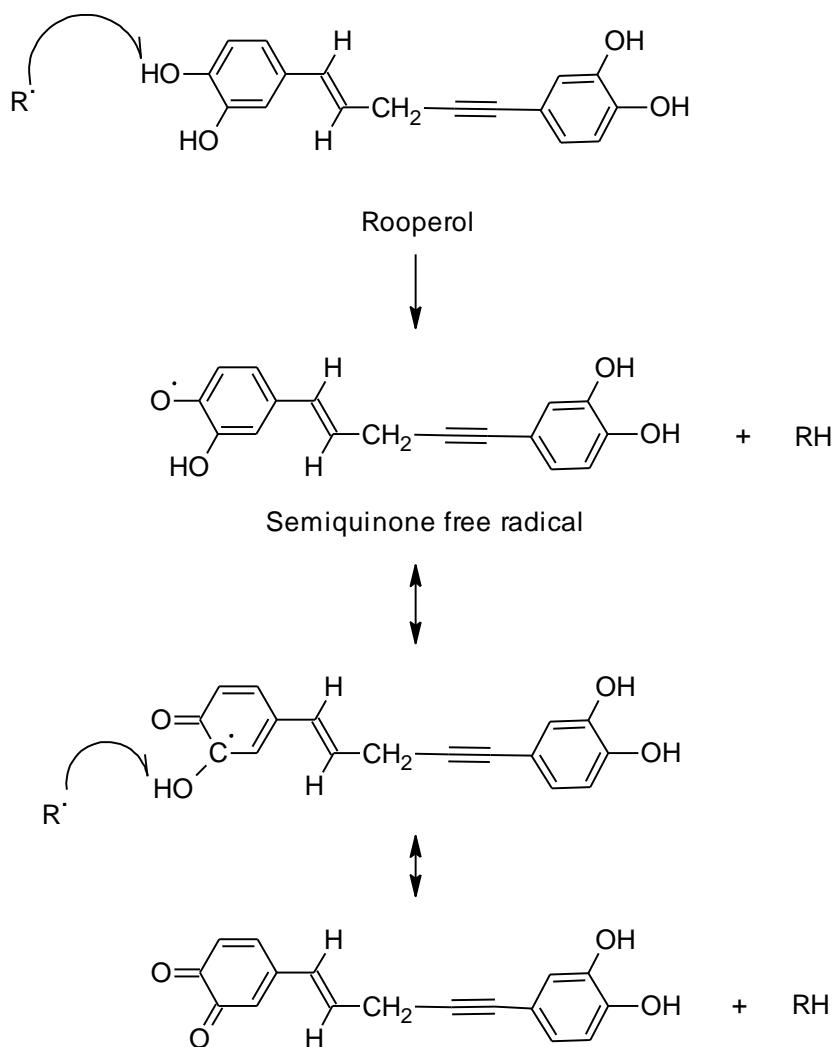


Figure 1.3: Rooperol acting as an anti-oxidant.

Rooperol acts like any anti-oxidant and has the required features of a good anti-oxidant, i.e. a benzene ring with 1,2-hydroxy or 1,4-dihydroxy groups. The function of anti-oxidants is to scavenge free radicals. The hydroxyl group interacts with the free radical and, ultimately, an *ortho*-quinone forms. In the process free radicals are destroyed (Drewes and Khan, 2004).

1.3 DRUGS EFFECTIVENESS

For a drug to be deemed effective, it must have a selective effect on the target cell. In this case this should be on the specific cancer type, either depressing cancer cell growth or metabolism. If it is selectively toxic to cancer cells and not normal cells, then it should induce cell death by apoptosis and not necrosis, as the latter may be life-threatening (Cooper, 1993). Apoptotic death may be induced by a variety of stimuli and via specific receptors. Not all cell types will die after treatment with the same compound, or at the same concentration. The latter too may determine whether the cell will die through apoptosis or necrosis and this is

important to assess as induction by necrosis may have life-threatening consequences (Bertho *et al.*, 2000; Pereira and Amarante-Mendes, 2011).

1.3.1 Cell death

Since the major aim of most therapeutic interventions is to induce apoptosis and not necrosis, the mechanisms of inducing either form of cell death are briefly described. Detection methods which may be used to assess which mode of cell death is induced will be described.

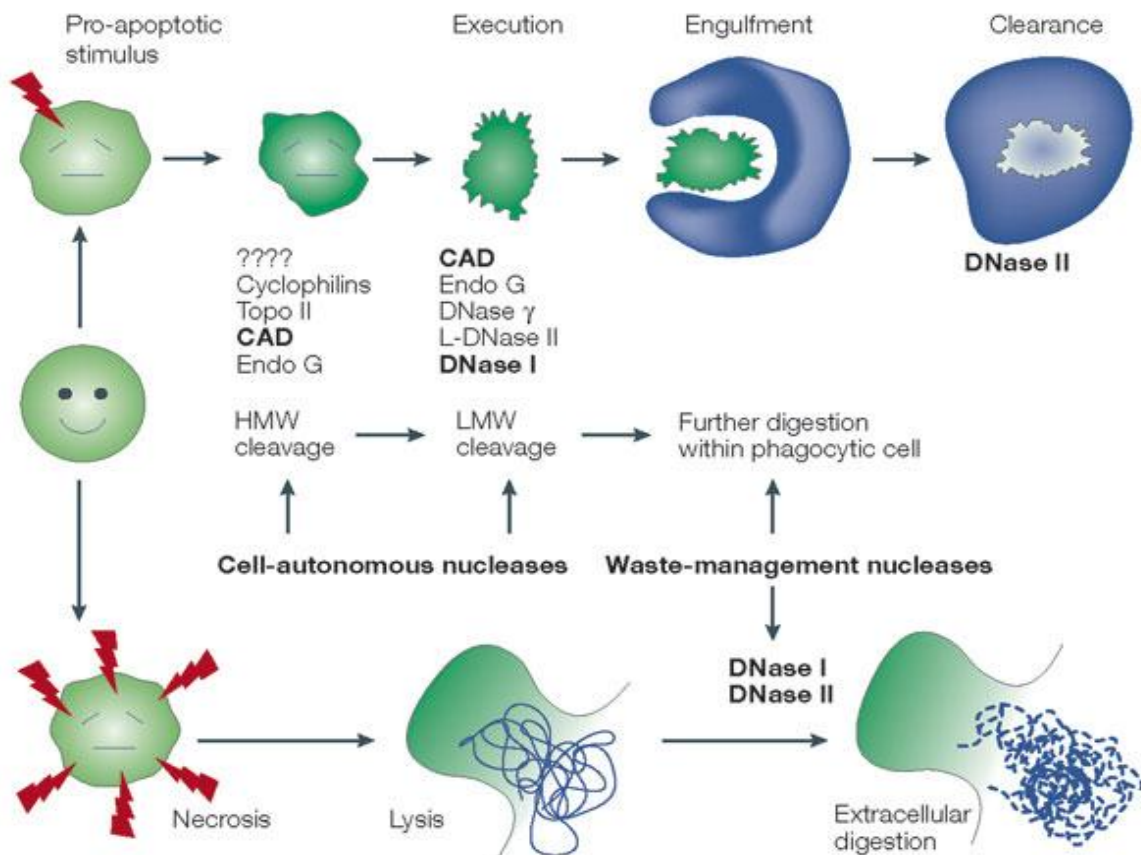


Figure 1.4: Differences between apoptosis and necrosis.

Apoptosis involves chromatin and nucleus condensation, blebbing of the plasma membrane, formation of apoptotic bodies and finally their engulfment and further digestion. Necrosis involves swelling of the necrotic cell, loss of plasma-membrane integrity and finally bursting of the cell, resulting in the release of the cytoplasm content and DNA to the surrounding cells causing inflammation. Caspase-activated DNase (CAD) DNase I and DNase II are the main nucleases involved, as indicated in bold. HMW cleavage = higher molecular weight cleavage of DNA, LMW cleavage = lower molecular weights cleavage of DNA (also called DNA ladders), topo II = topoisomerase II, endo G = endonuclease G. DNase I and II are referred to as waste management nucleases (Samejima and Earnshaw, 2005).

There are two major mechanisms of cell death that cells can employ when they are stressed or damaged, programmed cell death (apoptosis) or non-programmed cell death (lysis or

necrosis) (Figure 1:4). Apoptosis and necrosis can be distinguished according to their biochemical and morphological features (Leist and Nicotera, 1997). Whether the cell will die through apoptosis or necrosis depends on the intensity of the attacking onslaught. Some studies reported that ATP concentration influences the chosen type of cell death (Fadeel and Orrenius, 2005).

Apoptosis, is referred to as programmed cell death (PCD), has been widely recognized by diverse fields of scientific research (Darzynkiewicz *et al.*, 1992; Darzynkiewicz *et al.*, 1997). It was initially discovered by Carl Vogt in 1842 during an amphibian development study, and was called Programmed Cell Death (PCD). The term apoptosis which was suggested by James Cormack, a professor of Greek language, refers to the dropping off of leaves from a tree (Kerry *et al.*, 1972; Pereira and Amarante-Mendes, 2011).

Recently it has been discovered that there are actually three kinds of PCD patterns, i.e. apoptosis, autophagy and necroptosis (Peter, 2011). Apoptosis refers to the well-recognized type of cell death that is caspase-dependent, that has associated morphological changes that includes nuclear and cytoplasmic condensation, blebbing of the plasma membrane that eventually results in the cell breaking up into a membrane-enclosed apoptotic bodies (Fadeel and Orrenius, 2005). Autophagic cell death is regulated by the availability of nutrients for the cells but under limited nutrients the cell will digest itself until death (Peter, 2011). Necroptosis is a recently found kind of necrosis that shows sequential regulation by the kinase receptor interacting proteins (RIKP) family which shows some “cross talking” with apoptosis and is activated if the extrinsic apoptotic pathway is activated while apoptosis is inhibited (Declercq *et al.*, 2009).

Morphological features of necroptosis are the same as that of necrosis but its inducing stimulus and programmed nature is like that of apoptosis (Wang *et al.*, 2007) . In necroptosis studies, a specific small molecule inhibitor of necroptosis, necrostatin-1 has been identified. This provides an opportunity to evaluate significant functions of necroptosis although the mechanism is still not well understood (Li *et al.*, 2008).

Since apoptosis is a normal, physiologically active, and not accidental, with a clearly understood mechanism of induction, scientist have recognized that most, if not all, physiological cell death occurs through apoptosis (Fadeel and Orrenius, 2005). Apoptosis does not cause an inflammatory response as it does not release it's cellular content to the surrounding and it is tightly regulated and maintains homeostasis perfectly (Gavrilescu and

Denkers, 2003). Therefore, for chemotherapy, induction of apoptosis, rather than necrosis of diseased cells, is a desired outcome (Rastogi *et al.*, 2009). Selectively triggering apoptosis as a form of cell death in a premalignant cell line and not the normal cell line is, therefore, an aim in the current study.

1.3.2 Apoptosis

Apoptosis is a physiologically active process of cell death in which the cell itself devises a program for death and homeostasis (Bertho *et al.*, 2000; Darzynkiewicz *et al.*, 1997). The PCD process appears to play an important role in living organisms. In cellular development and aging it acts as a homeostasis mechanism for maintenance of cellular populations and acts as a defense mechanism, through the immune response, and induction of natural death of infected cells (Bertho *et al.*, 2000; Elmore, 2007).

Tumour growth is usually associated with loss of apoptotic regulation and radiotherapy and chemotherapy are designed to result in apoptotic tumour cell death. Compounds that can induce apoptotic tumour cell death are very important in cancer chemotherapy (Zamai *et al.*, 2001). Apoptosis can be initiated to work through two distinct apoptotic pathways, i.e. intrinsic and extrinsic as well as perforin/granzyme pathway (Figure 1.5). All these apoptotic pathways give rise to biochemically distinguishable initial events (e.g. they activate different caspases) and finally result in a common executioner pathway (Elmore, 2007) in which cytomorphic and other changes such as changes in membrane component distribution (Figure 1.4). The most important pathway relevant to induction of apoptosis in target cells is the Intrinsic Pathway (Figure 1.5).

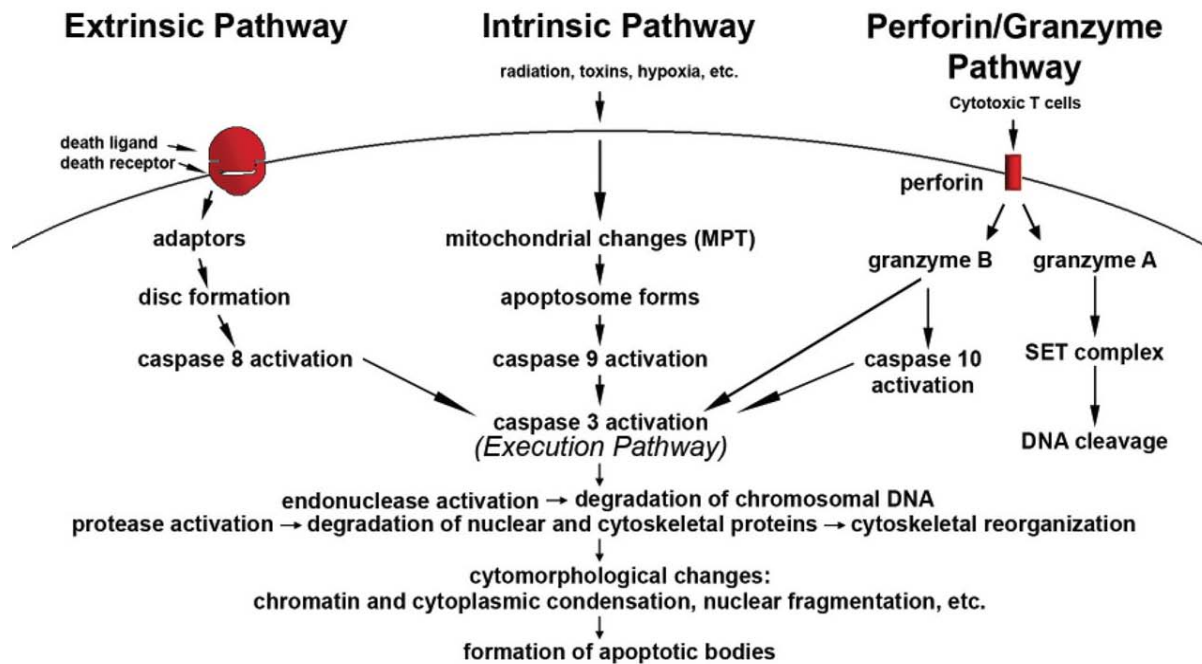


Figure 1.5: Different programmed cell death pathways.

All the apoptotic pathways result in the activation of the execution pathway. When the execution pathway is activated, a cascade of apoptotic events occur which all give rise to visible changes in the cell's physical appearance. The only mechanism relevant to drug-induced cell death is the intrinsic pathway. MTP = mitochondrial changes, SET complex = 270–420 kDa protein complex (adapted from Elmore, 2007).

1.3.2.1 Intrinsic apoptotic pathway

The intrinsic pathway of inducing apoptosis is a mitochondrion-dependent apoptotic pathway which usually responds to the extracellular signals and internal insults such as DNA damage, toxins, radiation, hypoxia, hyperthermia, viral infection and free radicals (Elmore, 2007) and is important in drug-induced cell death. This pathway is mainly regulated by members of the Bcl-2 family of proteins, found in mitochondria. These share one or more Bcl-2 homology (BH) domains. There are anti-apoptotic members (A1, Bcl-2, Bcl-X_L, MCL-1 and Bcl-W) with all four BH domains and pro-apoptotic members (BAX, BAK and BOK) with no BH4 domain.

There is another subset of special pro-apoptotic proteins. These display only the BH3 domain (BID, BIM, BAD, BIK, BMF, NOXA and PUMA) responsible for inter-molecular dimerization amongst the members, a process essential for their pro-apoptotic function. These proteins are referred to as “BH3 only proteins” and are capable of binding each other in an unusual way (Haupt *et al.*, 2003; Pereira and Amarante-Mendes, 2011) (Figure 1.6).

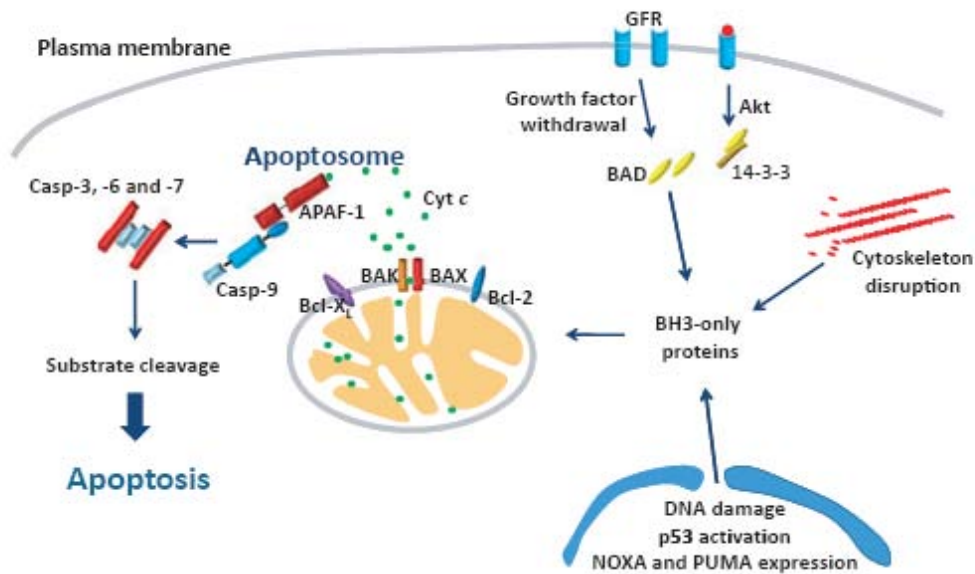


Figure 1.6: Mechanism of the intrinsic apoptotic pathway.

In response to DNA damage through chemotherapeutic drugs or ultraviolet radiation, the p53 gene is activated. This activates the expression of the BH3 only members, BIM and BMF. Growth factor withdrawals lead to the down regulation of the Akt pathway and, therefore, dephosphorylation of BAD and release from the 14-3-3 chaperon. When all the BH3 only members are activated they induce the BAX/BAK channel, leading to MOMP. This leads to the executioner pathway. Bcl-2 = B cell lymphoma 2, BH3 = Bcl-2 Homology domain 3, BAD = Bcl-2-associated death promoter, BAX = Bcl-2-associated X protein, MOMP = mitochondrial outer membrane permeability, BAK = bcl-2 homologous antagonist/killer, GRF = growth receptor factor (Pereira and Amarante-Mendes, 2011).

In response to the cell internal insult, the p53 is activated by the cascade of proapoptotic proteins and induces the over expression of regulatory pro-apoptotic proteins (i.e. NOXA and PUMA) (Figure 1.6). These proteins activate the over expression of the BH3 only proteins, BAX and BAK. The withdrawal of growth factors occurs and, therefore, the dephosphorylation of the BH3 only member, BAD, BAD subsequently is released from a cytoplasmic 14-3-3 chaperone. This directs BAD to the mitochondria. The cell internal stresses interfere with the cell's cytoskeleton dynamics and induce activation of the BH3 only protein members, BIM and BMF. This in turn induces mitochondrion-mediated apoptosis (Elmore, 2007; Rastogi *et al.*, 2009) (Figure 1.6).

A BAX and BAK channel is formed through the activation of the BH3 only proteins. This induces mitochondrial outer membrane permeability (MOMP) and, therefore, cytochrome c release. The mitochondrial cytochrome c binds to apoptotic protease activating factor 1 (APAF-1) and procaspase-9, activating the formation of the apoptosome complex (Figure

1.6). The clustering of procaspase-9 in such a complex results in its activation to caspase-9 which cleaves and activates the common executioner caspases, and subsequently the cell is committed to apoptosis (Schuler and Green, 2001) (Figure 1.6).

1.3.2.2 Extrinsic pathway

The extrinsic pathway is less likely to be involved in drug-induction of cell death as it is a receptor-mediated pathway mainly responsible for maintenance of tissue homeostasis (Fadeel and Orrenius, 2005) (Figure 1.7). This pathway is p53-tumour suppressor gene-dependent since the production of the trans-membrane receptor protein (i.e. Fas, DR5 and PERP) is dependent on the level of p53 expressed. This determines the level at which genes coding for the apoptotic trans-membrane proteins (Figure 1.7). These extrinsic pathway death receptors (DR) are characterized by their content of an 80 amino acids long domain referred to as death domain (DD) (Jonnalagadda *et al.*, 2008). This determines the specificity of the ligand for its receptor (Pereira and Amarante-Mendes, 2011). All the death receptors in this pathway belong to the tumour necrosis factor receptor (TNF-R) family. The T-cell secreted death-inducing protein FasL activates Fas. DR5, activated by binding to the TNF-related apoptosis inducing ligand (TRAIL), and the p53 apoptosis effector related to PMP-22 (PERP), cooperate to induce apoptosis by an, as yet, unknown mechanism (Haupt *et al.*, 2003).

Ligation of the death receptor, e.g. the FasL binding to the receptor Fas, induces the formation of a death-inducing signaling complex (DISC) which in turn recruits procaspase-8 (Figure 1.7). When the procaspase-8 levels increase, procaspase-8 is automatically activated to caspase-8. This sequentially activates the executioner caspases (3, 6 and 7) (Elmore, 2007). The cell will subsequently be directed to Type I extrinsic apoptosis or caspase-8 can process the BH3 only member BID to a shortened BID (tBID) which will be transported to the mitochondrion and induces mitochondrial outer membrane permeability (MOMP). This results in the release of cytochrome c into the cytoplasm. This sequentially induces the formation of the apoptosome (APAF-1/procaspase-9) complex and the activation of the executioner caspases. This subsequently results in mitochondrion-dependent apoptosis (Type II) (Haupt *et al.*, 2003; Pereira and Amarante-Mendes, 2011) (Figure 1.7). The alternative apoptotic pathway, not really relevant in drug-induced apoptosis, is the perforin/granzyme apoptotic pathway.

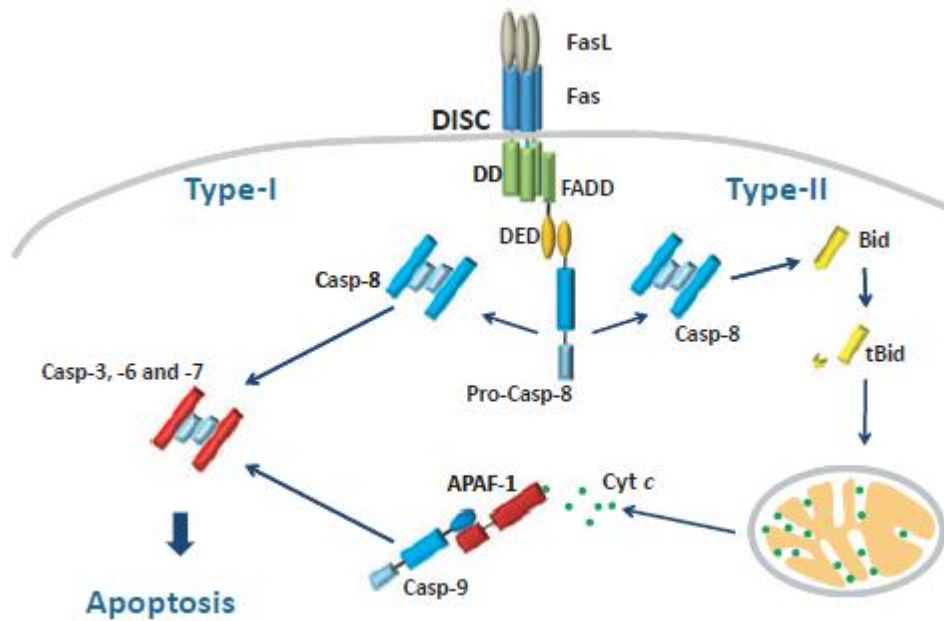


Figure 1.7: Extrinsic apoptotic pathway mechanism.

Clustering of the Fas L and Fas death receptors and induce the adaptor protein FADD and procaspase-8 can cleave the executioner pathway proteins or cleaves Bid into a truncated form. This is released to the mitochondrion and induces MOMP. Therefore, the release of cytochrome c is induced and the APAF-1/caspase-9 apoptosome is formed. This induces the executioner pathway. PERP = p53 apoptosis effector related to PMP-22, Apaf-1 = apoptosis protease-activating factor-1 (adapted from Pereira & Amarante-Mendes, 2011).

1.3.2.3 Perforin/granzyme apoptotic pathway

T-lymphocytes and natural killer cells use a perforin/granzyme pathway to target and destroy infected cells. If the lymphocyte detects some kind of abnormality in the cell, it will trigger apoptosis and either the FasL/FasR interaction or perforin/granzyme-dependent pathway (Fadeel and Orrenius, 2005). The perforin/granzyme pathway is the main mechanism used by the cytotoxic T lymphocytes, and, therefore, not important for drug discovery since, as mentioned before, toxins/drugs activate the intrinsic apoptotic pathway.

What happens in this pathway is that the lymphocytes secrete perforin and granzyme via granule exocytosis upon detection of any abnormality within any cell. Perforin is a membrane-disrupting protein that is capable of forming a pore in the surface of the cell membrane and granzymes are serine proteases. These proteins work together to induce apoptosis. Granzymes trigger apoptosis in the target cell and perforin delivers them appropriately into the target cell (Trapani and Smyth, 2002).

There are two kinds of granzymes, i.e. granzyme A and granzyme B. Granzyme B can cleave proteases at aspartate residues and will cleave caspase-10 (the initiator caspase). This will subsequently activate the executioner caspases. Granzyme B has been reported to cleave Bid (BH3 interacting domain death agonist) and, therefore, result in the induction of the mitochondrial-dependent death pathway. Again this protease can also directly activate caspase-3, inducing the execution phase of apoptosis (Elmore, 2007). Granzyme A drives apoptosis in a caspase-independent pathway where it cleaves the SET complex and thereby activates the DNase (NM23-H1) which will activate DNA degradation, thereby contributing to apoptosis (Calaf *et al.*, 1995). Apoptosis induced via the extrinsic, intrinsic and perforin/granzyme pathways can be distinguished biochemically by detection of caspase-8 (extrinsic), caspase-10 (perforin/granzyme) and caspase-9 (intrinsic) in early stages of apoptotic cell death. All these pathways at late stages of apoptosis give rise to the common caspase-dependent executioner pathway.

1.3.3 What do the common executioner caspases do?

In extrinsic, intrinsic and perforin/granzyme pathways the end point is the execution phase. This is considered the final stage of apoptosis. The execution phase is actually carried out by specific proteolytic enzymes such as caspase-3, caspase-6 and caspase-7. These are responsible for the actual physical effects seen late in apoptosis (Vaskivuo, 2002). All these caspases recognize different specific substrates in their reaction, as illustrated in Figure 1.8.

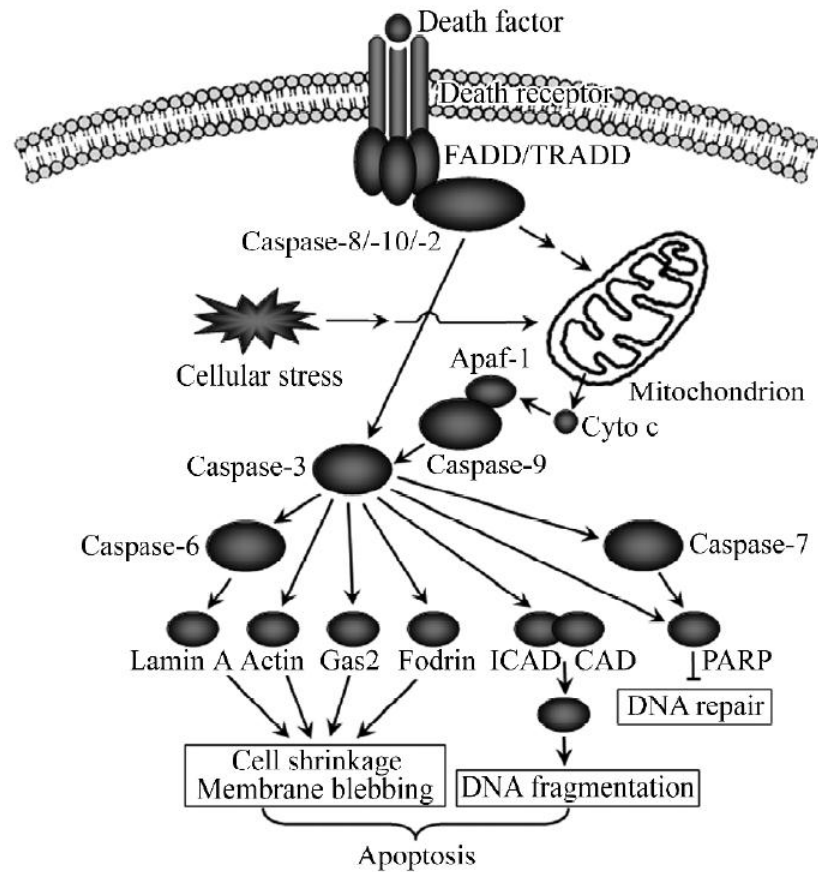


Figure 1.8: Executioner caspases and their substrate recognition for induction of apoptosis.

The common executioner pathway results in cell shrinkage, membrane blebbing, DNA fragmentation and inhibition of DNA repair genes. CAD = caspase-activated deoxyribonuclease; FADD = Fas-associated death domain; ICAD = inhibitor of caspase-activated deoxyribonuclease; PARP = poly (ADP-ribose) polymerase; TRADD = tumour necrosis factor receptor-associated death domain (adapted from Fan *et al.*, 2005).

Caspase-3 is recognized as the main enzyme in the execution phase and is activated by any of the initiator caspases (caspase-8, caspase-9 and caspase-10). This caspase cleaves the inhibitor caspase activated DNase (ICAD) and subsequently releases caspase-activated DNase (CAD). CAD is an endonuclease responsible for degradation of chromosomal DNA, and, therefore, causes chromatin condensation. It activates cytoskeleton disruption and the budding off into apoptotic bodies through cleavage of gelsolin, an actin-binding protein (Elmore, 2007).

Cleavage of lamin A and fodrin by caspases (as indicated in Figure 1.8) results in chromatin condensation and decomposition of nucleus and formation of apoptotic bodies. Poly ADP-ribose polymerase (PARP), DNA-dependent protein kinases (DNA-PK) and steroid response

element binding protein (U₁,70 KD) are the proteins involved in DNA repair, so once they are cleaved by caspases they become inactivated and, therefore, DNA degradation results (Fan *et al.*, 2005). Eventually, when all caspases are activated, a cell will undergo many physical changes and die (Figure 1.8).

1.3.4 Regulators of apoptotic cell death

In all apoptotic pathways caspases are a very important family of proteases referred to as aspartate-specific cystein proteases that mediate apoptosis. They are single chain proteins with an amino terminus pro-domain, large subunit in the middle with an active site and the carboxy terminal small subunit. To date about 14 caspases have been discovered and not all of them play a role in apoptosis. Caspases are regulated at post-translational level to ensure that they are regularly activated (Cohen, 1997; Pereira and Amarante-Mendes, 2011). There are inflammatory caspases (which includes caspases-1, -4, -5, -11, -12 and -13) and all the others are involved in apoptosis. The apoptosis-inducing caspases are divided into two groups. There are initiator caspases (-2, -8, -9 and -10) which are activated through dimerization through the effect of multimeric complexes like the apoptosome and death-inducing signal complex (DISC), and executioner caspases (-3, -6 and -7) already expressed as dimers and activated by cleavage of the pro-domain from the large and small subunit (Cohen, 1997; Fadeel and Orrenius, 2005; Nicholson, 1999; Pereira and Amarante-Mendes, 2011).

Another mediator of apoptosis is the p53 tumour suppressor gene or transcription factor that induces cell death to restrict irregular cellular growth. This gene restricts cellular growth through apoptosis.

1.3.5 Methods of assessing cell death (apoptosis or necrosis)

Apoptosis is not only a process for cell homeostasis but removes infected or damaged cells from the system (Martinez *et al.*, 2010). In chemotherapeutic testing of drugs, selective cytotoxicity is of importance and provides preliminary data for *in vivo* studies i.e. evidence that test drugs can induce apoptotic cell death *in vitro* in tumour cell lines, but do not affect a normal cell line (Zamai *et al.*, 2001).

Methods for evaluation of cell viability are mostly dependent on proliferation and metabolic activity. Other methods developed include those based on direct cell counting, differential

staining and DNA integrity (Wang *et al.*, 2010). Each checks a different, differential effect and all have some merit for the determination of the effect of a test compound, though each has its own weakness.

As the morphological characteristics of dead or dying cells include the loss of cell membrane integrity, many assays for cell viability depend on this characteristic. When fluorochromes like PI, ethidium bromide (EB), 7-amino-actinomycin D (7-AAD) and trypan blue (TB) are incubated with live and dead cells, the dyes will be excluded by the live cells with intact cell membrane, but stain the late apoptotic and necrotic cells showing loss of cell membrane integrity (Darzynkiewicz *et al.*, 1997).

Acridine orange (AO) and Hoechst (HO) are fluorochromes that are different from such dyes as they stain even the live cells with intact membranes. Use of one of these membrane-permeable stains, with one of the already mentioned non-cell-permeable dyes (in intact cells), allows one to distinguish between late apoptotic and necrotic cell death (stain green with AO and also red with PI, respectively), and early apoptotic and live cells (staining green with AO and without staining for PI) and is cheap and easy to use (Bradbury *et al.*, 2000). Whether necrosis and late apoptosis are distinguished, however, is unclear as staining intensity of propidium iodide has been reported to simultaneously detect living (PI-negative), apoptotic (PI-weak cytoplasmic staining) and necrotic (PI-bright staining) cells, when unfixed cells are exposed to supravital staining (Zamai *et al.*, 2001). The latter study contradicts the study by Bradbury *et al.* (2000), in that intensity of PI staining is used to distinguish apoptosis from necrosis whereas lack of PI staining is taken to indicate early apoptosis and PI staining to indicate necrosis in the results of Bradbury *et al.* (2000). PI, nevertheless, seems to represent one of the most important dyes for detection of cell death (Bradbury *et al.*, 2000).

Cell membrane disruption, during various insults, causing expression of thrombospondin binding sites, loss of sialic acid residues and exposure of phosphatidylserine (PS) by apoptotic cells, allows the development of cell viability detection methods. PS is a phospholipid normally present in the plasma membrane, facing the cytoplasm. During early apoptosis, the plasma membrane asymmetry is disrupted and the PS is exposed on the cell surface.

Annexin V is an expensive protein that binds phospholipids like PS, if exposed on the surface of a cell dying via apoptosis. Dye-labeled annexin V allows the detection of such surface-exposed PS. In early apoptotic cells, annexin V staining is positive and no staining for PI is

seen. Alternatively, staining with both detection systems can occur in late apoptosis and necrosis. Unfortunately, the two different types of cell death cannot be distinguished by this method (Verms *et al.*, 1995). It has been reported that annexin V staining is only suitable for apoptosis detection in cells occurring naturally in a suspension. Unfortunately, during application in studies on adherent cells, PS exposure may either occur as an artifact due to membrane damage caused by treatments used to dislodge cells. This may give rise to false annexin V binding and false positive results (Van England *et al.*, 1996). This limits the use of such a technique for adherent cells.

Caspase assays are similarly expensive and time consuming, though assays for caspase-8, -3 and -9, and caspase-10 may be used to detect induction of cell death via the extrinsic, intrinsic and perforin/granzyme pathways (Figure 1.5). For the current study, a high-throughput, simple, minimally expensive method was sought, and imaging and flow cytometry using an inexpensive dye was considered.

Imaging (microscopy), flow cytometry and transmission electron microscopy (TEM), at low and higher magnification may assist the simultaneous viewing and result assessment of a large number of cells (Krysko *et al.*, 2008). Finally it was thought that light and fluorescence microscopy may be best used if cost and time is a consideration.

When using simple light microscopy and performing cell counts using a hemocytometer, a popular dye to use for detection of dead cells is trypan blue (Coder, 1997). This constitutes a simple and cheap, but less time-consuming method for cell death assessment, trypan blue labelling cells with permeable membranes i.e. dying, late apoptotic or necrotic cells. For fluorescence microscopy, double staining with AO (green) and ethidium bromide (EB) (purple) or PI (red) is often used to similarly establish the percentage of viable (stained green), early apoptotic (stained green) as well, late apoptotic or necrotic cells (nuclei both stained red), like use of annexin V and PI systems, with similar results, though it seems that such dyes may not easily differentiate between apoptotic and necrotic cells (Baskić *et al.*, 2006), it seemed worthy of investigation.

Cell counts may be used to monitor both stimulation and depression of proliferation and indirectly the induction of cell death. Another way of indirectly assessing the effect of test compounds is using the (3-(4,5-dimethylthiazol-2-yl)-5-(3-carboxymethoxyphenyl)-2-(4-sulfophenyl)-2H-tetrazolium) (MTS) assay, a calorimetric method of estimating cell viability using assessment of metabolic activity. Here the metabolic rate of cells is a measurement as

metabolism is largely proportional to the number of viable cells (Bunger *et al.*, 2002). This method, however, is not reliable for use on its own as metabolic activity is not only proportional to the cell number, but the effect of a compound on the metabolism of the cells. Cells show depressed metabolic activity after treatment may also show no decreased cell numbers, or cell death, as decreased metabolic rate does not necessarily mean the cells are dying (Wang *et al.*, 2010).

Assays for metabolic activity check cytotoxic effects but are also highly depended on cell number. Cell numbers should, therefore, be checked, before and after treatment, to allow interpretation of results.

Imaging techniques, using dyes that indicate cell death are used to distinguish apoptosis from necrosis on slides seeded with adherent cells. These may not give an accurate reflection of the numbers of dead cell as cells may detach before dying. Flow cytometry, using the same such dyes, may detect those cells that have detached if cell supernatants are included in the assay. Though there are many ways to assess apoptosis, all have their weaknesses, as does the propidium iodide (PI) staining method used in this study. For this reason a number of methods should be employed to confirm results.

Flow cytometry is popular for the rapid analysis of a large group of individual cells (Bertho *et al.*, 2000). The morphological properties associated with cell death can be easily revealed by flow cytometry using the side scatter and forward scatter mode (see Section 3.2.6.1). Physical parameters such as DNA content, expression of antigens such as annexin V and membrane integrity can be assessed using the side scatter (for morphology) or forward scatter (for fluorescence) mode of analysis. This method has been proven to be very useful as it is rapid and may be used to assess a number of parameters (Telford *et al.*, 2004), but also compensate for cells not imaged using fluorescence microscopy, due to detachment before or during cell death. Flow cytometry, therefore, seemed an attractive option for the current study.

Assessment of DNA integrity, using methods such as DNA laddering, single cell gel electrophoresis (SCGE) (or Comet) assay, terminal dUTP nick end-labeling (TUNEL) and nick translation assays may also be used, but are technically challenging, time consuming and expensive. DNA laddering involves isolation and assessment of DNA using gel electrophoresis. Fragmentation of the DNA only becomes significant when a large proportion of the population of cells is apoptotic and DNA is easily sheered during DNA preparation giving false positive results indicating necrosis (smearing of bands). Therefore, this method

should generally not be used alone to draw conclusions (Abdullah *et al.*, 2010) . The presence of DNA fragments in a cell can also be confirmed by TUNEL assay.

The TUNEL assay involves detection of the fragmented DNA in individual apoptotic cells. The terminal deoxynucleotidyl transferase adds the dUTP to the 3'-OH end of the fragmented DNA. dUTP can be subsequently labeled with a variety of probes to permit detection with light microscopy, fluorescence microscopy and flow cytometry (Elmore, 2007). This technique is very sensitive and fast but very expensive. How many DNA breaks are needed for detection to occur is unknown. Therefore, another method of confirming results is required (Tumburrino *et al.*, 2011).

The Comet assay, where electrophoresis is performed on whole permeabilized cells, allows the visualization of a comet tail, indicating the DNA cleavage associated with either apoptosis or necrosis. This method is known for being very sensitive but technically difficult to perform and difficult to interpret (Yasuhara *et al.*, 2003) and, therefore, was not considered for the current study.

Cell counts, the MTS assay, supravital staining and imaging of PI and AO-treated cells on glass slides, and PI staining and flow cytometry (PI being used rather than annexin V as test cell lines to be used were adherent) were simultaneously assessed. Each compound was assessed on a model system of a normal MCF-10A breast epithelial cell line and its c-Ha *ras* transfected, premalignant, invasive derivative, to assess any differential effect of the parental HYP and its two derivatives.

1.4 MCF10A

The Michigan Cancer Foundation (MCF) developed a series of human mammary epithelial cell lines from a 36 year woman with fibrocystic disease (Miller *et al.*, 1993). The breast tissue from a 36 year old, premenopausal woman, with no family history of breast cancer was used. Histological examination of breast tissue revealed no malignancies, but extensive fibrocystic disease, characterized by an increase in fibrous tissue and a number of dilated mammary ducts, an abnormal increase in growth of ductal cells, with no evidence of abnormality (Soule *et al.*, 1990).

The immortal MCF10 cell line was isolated and characterized and found to spontaneously immortalize in culture. The mortal MCF10M cells were found to senesce when cultured in a media containing normal calcium concentrations (1.05 mM) but gave rise to an immortal cell

line that grows either as an attached cell, in normal calcium concentrations (MCF10A) or as a free floating cell line (MCF10F) in medium containing 0.04 mM calcium (Tait *et al.*, 1990).

The MCF10A cells are frequently used as a normal control in breast cancer studies since they show the morphological characteristic of normal breast epithelial cells (Zientek-Targosz *et al.*, 2008). These cells do not express any mutations in the p53 gene but show homozygous loss of the p16/p15 locus making them immortal, i.e. a phenotype similar to one in which p53 is mutated. They do not form tumours in mice or colonies in soft agar, but, at confluence, these cells do not form dome structures in tissue culture but form mammary spheres at 3D collagen culture (Zientek-Targosz *et al.*, 2008). The MCF10A cells have several advantages over other currently available cell lines because they are not treated with pro-carcinogens, the cells do not harbour SV40 genetic information, but are cells with normal polarized characteristics like normal breast epithelial cells, i.e. show a typical apical and basal domain, and their karyotype is near diploid with minimal rearrangements (Calaf *et al.*, 1995). If an oncogene's role in tumour progression is to be studied, introduction of such an oncogene into such a normal control allows the oncogene to be studied relative to a normal cell of the same genetic background, easily revealing the effect of the oncogene.

1.4.2 MCF10A transformation

More than 50% of breast cancers exhibit increased levels of activated Ras (Basolo *et al.*, 1991) and so to evaluate the selective effect of a compound on a cell line with increased levels of active Ras, a mutated (VAL-12) Harvey *ras* gene was introduced into a suitable acceptor cell, the MCF-10A cell line (Calaf *et al.*, 1995). This parental cell line was transformed to a premalignant cell line using transfection using the Homer 6 (Ph 06) plasmid, containing the neomycin-resistance gene for clone selection of transformed cells. The construct inserted into the plasmid contained the human T24 H-*ras* mutation or Val-12 mutated c-Ha-*ras* oncogene first isolated from a bladder cancer. Cells transformed with such a construct were subsequently called the MCF10A-NeoT cell line (Basolo *et al.*, 1991). Transformed MCF10A cells acquired a malignant phenotype, i.e. show clumping in high confluent cultures, 3-dimensional growths in collagen, show anchorage independence and are invasive (Russo *et al.*, 1991).

A combination of these two test cell lines, representing the normal and a premalignant invasive phenotype, represent a unique test system in which to explore the selective toxicity of a drug specifically aimed at H-Ras-related breast cancer malignancies.

1.5 RESEARCH AIMS AND OBJECTIVES

The aim of the current study was, therefore, to:

- Isolate and purify hypoxoside from the *Hypoxis hemerocallidea*, through extraction of its corms with ethanol and further isolation with pre-packed reverse-phase column.
- Prepare two derivatives from pure hypoxoside through methylation and acetylation, resulting in a dimethyl and a decaacetyl derivative, respectively.
- Confirm the purity of hypoxoside and the derivatives using NMR spectroscopy and HR-MS.
- Establish an inexpensive, rapid, high through-put method for the preliminary assessment of the selective effects and cytotoxicity of the prepared compounds using cell counts, metabolic assessment (MTS assay), imaging using flow cytometry, and fluorescence microscopy using dyes (especially supravital staining with propidium iodide which is claimed to be useful in distinguishing live from early apoptotic and late apoptotic/necrotic cells).

CHAPTER 2

HYPOXOSIDE: EXTRACTION, ISOLATION AND SYNTHESIS OF TWO DERIVATIVES

2.1 OVERVIEW

Plants produce phytochemicals, many of which have associated medicinal properties. Natural products have gained importance as being a possible primary source of commercial drugs (Chin *et al.*, 2006). Many older drugs are derived from plants e.g. cocimadin from sweet clover, aspirin from the bark of the yellow white willow and the malaria drug artemisinin sourced from *Artemisia annua L.* Many of the most effective cancer drugs are also derived from plants, e.g. vincristine, etoposide and paclitaxel that were isolated from the periwinkle, May apple and pacific yew tree, respectively.

For centuries in Africa, traditional healers were the only source of medical assistance for illness and diseases. Traditional healers use parts of plants for treatment of these diseases. Aqueous extractions of *Hypoxis* corms, for example, were traditionally used for intestinal parasites, barrenness, impotency, bad dreams, insanity and cardiac ailments. Since more diseases are now known, the *Hypoxis* extract has been used for treatment of cancer, headaches, dizziness, for testicular tumours, prostate hypertrophy and to boost the immune system (Drewes *et al.*, 2008). *Hypoxis hemerocallidea* is well known in Southern Africa. This plant is distributed in the wild areas from Eastern Cape, KwaZulu-Natal, Limpopo and Zimbabwe and has been chosen for this study because it has been reported to have a high concentration of hypoxoside compared to other *Hypoxis* species. A study carried out by Boukes *et al.* (2008) reported that 5 mg of *H. hemerocallidea* extract was found to contain 12.7 µg of hypoxoside, while *H. stellipilis* and *H. sobolifera* contained 7.9 µg and an undetectable amount, respectively (Boukes *et al.*, 2008).

As the *Hypoxis* extract became better known amongst the South African people, local entrepreneurs have prepared *Hypoxis* extracts for dispensing over-the-counter (OTC). These are readily available in pharmacies, health shops and supermarkets. Moducare[®] is one such product. The secret of Moducare[®] is that it contains the two sterols isolated from the *Hypoxis* extract (i.e. β-sitosterol and its glucoside). These are mixed in a given ratio to enhance human T cells growth (Boukes and Venter, 2012). Hypo Plus is also marketed as an OTC food supplement and immune booster. It consists of a *Hypoxis* extract, as well as a range of amino acids, vitamins and anti-oxidants. The Impilo African Potato product is also an OTC

preparation in a form of either a tablet or the capsule and is prepared from a *Hypoxis* extract (Drewes and Khan, 2004) .

The biological activity of the *Hypoxis* extract was initially associated only with steroid glycosides (Bettolo *et al.*, 1982; Laporta *et al.*, 2007a; Nair and Kanfer, 2006). Isolation of the active components from the crude extract is always important, as it reduces the possible negative effects of the other associated toxins or harmful compounds. The active principle was found to be hypoxoside and this was firstly isolated by Bettolo *et al.* (1982). Hypoxoside is referred to as a pro-drug as it is biologically inactive in its isolated form, but, as discussed in Chapter 1, it can be hydrolyzed to its active form, referred to as rooperol, by the enzyme β -glucosidase (Drewes *et al.*, 1984; Nair *et al.*, 2007). When β -glucosidase reacts with hypoxoside it is converted to the biologically active rooperol through the removal of the two sugar groups linked at their anomeric position to the benzene rings of hypoxoside (Figure 1.2). This enzyme has been reported several times to be present in tumours and hence tumours may activate this compound to their own detriment (Smit *et al.*, 1995). When hypoxoside is ingested (*in vivo*) it is converted to rooperol as there is a high content of activated β -glucosidase in the colon (Kruger *et al.*, 1994). On ingestion of the hypoxoside the compound is activated and may be absorbed to perform its curative role.

Hypoxis extracts have been studied for a number of ailments but more needs to be done to verify the claims by traditional healers and others. The phase I anti-cancer trial of hypoxoside carried out by Smit *et al.* (1995) did not show a significant effect on lung cancer patients, although patients were treated with high concentrations of hypoxoside. Subsequent reports on rooperol indicate that it has a strong antioxidant ability with a strong ability to inhibit lipid peroxidation (Laporta *et al.*, 2007b) . The hypoglycemic effect of the African potato extract was also reported but the active component causing this effect has not been identified (Zibula and Ojewole, 2000). The cardiovascular studies suggest that *Hypoxis* extract may be used as a natural treatment for some cases of cardiac dysfunctions and for hypertension (Ojewole *et al.*, 2006). The anticancer activity of the *H. hemerocallidea* extract on HeLa, MCF7 and HT27 cell lines showed it to have a lower anticancer activity than the anticancer activity of the *H. sobolifera*, a plant that has the lowest content of hypoxoside (Boukes *et al.*, 2008). The reason for this was not stated.

The aim of the current study was to isolate hypoxoside from *Hypoxis hemerocallidea*, and, in addition to hypoxoside, prepare two further derivatives from the pure hypoxoside, and

subsequently to investigate their selective cytotoxicity against a normal (MCF10A) and a premalignant (MCF10A-NeoT) breast epithelial cell line. Similar work has been done on the HeLa, HT-29 and MCF-7 cancer cell lines, respectively. This showed that hypoxoside has cytotoxic effects on cell lines such as cervical, lung and breast cancer cell lines (Boukes and Van de Venter, 2011). The current research will be different in that two derivatives, the dimethylhypoxoside (DMH) and decaacetylhypoxoside (DAH) previously prepared by Bettolo *et al.* (1982) have been prepared from hypoxoside, and further tested against both a normal and a premalignant invasive breast epithelial derivatives. These derivatives have never been evaluated for their activity, but were evaluated in the hope of finding better anti-cancer compounds for the treatment of invasive breast cancers.

In order to perform the derivatization and ensure the correct compound and plant corm was extracted, the plant had to be collected and identified.

2.2 COLLECTION AND IDENTIFICATION OF THE CONSTITUENTS IN *H.*

hemerocallidea

Hypoxis hemerocallidea (Figure 2.1) corms were collected from the Hayfields commonage along Military Way, Pietermaritzburg and identified by Dr Christina Potgieter of the John Bews Herbarium, School of Life Sciences, University of KwaZulu–Natal, Pietermaritzburg and a voucher specimen was deposited in the John Bews Herbarium (Catalogue No. SED 15).



Figure 2.1: Corm and flower of the collected *Hypoxis hemerocallidea* (photographed by Prof S.E. Drewes).

2.3 EXTRACTION AND ISOLATION

There is a growing demand for the pharmaceuticals based on medicinal plant extracts. The market volume of herbal extracts for food additives amounted to Euro 6.7 billion in Europe for 2003 alone and Euro 17.5 billion in the world. Continuous demand spontaneously drives the task of developing new and effective extraction methods (Ivanov *et al.*, 2006).

There are many methods that have been developed throughout the world for commercial extraction of plant materials. The general techniques include maceration, infusion, percolation, digestion, decoction, hot continuous extraction (Soxhlet), aqueous-alcoholic extraction by fermentation, counter-current extraction (CCE) and supercritical fluid extraction (Golovanchikov and Popov, 1998).

Extraction of the components from traditional plants in traditional medicine is generally based on extraction with various solvents at room temperature or on heating (Golovanchikov and Popov, 1998).

2.3.1 Materials and equipment

The reverse-phase column (3.5 x 2.7 cm) used in this study was a product from Phenomenex. The solvent used for extraction was ethanol (Merck), for isolation of hypoxoside, methanol (Merck) was used, a mixture of n-butanol (Kleber chemicals), H₂O, toluene (Merck) and MeOH (Merck) was used for identification of hypoxoside using TLC (silica gel 60 F₂₅₄, Merck, Germany). The separation was effected with cartridges packed with C-18 reverse-

phase silica using a standard vacuum manifold assembly. Chemicals used for methylation were methylamine (BHD Laboratory reagents), sodium nitrite (Sigma), urea (Saarchem), hydrochloric acid (Merck), sulfuric acid (Merck) and potassium hydroxide (Saarchem). The acetylation procedure was carried out with the following compounds: pyridine (Saarchem), acetic anhydride (Merck), followed by drying with anhydrous magnesium sulfate (Merck).

For obtaining the extract in a solid form, it was freeze dried using a VirTis machine (Polychem Supplies). For characterization of hypoxoside and its derivatives, a Bruker NMR spectrometer (500 MHz) and Waters Micromass LCT Premier TOF mass spectrometer were used.

2.3.2 Extraction and isolation procedures

This part of the work was performed in the Department of Chemistry in the University of KwaZulu-Natal, Pietermaritzburg. The extraction was done according to the method used by Drewes *et al.* (1984) with a few modifications. Freshly collected corms (1.65 kg) of *Hypoxis hemerocallidea* were thoroughly washed under running tap water. They were cut into thin slices, macerated and subsequently soaked in ethanol (2 L) at room temperature for 48 h. The extract was filtered and concentrated *in vacuo*, followed by freeze drying to give approximately 56 g of brown residue. Thereafter, 200 mg of the crude material was dissolved in a MeOH-H₂O (1:1) mix and separated on a pre-packed C-18 reverse-phase column (Phenomenex 3.5 x 2.7 cm) using a standard vacuum manifold assembly. The isolation procedure was repeated five times. Hypoxoside was detected in the fractions by TLC using an n-butanol-H₂O-toluene-MeOH (4:2:2.5:2) solvent system and *para*-anisaldehyde for visualization. Fractions containing a single compound were combined and concentrated in a rotary evaporator. The resultant aqueous fraction was freeze dried to give pure hypoxoside (~100mg). The purity and structure of hypoxoside was confirmed with NMR spectroscopy. The experiments used were ¹H NMR (for identification of protons), COSY45 (correlated spectroscopy, a 2-D NMR experiment that reveals correlation between neighboring protons), ¹³C NMR (to identify all carbons), DEPT (distortionless enhancement polarization transfer, to distinguish CH₃ from CH's and CH₂'s, carbons), and heteronuclear single quantum coherence (HSQC) and, heteronuclear multiple bond correlation (HMBC) experiments to detect correlations between the ¹H and ¹³C nuclei. Details are given in the Section 2.3.4.2 below.

2.3.3 Results

Table 2.1: Collected masses of the hypoxoside and derivative weights.

<u>Material type</u>	<u>Mass (g unless otherwise stated)</u>
1. Fresh corms	1650
2. Crude extract	56.6 (3.4%)
3. Hypoxoside	291 mg (yield from 1 g crude extract, therefore 29% was produced)

Table 2.1 shows the mass of the isolated products and hypoxoside. A good separation of the major product was achieved using a reversed phase column chromatography, as indicated by examination by TLC, though minor contamination was present in the initial fractions (Figure 2.2).



Figure 2.2: TLC plate showing fractions collected from a reverse phase chromatography column in the manifold assembly.

The spots of the collected fractions were plotted on the TLC plate and the tubes 6, 7, 8, 9 and 10 were used for derivatization. The 1st spot represented with an “s” is the starting material before it was introduced on the column. The second spot represented by 3 was the 3rd fraction collected from the column and the fractions were collected up to the 12th tube/fraction.

2.3.4 Elucidation of the hypoxoside structure by ¹H and ¹³C NMR spectroscopy

The structure of the hypoxoside isolated and selected, as described above, was confirmed by examining the ¹H and ¹³C NMR spectra recorded at 500 MHz and 125 MHz, respectively.

2.3.4.1 Procedure

The isolated hypoxoside was diluted with deuterated methanol (approximately 2 ml) and the ^1H and ^{13}C NMR spectra recorded at 500 MHz and 125 MHz, respectively (Bruker Instrument). In order to allocate all protons and carbons in the spectra, use was made of two-dimensional NMR experiments such as COSY, DEPT, HSQC and HMBC to identify the position and relationships of the relative atoms.

2.3.4.2 Results

The analysis of the spectra is shown in Table 2.2 below (all spectra shown in Appendix A).

Table 2.2: NMR chemical shifts for hypoxoside in CD_3OD .

^1H NMR		^{13}C NMR
Assignment	Chemical shifts (ppm)	Chemical shifts (ppm)
C-1	6.57 (1H, <i>d</i> , $J = 15.7$ Hz)	131.8
C-2	6.13 (1H, <i>dt</i> , $J = 15.7; 5.0$ Hz)	120.3
C-3	3.30 (2H, <i>d</i> , $J = 5.0$ Hz)	23.3
C-4	-	86.3
C-5	-	83.3
C-1''/C-1'	-	134.6, 120.9
C-2''/C-2'	6.92 (1H, <i>d</i> , $J = 2.1$ Hz); 6.90 (1H, <i>d</i> , $J = 2.1$ Hz)	120.1
C-3''/C-3'	-	146.8, 146.3
C-4''/C-4'	-	148.5, 148.3
C-5''/C-5'	7.12 (2H, <i>d</i> , $J = 8.3$ Hz)	124.7, 124.5
C-6''/C-6'	6.87 (1H, <i>dd</i> , $J = 8.3; 2.1$ Hz); 6.82 (1H, <i>dd</i> , $J = 8.3; 2.1$ Hz)	118.9, 118.5
Glucose		
C-1''/C-1'	4.75 (2H, <i>d</i> , $J = 7.3$ Hz)	104.0
C-2''/C-2'	<i>a</i>	78.2
C-3''/C-3'	<i>a</i>	71.3
C-4''/C-4'	<i>a</i>	74.9
C-5''/C-5'	<i>a</i>	78.4
C-6''/C-6'	3.89 (2H, <i>bd</i> , $J = 7.0$ Hz), 3.72 (2H, <i>bd</i> , $J = 7.0$ Hz)	62.5
<i>a</i> - Multiplet, 3.35-3.75 ppm		

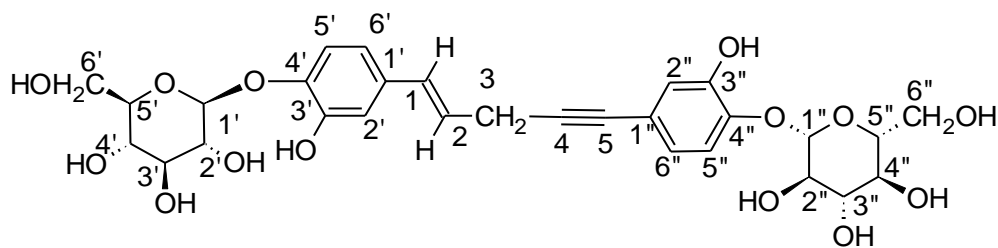


Figure 2.3: Numbering of carbons in the hypoxoside structure.

The two benzene rings are separated by a chain of five different carbons (single, double and triple bond). This causes the protons on one ring to have slightly different chemical shifts to those on the other ring, but the splitting patterns (AMX) remain the same. The ring that will have more deshielded protons will be the one closer to the triple bond. In the region δ_H 6.8-7.2, the six protons present on the two benzene rings confirm the hypoxoside structure as follows: the first doublet peak at δ_H 7.12 shows protons 5''/5', overlapping exactly with coupling constant of $J=8.3$ Hz (*ortho*-coupling). The second two doublet peaks at δ_H 6.92 and 6.90 represent the 2''/2' protons. The third set of peaks at δ_H 6.82 and 6.87 represent the 6''/6' protons, shown as a double pair of doublets due to the *ortho*-splitting by H-5''/5' and *meta*-splitting by H-2''/2'. Overall the protons are a clear example of the AMX pattern in which two systems are imposed on one another.

From the 5 carbon chain linking the two benzene rings, three protons can be seen. The proton on C1 resonates at δ_H 6.57 as a doublet with $J = 15.7$ Hz (*trans* configuration). The proton on C2 resonates at δ_H 6.13 and is a doublet of triplets (as anticipated) with $J = 15.7$ and 5.0 Hz. The protons on C3 (CH₂) resonate further upfield at δ_H 3.29.

The only CH₂ groups in the molecule (at C-3, and at C-6 on glucose) were readily located from the DEPT analysis. The proton spectrum is well resolved and much clearer than the original spectrum produced by Marini Bettolo and his co-workers in 1982 (Bettolo *et al.*, 1982). The ¹³C NMR shift values listed in Table 2.2 are in good agreement with the values quoted earlier (Bettolo *et al.*, 1982).

2.4 PREPARATION OF HYPOXOSIDE DERIVATIVES

The numerous uses of the *Hypoxis* extract have drawn much interest in the synthesis and derivatization of rooperol, the biologically active form of the *Hypoxis* extract's major compound, hypoxoside. Initially, when hypoxoside was isolated, three derivatives were made from hypoxoside (i.e. decaacetylhypoxoside, dimethylhypoxoside and dimethyloctaacetyl

hypoxoside) and other derivatives were made from rooperol which include the tetramethyl aglucone and tetraacetyl aglucone (Bettolo *et al.*, 1982). None of these compounds have been tested for biological activity and the current research was carried in the hope that the derivatized compounds had increased anticancer activity compared to the parent compound.

A patent filed in 1987 contains a number of rooperol analogous and related compounds. Selected compounds recorded in the patent were tested against selected cancer cell lines and rooperol was found to have the best selective toxicity against most cancer cell lines (Drewes and Liebenberg, 1987). These derivatives were not, however, those investigated in the current study i.e. DMH and DAH.

2.4.1. Methylating hypoxoside

In order to prepare the dimethylhypoxoside, nitrosomethylurea, precursor for the diazomethane procedure, needed to be prepared. Diazomethane is a well-known methylating agent.

2.4.1.1 Preparation of nitrosomethylurea (diazomethane precursor)

The nitrosomethylurea was prepared according to Arndt *et al.* (1935) with no modifications (Arndt *et al.*, 1935).

2.4.1.2 Precursor preparation procedure

A 33% aqueous solution of methylamine (145 g) and an aqueous solution of 32% hydrochloric acid (~155 ml) were mixed in a 1 l flask, with the acid added until the solution was acidic to methyl red. Water (~100 ml) was added to bring the total volume to about 500 ml. The solution was mixed with urea (300 g) and boiled under gentle reflux for 2.75 h and vigorously refluxed for a further 15 min. The solution was cooled overnight at room temperature (~ 15°C) and a 2% (m/v) sodium nitrite (10 g) was dissolved in the cooled solution (500 ml), which was further cooled to 0°C. A mixture of ice (600 g) and a 98% sulfuric acid (54 ml) was placed in a 3 l beaker surrounded by sufficient freezing mixture (ice mixed with coarse salt). The cold methylurea-nitrite solution was slowly poured into the H₂SO₄-ice mixture with mechanical stirring. The temperature was not allowed to rise above 0°C. The resulting white nitrosomethylurea precipitate was filtered and stored at low temperature.

2.4.1.3 Methylation step of hypoxoside

The nitrosomethylurea prepared in Section 2.4.1.1 was used to prepare the diazomethane popularly known as a methylating agent to produce the required methylated hypoxoside derivative (DMH).

2.4.1.4 Methylation procedure

A 40% (m/v) aqueous solution of KOH (15 ml) was added to diethyl ether (80 ml) while stirring. The mixture was surrounded by an ice bath at 0°C. Nitrosomethylurea (4 g) was added to the KOH/ether solution in small portions while stirring and keeping the temperature at 0°C. When the bubbling was complete the yellow upper layer was transferred into a conical flask with KOH pellets (stored at 0°C) in order to dry the ether layer. The ether layer was transferred into a second flask with KOH pellets and was left there for 10 minutes. The hypoxoside (100 mg) was dissolved in methanol (10 ml) and allowed to cool to 0°C. The yellow ethereal solution of diazomethane was subsequently poured into a methanolic solution of hypoxoside. The mixture was stored at 15°C for up to 4 days. The TLC examination showed a single component and the product was subsequently concentrated *in vacuo*. The material was dissolved in distilled water and freeze dried to give dimethylhypoxoside (107 mg).

The DMH produced was subsequently analyzed by ¹H NMR and to further confirm the identity of DMH, a high-resolution mass spectrum (HR-MS) was run (Waters Micromass TOF spectrometer).

2.4.1.5 Results

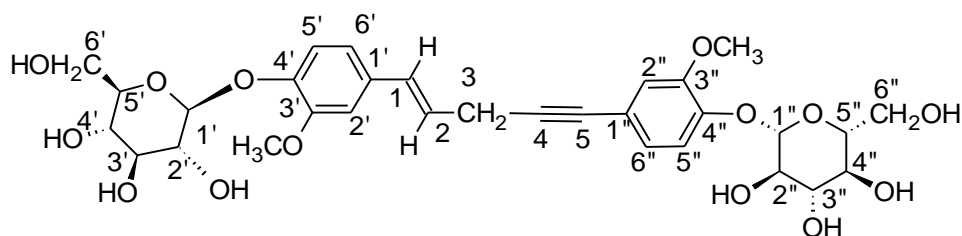


Figure 2.4: Numbering of carbons in the dimethylhypoxoside structure.

From 100 mg hypoxoside, 107 mg of DMH was obtained. The DMH derivative differs from hypoxoside only in the fact that the two free OH groups on the aromatic rings have been methylated. The proton NMR spectrum is virtually super-imposable on that of hypoxoside apart from the fact about the strong methoxy signals (2 x OMe) found at δ_{H} 3.95. This was further confirmed with the high-resolution mass spectrometry (HR-MS) results as follows:

Calculated mass for $\text{C}_{31}\text{H}_{38}\text{O}_{14}\text{Na} = 657.2159$ g/mol. (Na^+ adduct formed in mass spectrometer)

Observed mass of the derivative = 657.2153 g/mol.

2.4.2 Acetylation of hypoxoside

Acetylation of hypoxoside and acetylation of hypoxoside was carried out as described by Bettolo *et al.* (1982).

2.4.2.1 Procedure

A 1:1 mixture of pyridine and acetic anhydride (4 ml) was prepared. The hypoxoside (100 mg) was added to the mixture and allowed to stand for 72 h. Distilled water (10 ml) was added and a white precipitate formed. The product was extracted with ethyl acetate and two layers formed, which were separated. The aqueous layer was further extracted with ethyl acetate. The ethyl acetate extracts were dried over anhydrous magnesium sulfate and concentrated in the rotary evaporator at 50°C for 30 min. A small amount of pyridine was left, to which 20 ml distilled water and few drops of 32% (v/v) HCl were added. The solution was again extracted with ethyl acetate, dried over magnesium sulfate and concentrated to dryness at 50°C.

The DAH produced was subsequently analyzed by ^1H NMR and to further confirm the identity of DAH, a high-resolution mass spectrum (HR-MS) was run (Waters Micromass TOF spectrometer).

2.4.2.2 Results

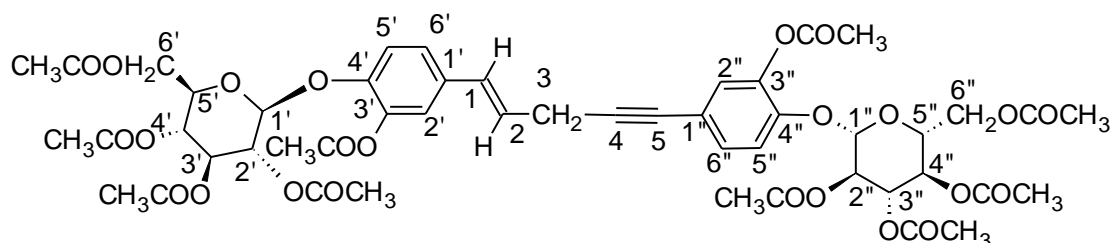


Figure 2.5: Numbering of carbons in the decaacetylhypoxoside structure.

Treatment of hypoxoside with acetic anhydride/pyridine afforded the decaacetyl derivative (109 mg of DAH from 100 mg hypoxoside). It was clear that acetylation of the eight hydroxy groups on the glucose moieties as well as the two free phenolic groups at the C-3'' and C-3' positions had taken place. The ^1H NMR spectrum is closely related to that of the HYP for most of the protons, but also revealed a strong acetyl signal at 2.1 ppm (10 x OCOCH_3) as a sharp multiplet. The final confirmation of the structure came from the high-resolution mass analysis.

Calculated mass for $\text{C}_{49}\text{H}_{54}\text{O}_{24}\text{Na} = 1049.2903$ g/mol.

Observed mass of the derivative = 1049.2903 g/mol.

The HYP, DMH and DAH derivatives prepared were now considered suitable for subsequent testing for their selective cytotoxicity on the model cancer cell lines selected for the current study (Chapter 3).

CHAPTER 3

ASSESSMENT OF ANTI-CANCER SELECTIVE CYTOTOXICITY OF THE HYPOXOSIDE AND TWO DERIVATIVES

3.1 INTRODUCTION

The main goal of chemotherapy is to adversely affect cancer cells and leave the normal cells unaffected. Assessment of the relative toxicity of drugs on normal and abnormal cells is important and this is called the assessment of “selective cytotoxicity” (Crawford *et al.*, 2003; Yang *et al.*, 2011). A problem faced is that selective cytotoxicity may depend on cell type, i.e. a drug may be selectively toxic to a certain normal cell or one kind of cancer cell and not to another (Henderson, 1969).

Cancer cells, however, go through marked molecular changes during transformation from normal to malignant cells and such changes may fortuitously bring susceptibility to specific cytotoxic drugs. Some genes have been identified to be associated with a specific cancer phenotype and identifying such molecular changes or genes may assist in drug choice (Simon *et al.*, 2000). A study of genes that contribute to the sensitivity of the cancer cells to anti-cancer drugs has been carried out in yeast cells, but how reliable and valid such a study may be questionable due to cell differences (Simon *et al.*, 2000). The availability of a unique normal and premalignant breast epithelial test cell line model, the MCF10A and MCF10A-NeoT cell lines (Section 1.4.2 and 1.4.3), in which the effect of specific cancer progression-inducing mutations, e.g. transformation with the (Val-12) mutationally activating H-*ras* oncogene may be tested, has given rise to a much more suitable system and has been used extensively for this purpose to date (Miller *et al.*, 1993).

Single-stranded DNA-drug constructs (anti-cell aptamers) that specifically bind to the surface of a certain type of cancer cell have been developed. When polymerized with a synthetic linker, “acrydite”, and conjugated with the novel drug, binding and being internalized by target cells may cause sensitive cells to die (Yang *et al.*, 2011). Such a new approach represents one possible strategy for specifically targeting a specific tumour type, known to be sensitive to a particular drug.

Malignant tumours are different to normal cells in that as they grow into large disordered masses and they are, therefore, soon deprived of oxygen supply from blood vessels.

Adaptation to growth under such conditions assists malignant tumour survival. This is promoted by a protein known as hypoxia-induced factor-1 (HIF-1) which stimulates angiogenesis, expression of glucose transporters and glycolytic enzymes and also promotes glycolysis to produce lactate. This allows cancer cell survival under anoxic conditions via the Warburg metabolic route, while blocking mitochondrial oxidative phosphorylation and production of reactive oxygen species (ROS) by mitochondria as excess ROS is damaging (Nagy, 2011). Hypoxic cells produce ROS but low levels are found to stabilize HIF-1 under anoxic conditions. HIF-1, therefore, prevents pyruvate entering the TCA cycle, and oxidative phosphorylation, through the induction of an inhibitor protein, kinase D-1 (PKD-1), facilitating survival of cancer cells (Nagy, 2011).

HIF-1 expression, therefore, changes the metabolism of cancer cells to alleviate ROS stress and, to compensate for the inefficiency of Warburg metabolism. Cancer cells also try to ensure survival by stimulating glutaminolysis to provide compensating ATP energy. As the deglycosylated derivative of hypoxoside, rooperol is described to have anti-oxidant activity (Laporta *et al.*, 2007b), treatment with hypoxoside (converted to rooperol after oral uptake), may stress the cancer cells as total neutralization of ROS may destabilize HIF-1 activity. It is thought that rooperol may, therefore, have therapeutic potential, potentially allowing malignant tumours to be selectively targeted, as they, and not normal cells, survive using the Warburg metabolic pathway. For this reason, purified *Hypoxis* extract (hypoxoside) and two derivatives were tested for their selective cytotoxicity on the normal MCF10A breast epithelial cells and the H-*ras* transfected premalignant MCF10A-NeoT derivative, as a model of a normal and premalignant breast epithelial cell, in the progression to invasive cancer. HIF-1 is also responsible for the induction of cell migration and invasion as is the mutationally activated H-*ras* (Kim, 2007).

3.2 HYPOXOSIDE AND TWO DERIVATIVES AS POTENTIAL ANTI-CANCER DRUGS

As activation of H-*ras* has been associated with upregulation of the invasive phenotype (Moon *et al.*, 2000) and HIF-1 is associated with an increased Warburg effect, and an invasive phenotype, the H-*ras* transfected MCF10A derivative seems to give rise to a suitable model on which to screen hypoxoside and its derivatives for activity for effect on breast cancers with a similar profile. Two derivatives, as well as hypoxoside, were tested as hypoxoside from other AP species has been tested on cancer cell lines before, with some success (Boukes, 2008; Boukes *et al.*, 2010; Boukes and Van de Venter, 2011) but with little

success in clinical trials (Albrecht *et al.*, 1995a; Albrecht *et al.*, 1995b; Boukes, 2008; Boukes *et al.*, 2010; Boukes and Van de Venter, 2011). The two derivatives of hypoxoside from *H. hemerocallidea* that have been synthesized for this study have never been tested previously.

A high-throughput preliminary screening method was also sought. PI methods have been specifically mentioned to be suitable for the assessment of early and late apoptosis, as well as necrosis (Zamai *et al.*, 2001). Effects of test compounds on metabolism (O'Toole *et al.*, 2003) (i.e. MTS assay) and also cell numbers were explored in the current study. As such a study constitutes a “range find” assessment for further future investigations, an exposure time that was both convenient, time efficient, and yet considered long enough to assess effects, was chosen to allow at least early effects and trends to be established (Malich *et al.*, 1997). Though some studies extend the exposure time to approximately 72 h (O'Toole *et al.*, 2003), since a rapid and preliminary cytotoxicity assessment of the prepared hypoxoside and its derivatives was required, a 24 h exposure was chosen. In order for such a test to be completed, however, the more hydrophobic derivatized compounds had to be initially solubilized in an organic solvent at a non-toxic level. So that the solvent effect could be maintained as low as possible, a dilution series of the test compounds was established to maintain solvent levels at a constantly low, non-toxic level.

3.3 EXPERIMENTAL

3.3.1 Materials and equipment

MCF10A and MCF10A-NeoT cell lines were supplied by Prof Sloane (Department of Pharmacology, Wayne State University, Detroit, MI). The chemicals used were of the highest purity available (analytical reagents). Cells were cultured in Dulbecco's modified Eagle's medium (DMEM)-Ham's F12 nutrient medium from Sigma (St. Louis, Mo, USA) containing 5% horse serum and Fungizone was purchased from Gibco (Paisly, UK), and supplemented with insulin and hydrocortisone from Sigma (St. Louis, Mo, USA), and recombinant human epidermal growth factor purchased from Upstate Biotechnology (Lake Placid, USA). Hank's balanced salt solution (HBSS), phenazine methosulfate (PMS), 3-(4,5-dimethylthiazol-2-yl)-5-(3-carboxymethoxyphenyl)-2-(4-sulfophenyl)-2H-tetrazolium (MTS), dimethyl sulfoxide (DMSO), acridine orange, propidium iodide, cyclohexamine, sodium bicarbonate and trypsin-ethylenediaminetetra-acetic acid were all purchased from Sigma Aldrich (St. Louis, Mo, USA).

The absorbance was read using a Fluostar OptimaVersamax (Labtech, Taiwan). Cell counts were performed using a Beckman Coulter Epics XL flow cytometer or improved Neubauer haemocytometer counting chamber. Dead or alive cells were distinguished using AO/PI staining. Staining was viewed using the Olympus Provis AX70 fluorescence microscope and AnalySiS v3.0 Soft Imaging System, colour view camera and software. Cells were also viewed under an Olympus inverted light microscope during culture. The sterile cell culture flasks (25 and 75 Ti), and 96 and 24 Transwell tissue culture plates, 15 and 50 ml screw top Falcon tubes, round coverslips (30 mm) and micropipettes were from Nunc (Roskilde, Denmark) or Bibby-Sterilin (Staffordshire, UK).

3.3.2 Preparation of the stock and working solutions of hypoxoside and hypoxoside derivatives

All the derivatives of hypoxoside produced were soluble in ethyl acetate but this solvent is toxic to cells. The most common solvent used in dissolving compounds for cell culture purposes, due to its low cell toxicity at low temperatures, is dimethyl sulfoxide (DMSO). This solvent is, therefore, usually used to preserve and store cells in liquid nitrogen, as it protects them against ice crystal damage at lower temperatures. It is also known to trap free radicals and is often used as a free radical scavenger. It is still poisonous at temperatures above -80°C , however, and has been reported to decrease viability of cells via the up-regulation of the apoptosis promoter BAX at 1% DMSO in media (Cao *et al.*, 2007). For this reason levels of DMSO should be kept as low as possible (and below 1%) and exposure of cells limited by dilution or washing of cells as soon as possible. This is especially true on thawing of cells stored in liquid nitrogen to which the freezing medium (20% horse or bovine serum, 10% DMSO and 70% culture medium) is added prior to freezing.

Though HYP and DMH were soluble in aqueous media, the DAH was not completely soluble in such a solvent. It was, therefore, decided to dissolve all the compounds [hypoxoside (HYP), and the two derivative dimethylhypoxoside (DMH) and decaacetylhypoxoside (DAH), synthesized from hypoxoside as described in Chapter 2], in the lowest final concentration of DMSO possible.

The three compounds were dissolved completely in pure DMSO. As the % of DMSO that the MCF10A cells can withstand without any cytotoxic effects was established to be approximately 0.001% DMSO (unpublished results), this required the development of a

complex dilution series so that all compounds were dissolved in the same final % of DMSO (i.e. the final concentration of 0.001% DMSO), to allow effects of compounds to be more directly comparable.

3.3.2.1 Reagents

Hypoxoside stock solution (300 mM)

Hypoxoside (18 mg) was dissolved 100 μ l of pure DMSO in a 100 μ l cryo-vial (making up a stock solution of 300 mM) and stored at 0°C.

Dimethylhypoxoside stock solution (300 mM)

Dimethylhypoxoside (19 mg) was solubilized in a 100 μ l cryo-vial tube, making up a final stock solution of 300 mM, and stored at 0°C.

Decaacetylhypoxoside stock solution (300 mM)

Decaacetylhypoxoside (15.4 mg) was dissolved in 50 μ l in DMSO resulting in a final stock solution of 300 mM and stored at 0°C.

3.3.2.2 Procedure

Stock and working solutions of hypoxoside and its various derivatives were prepared as illustrated below (Fig 3.1) in an effort to maintain the overall concentration of potentially toxic DMSO at a minimum, while achieving a concentration of 4.8-300 μ M of the various test drug derivatives. The dilution series from 300 μ M to 19 μ M (Figure 3.1) was made by adding 100 μ l of hypoxoside or 100 μ l for DMH or 50 μ l for DAH stock solution, and DMSO into cryo Eppendorf tube (containing 100 or 50 μ l of DMSO, respectively) to make 300 mM stock solution.

To make up the a dilution series from this stock solution, serial double dilutions (300 mM to 19 mM) in DMSO were carried out (Figure 3.1, top row), and were extended to produce a 9mM- down to a 4.8 mM concentration in a similar manner (details not shown) and used to make working solutions, or stored at 5°C. The working solutions were prepared by aliquoting 3 μ l of each stock solution and diluting it with 3000 μ l DMEM: F-12 complete media (1 in 1000 dilution) and always freshly prepared before use (Figure 3.1, second row).

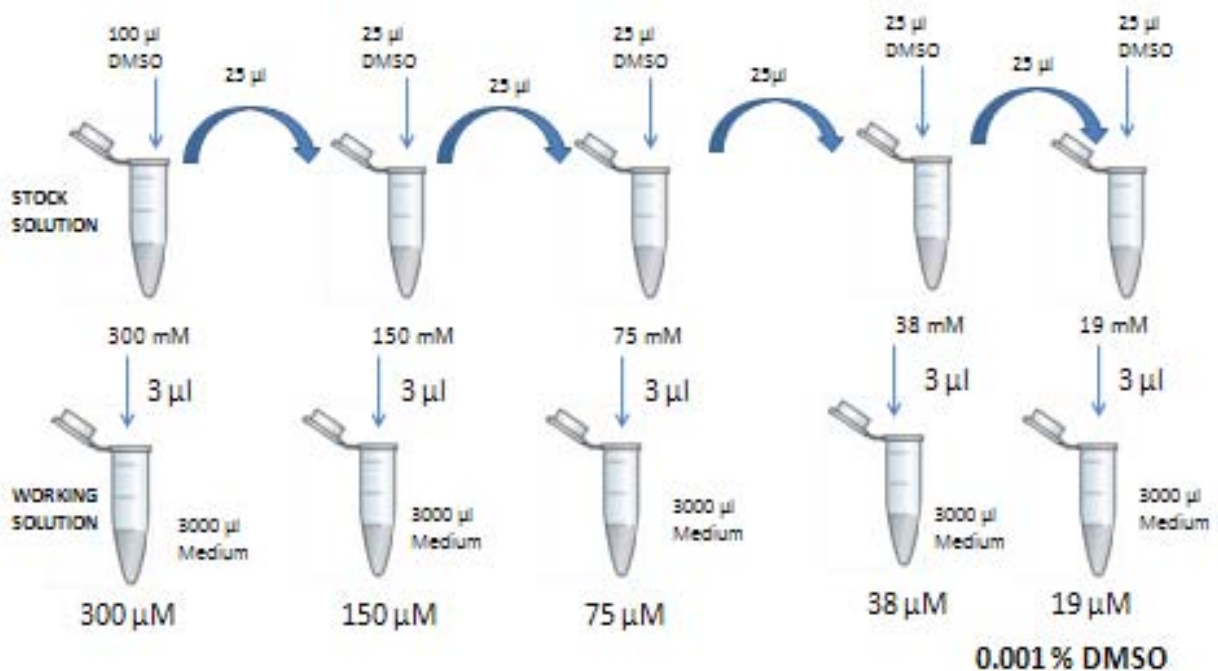


Figure 3.1: The preparation of solutions of hypoxoside and derivatives.

Stock solutions were prepared in 100 µl cryo Eppendorf tubes in 100% DMSO, as described in Section 3.2.2.2, from the highest concentration (300 mM) using a 1:1 serial dilution in DMSO to produce a 4.8 mM, lowest concentration. To produce the final working concentration the initial stock solution (top row) was diluted in a 1/1000 dilution with DMEM: F-12 complete media resulting in an equivalent µM unit concentration.

These dilutions were dispensed into multiwell plates seeded with subconfluent monolayers of MCF10A and MCF10-NeoT cells.

3.3.3. Culturing MCF10A and MCF10A-NeoT cell lines

Use of cell cultures has made preliminary testing of drugs far easier by removing ethical and statistical problems associated with animal models. Replicates and many cells may be assessed, though the behaviour of such cells may not be a highly representative of cells *in vivo*.

The first human cancer cell line to be established, over 50 years ago, was the immortal Henrietta Lacks (HeLa) cell line, isolated from a young black woman with cervical cancer. Over a thousand cell lines have been used as a tool to study the biochemistry and molecular biology of cancers. These have also assisted in understanding of cancer and normal cell behavior (Langdon, 2004).

The MCF10A was isolated from the patient with fibrocystic breast disease cells but has normal epithelial cell characteristics (Soule *et al.*, 1990; Tait *et al.*, 1990), though these cells are immortal. The MCF10A-NeoT derivative, established by transfection with the *c-Ha-ras* proto-oncogene, converted into a mutationally activated oncogene by a VAL-12 mutation (Basolo *et al.*, 1991; Calaf *et al.*, 1995) has been reported to give rise to premalignant cell characteristics (Russo *et al.*, 1991). When these two cell lines are used together, as they are from the same genetic source, they most validly, of all models, allow assessment of the test compounds on a near normal and premalignant breast cancer cell. Further derivatives harbouring further mutations, replicating the progression to a malignant phenotype are also available (Miller *et al.*, 1993). Here we limit testing to the MCF10A and MCF10A-NeoT cells, usually used as models of normal and premalignant cell lines, respectively. This is a good model because the “normal” cell line is used to establish the baseline levels of drug non-toxic to normal cells but toxic to premalignant cells of the same genetic background, i.e. selective cytotoxicity levels.

Cell culture is widely practiced worldwide and it involves allowing the cells to grow and be maintained outside the body. The cell culture techniques have been developed over many years. The cells need nutrients supplements to survive outside the body, and they are usually cultured in a basic media, complemented with some additives. The basic media usually contains amino acids, glucose, salts, vitamins and other nutrients. The additives include L-glutamine (mostly included in the basic media), antibiotics (streptomycin and penicillin usually used), growth factors, antimycotics and serum, and the pH is carefully controlled by a bicarbonate buffering system (Phelan, 1996). The choice of culturing medium is selected after experimentation and according to the experience during establishment of the cell line (Phelan, 1996).

For the MCF10A and its derivative cell culture, the DMEM: F-12 basic media was used and it was supplemented with horse serum, insulin, hydrocortisone, penicillin/streptomycin, epidermal growth factor, as illustrated in the following section.

3.2.3.1 Reagents

DMEM: Ham's F-12 incomplete medium.

Commercially pre-weighed medium and sodium hydrogen carbonate (1.2 g) were dissolved in distilled water (\approx 900 ml) using a magnetic stirrer. The pH was adjusted to 6.9 ± 0.3 range

if necessary and the solution made up to 1 L with distilled water. Sodium carbonate (1.2 g) was added to the solution and allowed to completely dissolve. The medium was filter sterilized and aliquoted into 200 ml sterile quanta and incubated at 37 °C overnight to check for contamination. The media was stored at 5 °C, but incubated at 37 °C before use.

Hank's balanced salt solution (HBSS).

Commercially pre-weighed HBSS powder was dissolved in distilled water (900 ml), stirred with a magnetic stirrer to ensure dissolution, sodium carbonate (0.35 g) was added and the pH was adjusted within a range of 7.3 ± 0.3 with HCl or NaOH if necessary. HBSS was filter sterilized into autoclaved bottles and incubated at 37°C to assess contamination, before storage at 5°C.

Horse serum.

Commercially available bottles of horse serum were incubated on a water bath at 56°C for 30 minutes to denature complement components. The horse serum was aliquoted into 10 ml volume in a 15 ml Falcon tube and stored at -20°C.

Insulin.

The prepared HBSS (16.5 ml) was used to dissolve insulin (10.2 mg) with the addition of 0.1 M NaOH (500 µl) and stored at -20°C before used.

Epidermal growth factor (EGF) (50 µg/ml)

Sterile EGF (100 µg) was aseptically dissolved in autoclaved Milli-Q water (2 ml) and stored at -20°C.

Hydrocortisone (3.33 µg/ml)

Hydrocortisone (10 mg) was dissolved in absolute ethanol (3 ml) and stored at -20°C.

DMEM: Ham's: F-12 complete medium.

The incomplete medium was supplemented with the de-complemented horse serum (10 ml), insulin (3 ml), fungizone (2 ml), EGF (80 µl) and hydrocortisone (30 µl). Then the complete medium was pre-incubated at 37°C, to check contamination and was stored at 5°C.

Fungizone (250 µg/ml)

Fungizone (5 mg) was dissolved in distilled H₂O (20 ml) and was subsequently stored at -20°C and will be defrosted to 37°C before use.

Penicillin/Streptomycin.

Pen/strep was commercially prepared and used as prescribed.

1 x Trypsin-EDTA.

Commercially available 10 x trypsin-EDTA (1 ml) was aliquoted in 15 ml Falcon tube and stored at -20°C. When about to use the aliquots were incubated at 37°C and subsequently diluted in a 1:10 dilution with prepared HBSS (9 ml).

3.2.3.2 Procedure

The cells were cultured (37°C, 5% CO₂/70% relative humidity) in a H₂O jacketed incubator (Nuair, US Autoflow) in 25 or 75 T_i culture flasks for 3-4 days. When cells reached 70% confluence they were passaged by washing with HBSS, covering the monolayer with trypsin-EDTA (± 1 ml) and incubation (37°C, 5% CO₂, approximately 15 min). To detach the cells, they were given a gentle tap with the palm of the hand and checked with an inverted light microscope every 7 minutes to assess complete detachment of cells. The complete DMEM: Ham's F-12 (10 or 20 ml of medium, respectively, depending on the capacity of the culture flask) was, subsequently added to neutralize the trypsin-EDTA. The suspension was split into two T_i (25 or 75) culture flasks (1:2).

It is important to freeze down stock cells before they become fully confluent and keep passage numbers low (to prevent genetic "drift", especially as the MCF10A cell line has a p53 mutation). Freezing the cells involves trypsinizing (1 ml) the actively growing cells allowing them to dislodge. When the cells have dislodged, an ice cold media (1 ml) consisting 20% horse serum, 10% DMSO and 70% media was introduced to the cell suspension. The cell suspension was aliquoted into 4 cryovials (0.5 ml each) and immediately transferred to a minus 80°C freezer overnight and into liquid nitrogen within the next 2-5 days.

3.3.4. MTS Assay optimization, compound exposure and data analysis

The availability of various cell lines of various types has allowed drugs for specific purposes to be tested at least in a preliminary way. Though the MTS assay is known as a cytotoxicity assay, it actually measures metabolic activity of metabolic enzymes, the assumption being that assessment of a treated and untreated cell line will allow an effect on metabolism to be assessed. Measurements are highly dependent on cell numbers. The assumption is often made that if the metabolic activity decreases, cells must be dying. We consider simultaneous assessment of cell numbers, however, to be essential, as this may not be the case.

Producing a soluble reaction product, MTS cytotoxicity assay is a superior alternative to the widely used MTT assay, in which the reaction product is water insoluble (O'Toole *et al.*, 2003). The MTS assay is usually used as a screen for viability of cells or rather their metabolic activity after treatment with compounds, though as explained above. When metabolites like glyoxylate or pyruvate undergo enzymatic oxidation to oxaloacetate, this is accompanied by reduction of NAD^+ to NADH. The NADH facilitates the reduction of the colourless MTS tetrazolium salt, to a coloured, soluble formazan product, in the presence of phenazine methosulfate (PMS). The intensity of colour generation is used as a measure of the metabolic activity of cells, and, therefore, their viability (Malich *et al.*, 1997; O'Toole *et al.*, 2003).

Initial optimization of cell numbers to be used to obtain a linear calibration response curve in the MTS assay was necessary before proceeding with the assessment of compound toxicity. This was necessary in order to establish a linear correlation between cell number and the product produced in a specific time, to ensure the production of reliable results. For most tumour cells hybridomas and fibroblast cell lines, 5000 cells/well is recommended for proliferation studies (Promega, 2009).

Subsequent to the optimization MTS assay was carried out with the various compounds at various concentrations and the data analyzed to assess possible selective effects on the premalignant, MCF10A-NeoT cell line compared to the normal MCF10A cell line. Due to the large number of data points and number of test compounds to be compared, the ANOVA test was selected. The ANOVA (analysis of variance test), unlike the students t-test, which is a test for the significance between two means (two-sample t-test) or between a mean and a hypothesized value (one-sample t-test), is a test of significant differences between multiple

means, assessed by comparing variances. This program requires that data (responses) are normally distributed (outcome is normally distributed). Like the t-test, therefore, ANOVA requires that data is checked for a normal distribution. This was, therefore, carried out. The program also requires that there is homogeneity of variance, i.e. similar variance between data points and hence the standard error of the means (SEM) was assessed (<http://www.dorak.info>). A normal distribution (Gaussian distribution) can be described by two parameters: mean (μ) and variance (σ^2), where $X \sim N(\mu, \sigma^2)$ and the distribution is symmetrical with mean, mode, and median, and equal at μ . In the special case of $\mu = 1$ and $\sigma^2 = 1$, this is known as the standard normal distribution.

A diagnostic test for the assumption of normal distribution of residuals in linear regression models is given by a plot of the normal probability of the residuals (difference between observed values of results and the corresponding fitted values predicted by regression). Each residual is plotted against its expected normal value. A plot that is nearly linear suggests normal distribution of the residuals. Such a plot was, therefore, used in the current study.

All in all analysis of variance (ANOVA) is a statistical set of models that allow for different sources of variance between the means of several groups to be measurable. General ANOVA was carried out from GenStat, giving p (or F pr) values (according to the null hypothesis) to assess overall significant differences (see Table 3.1 below). There are three different kinds of ANOVA from which to choose in the GenStat software i.e. one-way, two-way and general ANOVA. One-way ANOVA can be used, for example, to determine the metabolic activity of two different cancer cell lines, where there is only one factor that could affect the metabolic activity of the different cell lines (Bewick *et al.*, 2004). Once another factor is added, however, and for example, one of the cells were treated with three different compounds, due to the addition of another factor, there are now two factors in total (i.e. cell type and treatment compound type), and a two-way ANOVA can be used (Ekermans *et al.*, 2010). The General ANOVA is, on the other hand, a general way of determining the significance effect regardless of the number of factors involved and was, therefore, used in this case.

In analysing significant differences it is assumed that the treatment has induced no difference, i.e. that the null hypothesis is true. If the null hypothesis is true there are no differences in the mean effect between the groups or treatments in the populations and, therefore, the explained (regression) sum of squares (ESS) (or variance estimated between groups, or the sum of squares (ss) divided by the degrees of freedom (df) or ms in GenStat) divided by the residual

sum of squares (RSS) [or variance within a group or F or variance ratio is 1]. This can be better explained by the formula below (Armitage and Colton, 2005):

$$F = \frac{\text{Variance estimated between groups (ESS or MSG)}}{\text{Variance estimated within a group (RSS or MSE)}}$$

Where MSG = mean sum of squares between groups and MSE = mean sum of squares within a group.

If the null hypothesis is not true, this will give a low significance p-value (or F pr from the GenStat ANOVA table, automatically generated by the GenStat programme) i.e. $p < 0.05$. This indicates that the null hypothesis (H_0) should be rejected in favour of the alternative (H_a), as illustrated below, as there is evidence that at least one pair of means is not equal. Depending upon which group is compared, this was used to give information about such a group in relation to the other groups.

The assumptions made in the general ANOVA used are, specifically that values are randomly assigned to one of “n” groups and the distribution of the means by group are normal with equal variances. Sample sizes between groups do not have to be equal, but large differences in sample sizes by group may affect the outcome of the multiple comparisons tests. This was not so in our experimental design and hence was the program chosen.

The hypotheses for the comparison of independent groups are:

$$H_0: u_1 = u_2 \dots = u_k \text{ (means of the all groups are equal)}$$

$$H_a: u_i \neq u_j \text{ (means of the two or more groups are not equal)}$$

Where k is the number of groups, H_0 stands for the null hypothesis statement; H_a is an alternative statement to the null hypothesis and u represent means of the data points

The test performed is represented in an Analysis of Variance (ANOVA) table. This test is an F pr (F probability) test with N-1 degrees of freedom (df), where N is the total number of tests or samples. As mentioned, a low p-value or F pr value (i.e. $p < 0.05$) indicates evidence to reject the null hypothesis as there is evidence that at least one pair of means are not equal (<http://www.dorak.info>).

Results from ANOVA are subsequently displayed in a table such as Table 3.1:

Table 3.1: An example of the ANOVA table from GenStat.

Analysis of Variance for days

Source	df	ss	ms	F	P
Treatment	2	34.74	17.37	6.45	0.006
Error	22	59.26	2.69		
Total	24	94.00			

Where df = degrees of freedom, ss = sum of squares, ms = mean sum of squares, F (also referred to as vr) = variance ratio and F pr (also referred to as p value) = F probability

Formulas:

$$df = N - 1$$

$$ss = \sum_{obs} (\bar{x}_i - \bar{\bar{x}})^2$$

$$ms = \frac{ss}{df}$$

in this case

$$F = \frac{MSG}{MSE} = \frac{(\bar{x}_i - \bar{\bar{x}})^2}{(x_{ij} - \bar{x}_i)^2}$$

Where N is the number of individual groups, \bar{x} is the mean for the entire data set, \bar{x}_i is the mean group for i , x_{ij} is the value for individual 'j' in group 'i', and P value does not have any formula it is normally figured out from the F table (a simple comparison in this case).

The ANOVA analyses the combined effect of the variables. It does not allow individual variables to be compared, unless a further output tests, e.g. a plot of the mean metabolic activity against concentration compared to the average standard error of the difference of the means under the general ANOVA (see Fig 3.8) or the Duncan's multiple range test is added.

Standard error is a measure of chance variation and not actually error or mistake. Standard error (SE) of the mean is the standard deviation (SD) of the means in a sampling distribution and tells us how much variability can be expected among means. Therefore, any observed difference that is greater or less than the SE is a significant (significantly different) result.

The Duncan's multiple range test was chosen from GenStat under general ANOVA to also better reveal the relative significance (effect) of three factors assessed on individual samples (i.e. compound type, concentration and replication). The Duncan's multiple range test was chosen over the t-test because it can compare multiples of variables while the t-test only

compares two set of variables at a time. This was carried out to closely compare the effects of e.g. a specific treatment at a specific concentration on different individual test samples.

In statistics, a problem in multiple comparisons on random simultaneous experiments (Miller, 1981) or deductions made on selected observed values (Benjamini, 2010) arises via inference errors. These arise in parameters such as confidence intervals where population parameters are not considered or in hypothesis tests where the null hypothesis is incorrectly rejected. These are more likely to occur when the data set as a whole is considered. Techniques developed to prevent this, but allow significance levels for single and multiple comparisons to be directly compared, generally require a stronger level of evidence in order for individual comparisons to be considered "significant" and to compensate for the number of extrapolations made.

For hypothesis testing, a problem for performing multiple comparisons is the increase in type I error that occurs when statistical tests are repeatedly applied. An experiment-wide significance level α , for n independent comparisons also termed „family wise error rate“ (FWER), is given by

$$\alpha = 1 - (1 - \alpha_{\{\text{per comparison}\}})^n$$

is used to compensate for such error and allow a significance level to be assigned. Unless the tests are dependent, α increases as the number of comparisons increase. If the comparisons are not assumed to be independent, then:

$$\alpha \leq n \cdot \alpha_{\{\text{per comparison}\}},$$

There are different ways to assure that the FWER is at most $\bar{\alpha}$. The most reliable, free of independency and distribution assumptions, is known as the Bonferroni correction $\alpha_{\{\text{per comparison}\}} = \bar{\alpha}/n$. In the current study, the significant difference was assessed using the Duncan's test, which uses such a correction indicated by differences in assigned letters next to the metabolic activity mean values, allowing different concentration differences to be assessed. If there are no common letters between two variables that means that those variables are significantly different. The level of significance in this test is based on the number of treatments that are being tested. The level of significance is usually measured using the following formula:

$$\alpha_p = 1 - (1 - \alpha)^{p-1}$$

where α is the level of significance and p is the total number of treatments.

Methods where total α never exceeds 0.05 under any conditions provide "strong" control against Type I error, in all conditions, including a partially correct null hypothesis. Such a method is the Duncan's multiple range test, where $\alpha P \leq 0.05$ (i.e. results are significant at $p < 0.05$) (Duncan, 1955). This was chosen for the current study.

3.3.4.1 Reagents

Dulbecco's phosphate buffered saline (DPBS)

A small volume of deionized water was added at room temperature to KCl (0.2 g), NaCl (8.0 g) and KH_2PO_4 (0.4 g) and the $\text{MgCl}_2 \cdot 6\text{H}_2\text{O}$ (100 mg) and $\text{CaCl}_2 \cdot 2\text{H}_2\text{O}$ (133 mg) were added to the solution and mixed thoroughly before making up to a final volume of 1 L. The pH was adjusted to 7.35 with 1N HCl or NaOH, if necessary, and stored at 4°C.

MTS in DPBS, 2:1 (mg: ml)

MTS (30 mg) was dissolved with a magnetic stirrer in DPBS (15 ml), filter-sterilized through a 0.22 μm filter and stored in a dark container to prevent exposure to light. The solution was stored at -20°C for up to 14 days.

PMS in DPBS, 0.92: 1 (mg: ml)

Phenazime methosulfate (0.736 mg) was dissolved in DPBS (800 μl) with a magnetic stirrer. The solution was filter sterilized and poured into a dark autoclaved bottle. It was stored at -20°C for up to 14 days.

MTS/PMS (1: 20)

Phenazine methosulfate solution (750 μl) was mixed with 15 ml of MTS and the solution filter sterilized into a dark bottle and stored at -20°C for not more than three days.

3.3.4.2 Procedure

Cells were cultured in a 75 Terasaki (Ti) flask, grown to 80% confluence, trypsinized (1 ml) and neutralized with media (2 ml). The suspension was transferred into a 5 ml Falcon tube for easy pipetting and 30 μl was taken to perform the cell count. The volume of the cell suspension was adjusted so that the cell number required for the chosen range (i.e. 1000 - 10

000 cells/well) was contained in 100 μ l for inoculation into each well of a 24 well tissue culture plate. When pipetting and performing counts, the suspension was mixed continuously to allow even distribution of cells. The cell suspensions were pipetted into the various wells increasing cell numbers in triplicate and repeated three times over. Subsequently each well was made up to 100 μ l with warm media. For blanking purposes, a similar treatment series was set up, but no cells were added.

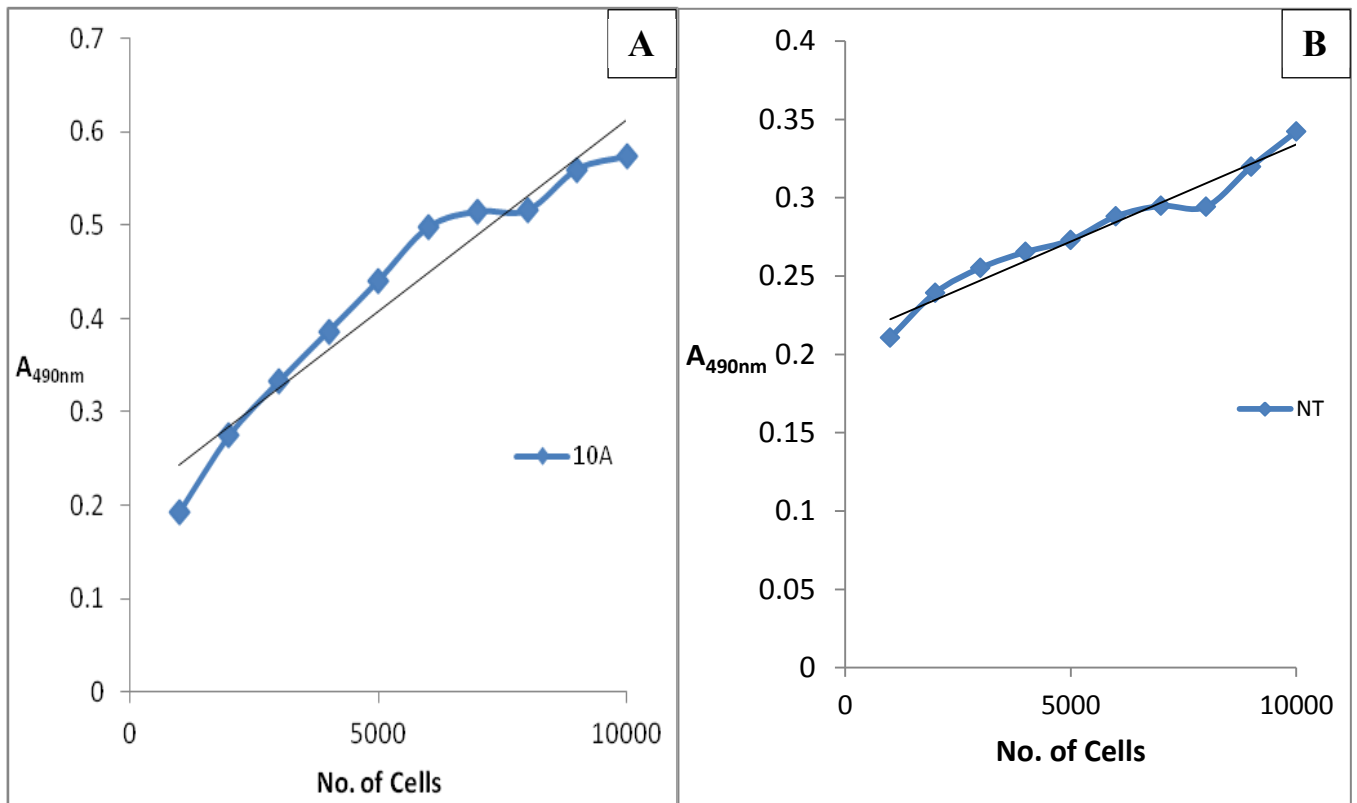


Figure 3.2: The calibration curves for MCF10A (A) and MCF10-NeoT (B) optimization for the MTS Assay.

The cells were seeded in a 96-well plate from 1000 to 10000 cells per well, and were incubated overnight. Subsequently MTS/PMS solution was introduced to the wells seeded with cells and incubated for 3 h. This was done to test the optimal reactivity of the MTS/PMS solution with the cells and that reactivity was measured spectrophotometrically at 490 nm. The graphs of MTS/PMS reactivity vs. seeded number of cells was plotted from which the linear range was identified and the points (number of cells) making up that linear range were added together and divided by the number of those points, which gave the optimal number of cells to be used for the MTS assay.

The cells were allowed to adhere overnight at 37°C, 5% CO₂. The PMS/MTS solution (20 μ l) was added and the solution incubated (37°C, 5% CO₂, 3 h). The plate was read at 490 nm with a Versamax spectrophotometer and the results exported to Excel. The data were

subsequently plotted (absorbance at 490 nm, versus number of cells seeded), a linear range identified, and the optimal seeding number determined to be 4000 cells/well for both cell lines (Figure 3.2).

After optimal numbers were established, the optimal number of cells (4000 cells/well) was seeded into a non-binding 96 well plate in triplicate for each treatment group. The cell suspension was made up to 100 μ l with warm culture media and incubated at 37°C, 5% CO₂ overnight.

After overnight exposure, medium was aspirated off and cells washed with HBSS and fresh media replaced. Cells in triplicate, were treated with 100 μ l of different concentrations (4.8, 9.5, 19, 38, 75, 150 and 300 μ M) of the three prepared hypoxoside or derivative compounds (prepared with 0.001% DMSO in culture medium). Two controls were included i.e. medium and 0.001% DMSO control, to ensure that the solvent is not responsible for cell death. For blanking purposes and to overcome any compound-chromogen disturbances, a same series of treatment was prepared, but this time with no addition of cells as before. The spaces around the 96 well plates were filled with sterile distilled water to reduce thermal gradient and media evaporation. The plate was incubated overnight at 37°C, 5% CO₂. After which the prepared PMS/MTS solution (20 μ l/well) was added and incubated (37°C, 5% CO₂, 3 h).

The plate was read at 490 nm with a Versamax spectrophotometer and the data was plotted in Excel as metabolic activity (expressed as a fraction of the metabolic activity seen in the DMSO control, to control DMSO effects) v.s. concentrations of the various compound types. The data was also assessed for a parametric or non-parametric, or normal or non-normal distribution. The standard error of the mean (SEM) of the three replicates was also calculated and plotted from Excel. To assess statistical significance/variation of the metabolic activity of the tested cell lines after treatment with the tested compounds, a general analysis of variance (ANOVA) test was carried from GenStat. This test, as mentioned Section 3.2.4.1, requires that the data is normally distributed. Therefore, residual (SEM) plots were carried out for data from both cell lines (i.e. MCF10A and MCF10A-NeoT) to check the normality of the collected data (Fig 3.3 below).

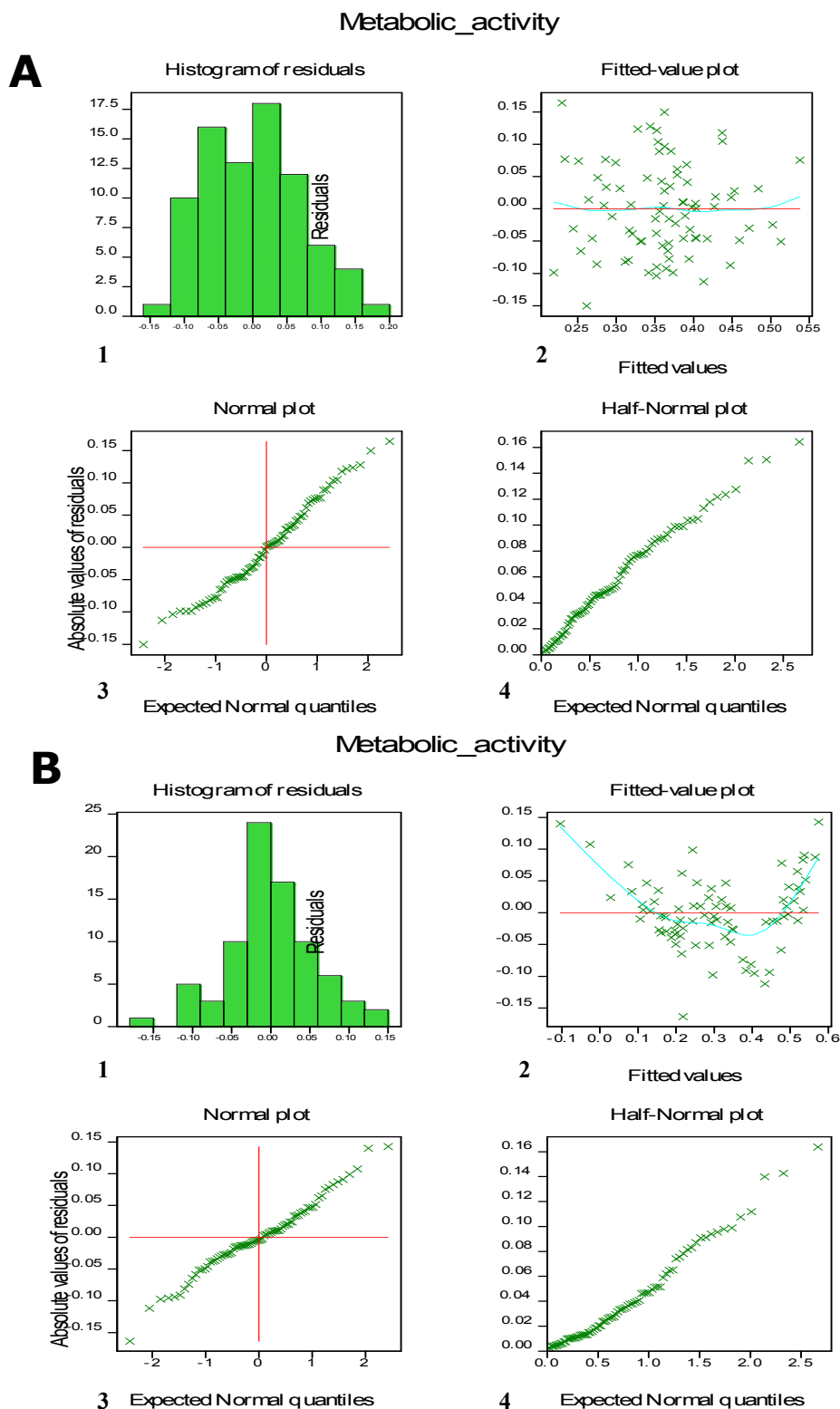


Figure 3.3: Residual plots of MCF10A (A) and MCF10A-NeoT (B) metabolic activity collected data after treatment with the three hypoxoside compounds.

Plots 1-4: a histogram of residual plotted as number of tests vs. error distribution, and is roughly bell shaped (i.e. normally distributed); a fitted plot, plotting residuals vs. fitted values (i.e. two middle lines should be aligned and points widely spread for a normal distribution); plots residuals against expected normal quantiles (should be a straight line for a normal distribution); resembles plot 3 except plots absolute residual values (a straight line for normal distribution).

Looking at the residual plots for both cell line it was concluded that the collected metabolic activity data was normally distributed and the general ANOVA could be performed as its requirements were met. Additional output tests (i.e. post hoc tests) were also performed to better appreciate the MTS assay results (i.e. mean plot graphs and the Duncan's multiple range tests for both cell lines).

3.2.5. Acridine orange/propidium iodide (PI) fluorescence microscopic assay

After assessment of the effect of test compounds on metabolic activity, assessment of how many cells were actually dead or dying was required. There are many methods of cell death assessment as described in Chapter 1. Some have advantages over others. Fluorescence microscopy is one of the widely known methods used for cellular studies and cell viability assessment. Cell counts and fixed cell assays using fluorescent staining allow quantitative measurement of such effects (Swedlow, 2003).

Fluorescence emissions occur when certain molecules are exposed to light of mixed or a specific wavelength, e.g. ultraviolet light, and emit light of a different colour and longer spectral wavelength. Fluorochromes, therefore, emit light of a specific longer wavelength (emission wavelength) when excited with light of a specific shorter wavelength (excitation wavelength) (Nikon, 2000-2012). Fluorescence microscopy, therefore, allows visualization of introduced or natural fluorescence light emitting fluorochromes within the sample prepared for imaging.

This form of microscopy may involve a simple staining procedure and is relatively rapid and inexpensive providing fluorescence microscopes are available (Swedlow, 2003). It also allows the user to view the internal details of a cell and is known for its facilitation of the detection of small amounts of the test material, with very high precision and sensitivity. The dependence on excitation and emission at a specific wavelength may be used to advantage, as different fluorophores of distinct excitation and emission wavelengths may be simultaneously viewed, as long they can be distinguished separately (Herman, 1998).

The principle behind fluorescence microscopy is that when white light strikes the first exciter filter, the optimal filter, chosen for the excitation of a specific fluorophore, must allow only the wavelength of light required to excite the chosen fluorophore to pass through the filter. The next component met, is the dichroic mirror. This must reflect the required excitation wavelength down onto the specimen labelled with a specific fluorophore, while allowing

unwanted inappropriate wavelengths to pass through (Figure 3.4). Generally such dichroic mirrors are named or labelled according to the wavelength at which light below that specific wavelength is reflected, i.e. wavelength just above the required excitation wavelength required to excite a chosen fluorophore. Wavelengths at or below the excitation wavelength required are reflected and allowed to strike the specimen (Figure 3.4).

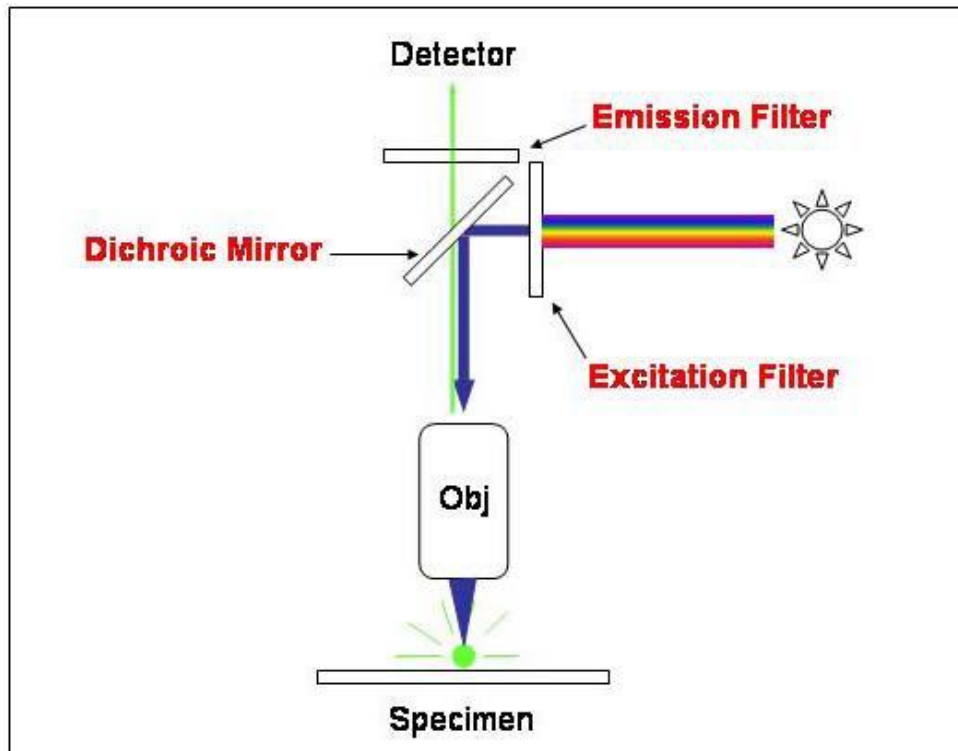


Figure 3.4: Epifluorescence microscopy set up.

The basic principle of fluorescence microscopy shown here is to allow excitation light through the exciter filter and not allow the wavelengths of light greater than that required to excite the selected fluorophore. The dichroic mirror reflects the light of wavelengths lower than the excitation wavelength of the selected fluorophore, to excite the specimen and the emitted light is usually greater than the excitation wavelength and will be allowed to pass through the dichroic mirror and through the emission filter which will only allow lower wavelengths of light than those emitted (Bradbury and Evennett, 1996).

When the specimen with the fluorophore is excited with the correct excitation wavelength, it emits light of a longer wavelength than the excitation wavelength, and reflects back up towards the optical tube and will pass through the dichroic mirror chosen, to the eye piece or detector or camera (Figure 3.4). Before reaching the eye-piece or detector, or camera, the emitted light will further pass through the emission filter, which only passes wavelengths at or greater than the emission wavelength of the specific fluorophore used (Figure 3.4),

eliminating unwanted stray, nonspecific fluorescence. This emission subsequently passes up to the objective or detector camera (Lichtman and Conchello, 2005).

Commonly used fluorochromes for imaging live and dying cells and cell nuclei under microscopy are AO, PI and HO, as discussed in Chapter 1. AO stains the live and dead cells green, HO stains both live and apoptotic cells blue and PI stains the late apoptotic and necrotic cells red. These dyes are usually combined, AO + PI, AO + HO and HO and PI in flow cytometry and for the microscopy. In the current study AO and PI were chosen as this combination is known to label viable (AO only) and late apoptotic (AO and PI) (Darizynkiewicz *et al.*, 1992; Foglieni *et al.*, 2001; Zamai *et al.*, 2001). Acridine orange and PI fluorochromes have excitation wavelengths at 502 and 536 nm, respectively, and emission wavelengths at 526 and 617 nm, respectively, so were considered easily distinguishable as there will be no emission spectrum overlap between the two fluorochromes and were, therefore, chosen.

In the current study, an Olympus Provis AX70 fluorescence microscope was used, and a U-MNIB cube for AO with an excitation filter of 470-490 nm and emission barrier filter of 515 nm. For PI the U-MWIG cube with the excitation filter of 520-550 nm and the emission filter of 580 nm. The dichroic mirror in these cubes for AO was 505 nm i.e. this reflects light wavelengths lower than 505 nm down onto the specimen and allows greater wavelengths to pass through (Figure 3.4). For PI the dichroic mirrors chosen reflects light wavelengths lower than 565 nm and allows wavelengths greater than 565 nm, through the barrier and camera filter (Herman, 1998; Olympus, 2012).

3.3.5.1 Reagents

Acridine orange (10 µg/ml).

A stock solution of 1 mg/ml was prepared by dissolving 1 mg of the AO powder in 1 ml of warm sterile HBSS. A 1:100 dilution of the stock solution was made to produce a working concentration of 10 µg/ml and the solution was stored at -20°C.

Propidium iodide (PI) (10 µg/ml).

A stock solution of 1 mg/ml was made up by dissolving 1 mg of PI in 1 ml warm HBSS. The solution was then diluted in a 1:100 dilution factor to make it up to the concentration of the working solution of 10 µg/ml, the solution was stored at -20°C.

Acridine orange/propidium iodide (1:1) (10 µg/ml).

The already prepared solutions of AO and PI were mixed in a 1:1 ratio before use.

Moviol (10% Moviol, 23 M glycerol in 0.1 M Tris, pH 8.5)

Moviol (2.4 g) was added to 0.2 M Tris (12 ml) covered with foil and stirred overnight, in a closed container. Glycerol (6 g) and dH₂O (6 ml) were added to the prepared solution and stirred overnight. The solution was then centrifuged (500 x g, 15 min), aliquoted and stored at -20°C.

3.3.5.2 Procedure

Round cover slips (3 mm) were placed into 24 well plates and the middle of the cover slips pretreated with DMEM: Ham's F-12 complete media for ≈2 h to condition the surface of the cover slips, so as to assist cells to adhere. A consistent number of cells (i.e. 10 000 cells/well) were seeded and a suspension media made up to a final volume of 200 µl after the cells were allowed to adhere for ≈ 2 h and allowed to grow overnight. The next day the media with non-adherent cells was aspirated off and cells gently washed with warm sterile HBSS. The media containing the hypoxoside, dimethylhypoxoside and decaacetylhypoxoside compounds (200 µl) at different concentrations (4.8, 19, 75 and 300 µM) was carefully added to the cells and three controls were set out, i.e. positive control with cyclohexamine (25 µg/ml, 3 h, 37°C, 5% CO₂), negative control with media only and 0.001% DMSO in media to check the effect of DMSO on cell death, as the compounds were also prepared in 0.001% DMSO. The plates were incubated overnight (37°C, 5% CO₂), the media was aspirated off and 20 µl of AO/PI (1:1, 10 µg/ml) stain was added in each well for 5 min (using a modification of the method of Zamai *et al.* (2001) previously optimized for the current cell line in our laboratory, data not published yet). The cover slips with cells were inverted onto a rectangular glass slide pretreated with Moviol mounting medium (2 µl) and cells were visualized and images captured with an Olympus Provis AX70 fluorescence microscope (with the UMIB and UMWIG filter cube for AO or PI) and images were subsequently annotated and processed using AnalySiS v.3.0 soft imaging system software and compared for PI/AO staining. Results were subsequently analyzed visually and amount of fluoresce assigned from +++ to – staining grading and recorded in a table.

3.3.6. Propidium iodide (PI) flow cytometric assay

A flow cytometer is one of the most commonly used instruments in the tests for detection of apoptosis, giving information such as the ratio of apoptotic to live cells, identifying nuclear changes resulting from DNA cleavage, assessing viability using dyes and probes which map membrane dynamics and integrity (Martinez *et al.*, 2010). Flow cytometry is a powerful technique used for multiple applications, from immunophenotyping to ploidy analysis, to cell counting and green fluorescence protein (GFP) expression analysis and detection of apoptosis (Luttman *et al.*, 2006).

A flow cytometer performs such analyzes by passing thousands of cells per second through the beam of a laser, using a flowing sheath of carrier fluid. The light that emerges as cells pass through allows data to be gathered and analyzed statistically by flow cytometry software to report cellular characteristics such as size, complexity, phenotype and health (Ormerod, 1994).

The principle behind the flow cytometer detection of fluorescently labeled cells is similar to that of the fluorescence microscope except the light path differs slightly (Figure 3.4 and 3.5). In the flow cytometer, as a cell passes through the laser beam it will refract or scatter light at all angles. The forward scatter (FS) or low angled light scatter is defined as that light scattered in the forward direction as laser lights strikes the cells and is used to analyse unlabeled cells. The magnitude of the FS signal is roughly proportional to the size of the cell and is detected by the forward scatter detector (Shapiro, 2003). The bandpass filter is always placed in front of the FS detector to prevent any intense laser light from reaching the detector. As the cell passes the band pass filter the signal generated is collected by the detector and translated into the voltage pulse. Small cells result in a small signal for the FS and large cells result in a large FS signal, therefore, the magnitude of voltage pulse recorded is proportional to cell size. If one plots a 1D-histogram for this data, the small cells will appear towards the left and the large cells towards the right. This kind of data represents only the size distribution within a population (Luttman *et al.*, 2006).

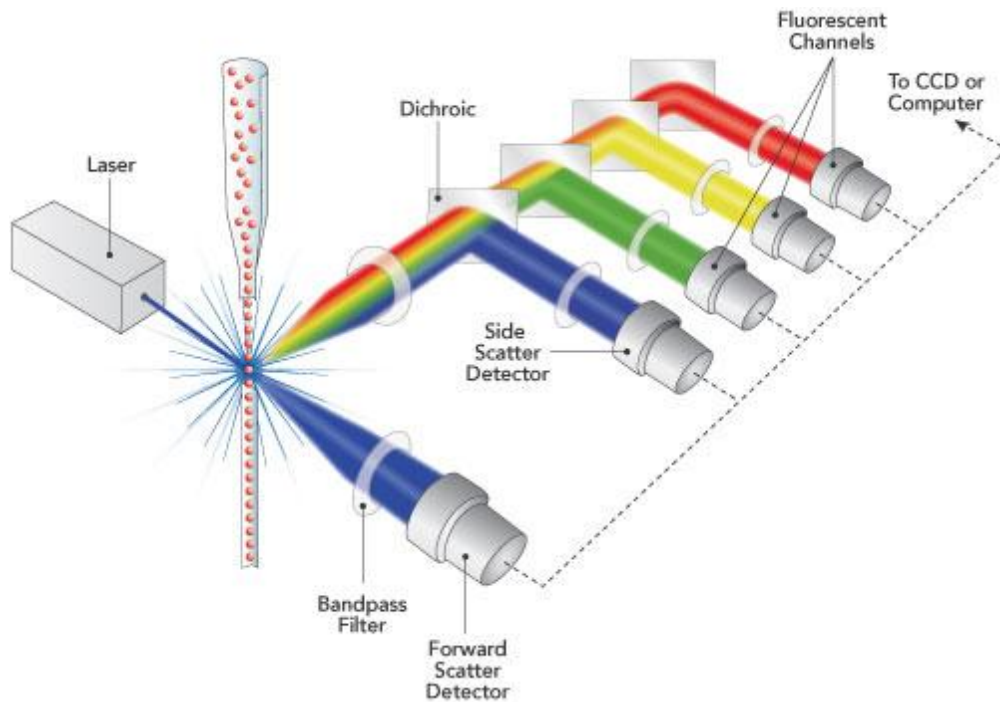


Figure 3.5: The layout of components in a flow cytometer.

The flow cytometer is divided into 5 systems, which includes the fluidic system guiding the sample to the interrogation point and taking away the waste, lasers as light sources for scatter and fluorescence assessments, the detectors which receive light and the electronics and computer system which convert the signals from the detectors into data and perform the necessary components necessary for flow cytometry analysis (adapted from Semrock, www.semrock.com/flow-cytometry.aspx).

The laser beam signal that is refracted by the cells, passing at higher angles, is called side scatter (SS) signal. The SS signal is generated by the granularity and structural complexity inside the cells. This light is focused through a lens system and collected by separate detectors usually situated at 90° from the laser path. The signals collected by the SS detector can be plotted in a 1D histogram, which then gives the complexity i.e. may reveal differences internal complexity of normal and damaged cell populations when represented in a scatter plot (Figure 3.6B, R1, R2 and R3).

What appears to be one stained population in a 1D-plot in a SS histogram (Figure 3.6A) is, in reality, multiple of populations that can be clearly seen in a 2D plot (Figure 3.6B), giving more information. The peaks from the 1D-plot will correlate with a population of dots in the FS and SS mode scatter plot (Ormerod, 1994).

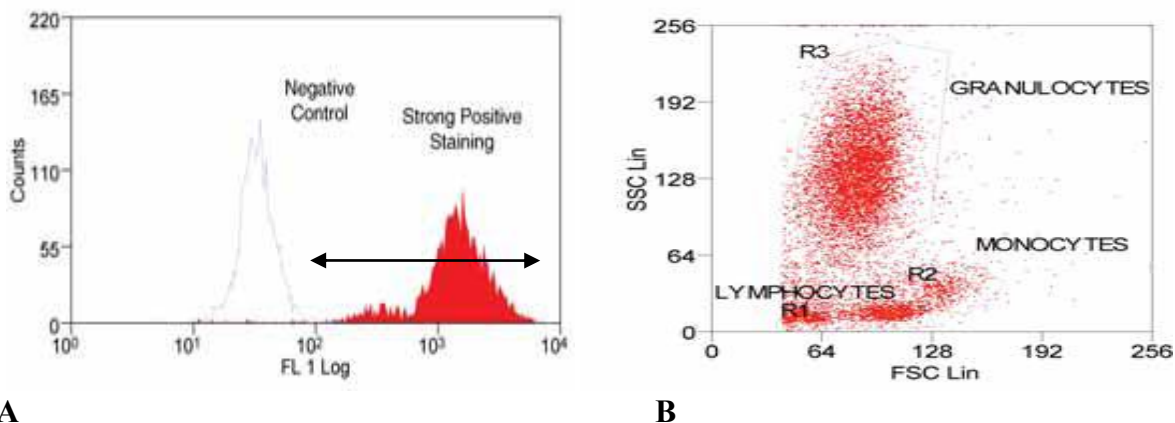


Figure 3.6: Multi-parameter flow cytometry analysis of blood cell populations.

The 2D scatter plot (B) showing granularity and the size of the analyzed cells, and reveals 3 populations, R1, R2 and R3. The 1D-histogram plot (A), shows only 2 stained populations of cells, the first region referred to as a negative control region (no staining region) and, thereafter, there is a weakly-and strongly fluorescently (FL) stained region. The 2D plot is gated to show only the stained populations (double headed arrow) which appear only to show only 2 populations in the 1D histogram.

An essential feature in flow cytometry, called “gating”, allows the selective visualization of particles of interest (Figure 3.6), with simultaneous “removal” of unwanted particles, like unwanted debris from the plot (Barrett *et al.*, 2011). In the current study, the separation of live and dead cells, after treatment with the prepared test compounds, was of interest. The PI positive (dead cells) were gated for a region, in a 1D histogram plot, and a % of events (PI stained cells) in that region was acquired for all test compounds at different concentrations.

Another parameter that gives information on the cell function and characteristics is the fluorescence, which as discussed in Section 3.2.5.1, is used to describe the excitation of a fluorophore to higher energy levels, followed by its return to the ground state with the emission of light (Shapiro, 2003). The energy of the emitted light is dependent on the energy with which the fluorophore is excited and the specific wavelength and consequently the specific colour of the beam of exciting light, the parameter that determines the specificity of the flow cytometric assays (Ormerod, 1994).

The common way of studying cellular characteristics through flow cytometry involves the use of added fluorophores. When the fluorophore is added to the cell sample it binds to the specific molecule on the cell surface or inside the cell either via histochemical affinity or

bound by an antibody. When a laser beam strikes the fluorophore on the cells, a fluorescence signal is emitted and it travels the same path as the SS (Figure 3.6B). As the light travels along this path it is directed through a series of filters and mirrors so that particular wavelength ranges are delivered to appropriate detectors in a manner similar to that desired for fluorescence microscopy (Section 3.2.5.1). This is achieved using a series of filters, i.e. excitation, dichroic mirror and emission or barrier filter, for fluorophores with increasingly lower wavelength detection (Luttman *et al.*, 2006) (Figure 3.5).

In a population of labelled cells some will be brighter than the others. As each cell passes through a laser, a fluorescence signal is generated and fluorescence light is then directed to the appropriate detector which is translated into a voltage pulse proportional to the amount of fluorescence emitted and all the voltage pulses are recorded and can be presented graphically in a histogram plot (Figure 3.6) (Shapiro, 2003). A two fluorophore experiment can be performed, but the two fluorophores must have emission peaks far enough apart, so that separated emission signals can be collected.

For the current study the Beckman Coulter Epics XL Flow Cytometer was used. This has the capability to analyse up to 4 colours of immunofluorescence from a single air-cooled laser. This machine uses a detector range of 300 nm - 800 nm, with a maximum analysis rate of >3300 cells/sec, and a minimum cell size of <0.5 μm . The fluorophore used in the current study was propidium iodide which is popular for the detection of cell death and is cheap. The method chosen was a previously optimized method of Zamai *et al.* (2001). The results were subsequently checked using the trypan blue method of detecting cell death and total counts, allowing estimate of % cell death to be calculated and increases or decreases in cell proliferation to be monitored.

3.3.6.1 Reagents

Propidium iodide (50 $\mu\text{g/ml}$)

A stock solution (1 mg/ml) was prepared by allowing 1 mg of PI to dissolve in 1 ml of warm sterile HBSS. The solution was diluted 1:20 in HBSS to give 50 $\mu\text{g/ml}$ working concentration and the solution was stored at -20°C .

3.3.6.2 Procedure

A consistent number (i.e. $\approx 200\,000$ cells/flask) of cells was seeded into 25 Ti flasks and incubated (37°C , 5% CO_2) overnight to allow cells to adhere and grow. The following day the media with non-adherent cells was removed and the cells washed gently with HBSS. The media containing the three test compounds at different concentrations (150 and 300 μM for HYP and 4.8, 19, 75 and 300 μM for DMH and DAH) (2 ml/flask/concentration) was added to the cells. Three controls were set out as in AO/PI staining protocol. The cells were incubated or treated overnight with the test compounds. The flask contents were decanted into respective 15 ml Falcon tubes with media. The adhered cells left in the flasks were trypsinized with 1 ml trypsin-EDTA and neutralized with the decanted media containing dead and floating cells. The cells were gently mixed and 500 μl withdrawn into a 5 ml culture tube for flow cytometric analysis and 15 μl placed into a 1.5 ml Eppendorf tube for the addition of trypan blue and counting in a hemocytometer chamber.

Propidium iodide (10 μl) was added into the culture tube for flow cytometric analysis, vortexed gently and incubated at room temperature in a dark area for 15 minutes. Cell viability was subsequently analyzed, within an hour, using a flow cytometer.

The flow analysis was carried out using an Epics XL flow cytometer (Beckman Coulter) equipped with a 488 nm Argon laser. The FSC and SSC fluorescence intensities were collected using a log scale, while the PI intensity (red dye) was collected with a linear scale. The emission filter used was 620 nm for PI. The medium flow rate used to analyze the tested cells was sufficient to ensure a minimum of 5000 counts per tested sample. Assessment of cytotoxicity was carried in triplicates and twice over, i.e. $n=2$.

3.3.7. Trypan blue hemocytometric assay

Use of the Improved Neubauer hemocytometer chamber is common and widely used for counting cells. This is because it provides a cheap and simple method for counting cells. For detection of cell death this method of counting cells is usually coupled with staining of cells with trypan blue dye, a dye that stains the nucleus of cells with damaged membranes, i.e. dead cells or late apoptotic or necrotic cells (van Dooren *et al.*, 2004). The cell membrane is naturally intact, but when the cell dies it is disrupted and allows bigger molecules to go through and trypan blue is one of those molecules (Strober, 2001).

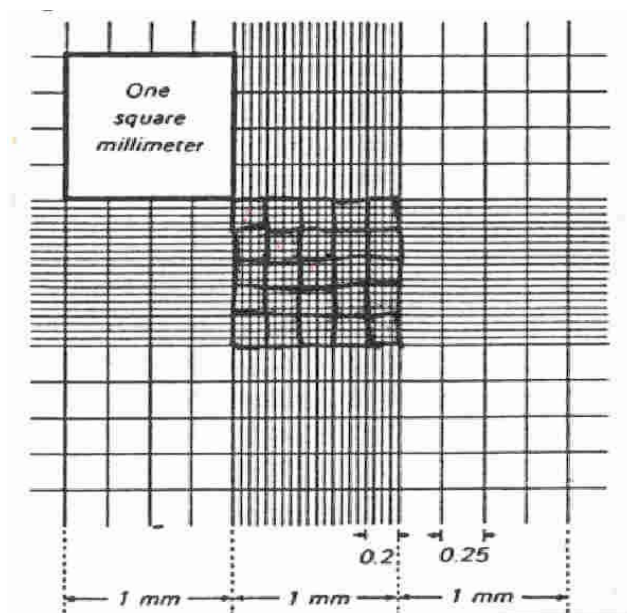


Figure 3.7: Improved Neubauer Hemocytometer counting chamber grid lines.

The grid lines of the large squares of the hemocytometer define one millimeter and the depth of the chamber is 0.1 mm allowing counts of cells per ml to be calculated (Dacie and Lewis, 1970).

A hemocytometer is a glass chamber, engraved with calibrated squares and with raised sides that will hold a coverslip at 0.1 mm above the chamber floor. The total volume of one large square is 0.0001 ml. The hemocytometer is filled with the cell suspension, containing uniformly dispersed cells for counting, by placing the pipette with the cell suspension at the edge of the hemocytometer and expelling the fluid slowly, so that the suspension is drawn uniformly into the chamber by capillary action.

There are two methods of counting cells from the hemocytometer chamber. The first one involves counting cells from the four outer big squares and calculating cell number using the equation and is used when cells are large and not too numerous:

$$\text{cells per ml} = \text{total cells counted} \times 2500 \times \text{dilution factor.}$$

The second method involves counting five squares in the middle block and calculating the cell number using the equation:

$$\text{Cells concentration per ml} = \text{total cells counted} \times 50000 \times \text{dilution factor.}$$

The choice of method depends on the cell concentration and the accuracy depends on the number of squares counted cells. This method was not anticipated to be as accurate as flow cytometry but it was required to give an idea of the effect of tested compounds on cell number and approximate number of dead cells in such total cell populations.

3.3.7.1 Reagents

Trypan blue (0.4%)

Trypan blue (40 mg) was dissolved in 10 ml HBSS, and was freshly prepared for use.

3.3.7.2 Procedure

The cells discussed in Section 3.2.6.3 were mixed with the 0.4% Trypan blue in a 1:1 ratio. The cells were mixed with a micropipette to prevent clumping and 30 μ l was introduced into both chambers of a prepared hemocytometer and placed on an inverted light microscope and the cells in four large squares were counted in both chambers, counting both live and dead cells (i.e. 8 x 1 cm grid squares), twice in duplicate. The following equation was used to calculate the total number of cells (averaged over 8 grid squares):

$$\begin{aligned} \text{Total number of cells} &= \frac{\text{total number of counted cells}}{8} \times 10\,000 \\ &= \text{cells/ml} \end{aligned}$$

The average total number of cells, both dead (blue stained) and live (not stained), was counted and averaged over at least two replicate repeat experiments and plotted as an additive/stacked column graph against the different concentrations of the different compounds, to reflect the effect of treatment and concentration on the cell numbers of normal and abnormal cell lines. A second graph was plotted as an un-stacked column plot, plotting the % cell death within each treatment group, corrected for (minus) the cell death induced by DMSO control, as a total cell number.

3.4 RESULTS AND DISCUSSION

3.4.1 The effect of hypoxoside, dimethylhypoxoside and decaacetylhypoxoside effect on the metabolic activity of MCF-10A and MCF-10A-NeoT cell lines.

All the hypoxoside test compounds (i.e. HYP, DMH and DAH) share a common core structure but differ in the methoxy substituents on the benzene rings and on the glucose moieties. The MTS assay was carried out to provide initial indications of the effect of the hypoxoside and its derivatives on the normal human epithelial cell line (MCF-10A) and premalignant human epithelial cell line (MCF-10A-NeoT).

The data from the MTS assay, for both the MCF10A and MCF10A-NeoT cell lines, was found to be normally distributed, according to the residual plots of normality from GenStat (Figure 3.3) and the SEMs calculated and recorded as error bars in Figure 3.8 seem to show no major variance within replicates. Since this was the case, and the data showed a normal distribution, the parametric test known as a general analysis of variance (ANOVA) could be used to explore any significance difference in results, both in terms of the overall treatment (compound type) as well as the overall effect of concentration within and between compound types. This was assessed by comparing the averaged effect using the mean plot of the mean metabolic activity and significant differences of all the factors (compound type, concentration and replication) using the most informative Duncan's analysis.

Inspection of the MTS results (Figure 3.8A, expressed as a fraction of the DMSO control) seems to indicate that the DAH has the most significant effect on the MCF10A cells with the DMH partially stimulating metabolic activity, especially at 38 μ M and depressing activity at 300 μ M. The DAH seems to depress activity almost to the same degree from a concentration of 9.5 μ M, but not significantly, and the HYP seems to have little effect over all concentrations. All compounds seem well tolerated, though effects of various compounds do seem to differ slightly. At this stage how significant these results and differences were, was not yet calculated.

Similar trends seem evident in the MCF10A-NeoT cells (Figure 3.8B) with HYP and DMH seemingly stimulating cell metabolism at concentrations 4.8-38 μ M, but the DAH apparently significantly depressed activity, especially from a concentration of 19-300 μ M (Figure 3.8B). Once again the significances of these differences between compound groups and different compounds concentrations only became evident after performing ANOVA analysis.

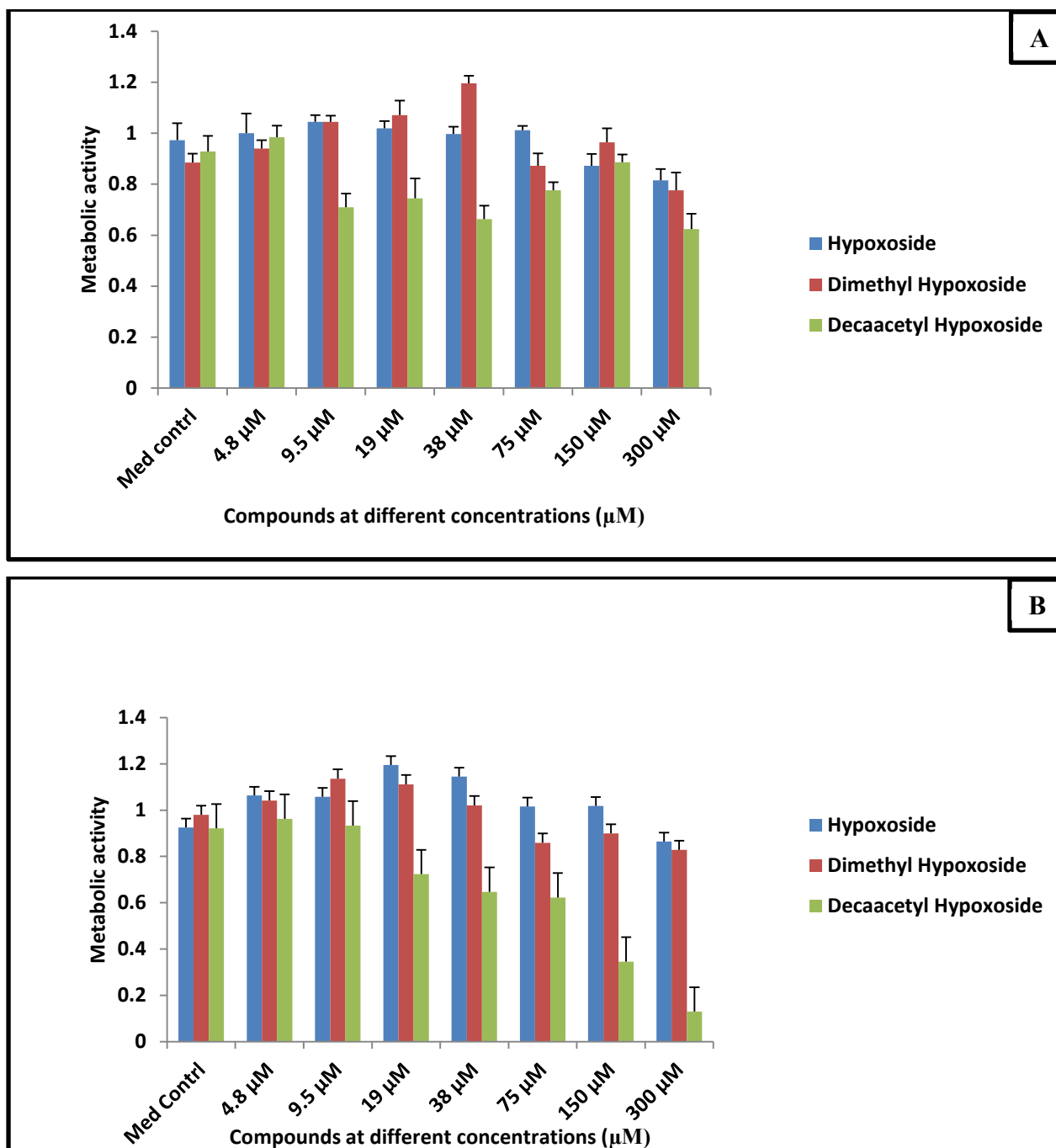


Figure 3. 8: MTS assay metabolic activity results of MCF10A and MCF10A-NeoT treated with three hypoxoside compounds.

The cells were seeded and allowed to adhere overnight, treated with three different compounds (i.e. HYP, DMH and DAH) at different working concentrations (i.e. 4.8-300 μM) in triplicate, and allowed to stand overnight. The tetrazolium salt, MTS was introduced and conversion to soluble formazan (for 3 h) and was analyzed spectrophotometrically at 490 nm on tests repeated 3 times and averaged. The effect of hypoxoside derivatives on the metabolic activity of the MCF10A cell line (A) and on the MCF10A-NeoT cell line (B), expressed as a fraction of the DMSO control to ensure effects were due to drugs and not diluting solvent were plotted using a bar graph and standard error of the mean (error bars, SEM), for n=3 and significance assessed using the ANOVA. **NOTE:** As each batch of samples were run at different times and DMSO and media controls varied slightly, the same symbol as the compound type is used for the controls.

Table 3.2: Analysis of variance (ANOVA) table from GenStat.

Variate: Metabolic activity

MCF10As

Source of variation	df	s.s.	m.s.	v.r.	F pr.
Replication stratum	2	0.017518	0.008759	1.18	
Replication.*Units* stratum					
Compound_type	2	0.182297	0.091149	12.24	<.001
Concentration	8	0.063772	0.007971	1.07	0.398
Compound_type.Concentration	16	0.090376	0.005649	0.76	0.722
Residual	52	0.387319	0.007448		
Total	80	0.741282			

MCF10A-NeoTs

Source of variation	df	s.s.	m.s.	v.r.	F pr.
Replication stratum	2	1.418709	0.709355	152.18	
Replication.*Units* stratum					
Compound_type	2	0.149490	0.074745	16.04	<.001
Concentration	8	0.190566	0.023821	5.11	<.001
Compound_type.Concentration	16	0.133313	0.008332	1.79	0.059
Residual	52	0.242383	0.004661		
Total	80	2.134462			

The general ANOVA analysis of the MTS results (Table 3.2, compound type), confirmed that compound type (i.e. HYP, DMH and DAH) had an overall significantly different effect on the metabolic activity of the MCF10A cells, as the p value (F pr) calculated was <0.001 (where "p<0.05" is the probability of this being so by chance at less than 5 percent). By visual inspection of graphical data in Figure 3.8A, this would seem to be true. It would seem that the DAH decreased the metabolic activity of the MCF10A cells relative to the control (Figure 3.8A), with HYP and finally DMH having lesser effects (Figure 3.8A). A similar effect is seen in the MCF10A-NeoT cell line (Figure 3.8 B) for the DAH and it appeared to be concentration-dependent for the range tested. Here the general ANOVA test confirmed visual inspection interpretation of graphical data by delivering an overall significant p value of p<0.001 for compound type (Table 3.2, compound type) supporting the rejection of the hypothesis that compound type has no significant effect.

Though it would seem from Fig. 3.8B, by visual inspection, that the DAH decreases the metabolic activity of the MCF10A-NeoT cells most, followed by the HYP and finally DMH (Figure 3.8B) i.e. this gave a similar trend for compound type, as seen in the MCF10A cells (Figure 3.8A), to assess such an effect on individual test concentrations within the group, relative to each other the Duncan's and mean plot (Figure 3.9) needed to be carried out. This was carried out after the general assessment on the effect of concentration on the test groups.

The average effect of changing concentration of the different compounds, on each individual cell line, explored using the ANOVA, showed no concentration-dependent significantly different effect on the metabolic activity of the MCF10A cells (giving a p value of $p = 0.398$, i.e. an effect which would seem less significant, according to the p value, than the effect induced by the compound type, which gave a p value of $p < 0.001$) (Table 3.2, concentration). The general effect of concentration on the MCF10A-NeoT cells appears significant ($p < 0.001$ compared to $p = 0.398$ for MCF10A cells), confirming what is visually seen (Figure 3.8A vs. B). Though the DAH did give a depression of activity, this depression on the metabolic activity of the MCF10A cells was similar, though more slight and less concentration-dependent, over a large range of concentrations (Figure 3.8A), unlike the increasing effect with increasing concentration on the MCF10A-NeoT cells (Figure 3.8B).

By visual inspection, the concentration producing the greatest effect on the MCF10A-NeoT cell line seems to be the 300 μM concentration of the DAH compound, i.e. this concentration significantly decreased the metabolic activity of the MCF10A-NeoT cell line compared to all concentrations of other compounds (Figure 3.8B). The ANOVA does not distinguish such an effect specifically as individual compound concentrations are analyzed within each compound type (Table 3.2, concentration) and not individual concentrations in each group in relation to each other individually. Therefore, a statistical package comparing individual concentrations within the group, e.g. the Duncan's comparison, was still required at this stage.

The results from the general ANOVA for the combined effect of concentration and the compound type for both MCF10A and MCF10A-NeoT (Table 3.2, compound type.concentration) were found to be $p = 0.722$ and $p = 0.0593$ (Figure 3.8A and B, respectively). As " $p < 0.05$ " this means that there was no significantly different effect on the MCF10A but an almost significant effect on the MCF10A-NeoT cell line using the 5% level

of discrimination i.e. the concentrations change and compound type produced similar trends in the MCF10A and MCF10A-NeoT cells metabolic activity, though this effect only just missed being significant overall by 0.093 (just greater than 0.05) for the MCF10A-NeoT cell line (Figure 3.8B). This is possibly because, when results of treatment type and concentration are considered as a group for the MCF10A and MCF10A-NeoT, differences in one treatment relative to the other treatment on each cell type may be obscured when being considered as part of the group.

Plots of the means of the metabolic activity against concentration of HYP, DMH and DAH were, therefore, plotted using GenStat, under general ANOVA, as a further output. This was done to facilitate the assessment of the effect of both treatment type and concentration on individual samples in either MCF10A or MFC10A-NeoT, and to assist in revealing significant differences not seen in general ANOVA analysis data (all values lying outside the av. SED being significant).

These graphs show the distribution of the collected data means and the distribution of points plot when the concentration of the three compounds (HYP, DMH and DAH) was altered (Fig 3.9). Such plots show the metabolic activity on the y axis and concentration of the various compounds on the x axis, and the various data points representing the various compounds plotted with differently coloured data points for both MCF10As and MCF10A-NeoTs (indicated by Fig 3.9 A and B, respectively).

The average standard error bar indicates the predicted values of the standard error of the section for the plotted graph (Figure 3.9). This plot of the means shows that the DAH derivative seems to depress the metabolism of MCF10A-NeoT cells in a more concentration-dependent manner than seen on the MCF10A cell line (Figure 3.9 B vs. A), with a depression in metabolic activity being significant over the 9.5-300 μ M range for the MCF10A-NeoT cells. The 150 and 4.8 μ M level of DAH induced less significant results on the MCF10A cells (Figure 3.9A), with lower metabolic activity values being induced in the MCF10A-NeoT cells, though trends were similar for the MCF10A cells. The 150 μ M and 300 μ M concentrations of DAH showed a marked effect on the MCF10A-NeoT cells, however, with the MTS values lying the furthest from the predicted SED (Figure 3.9B), indicating greater significance.

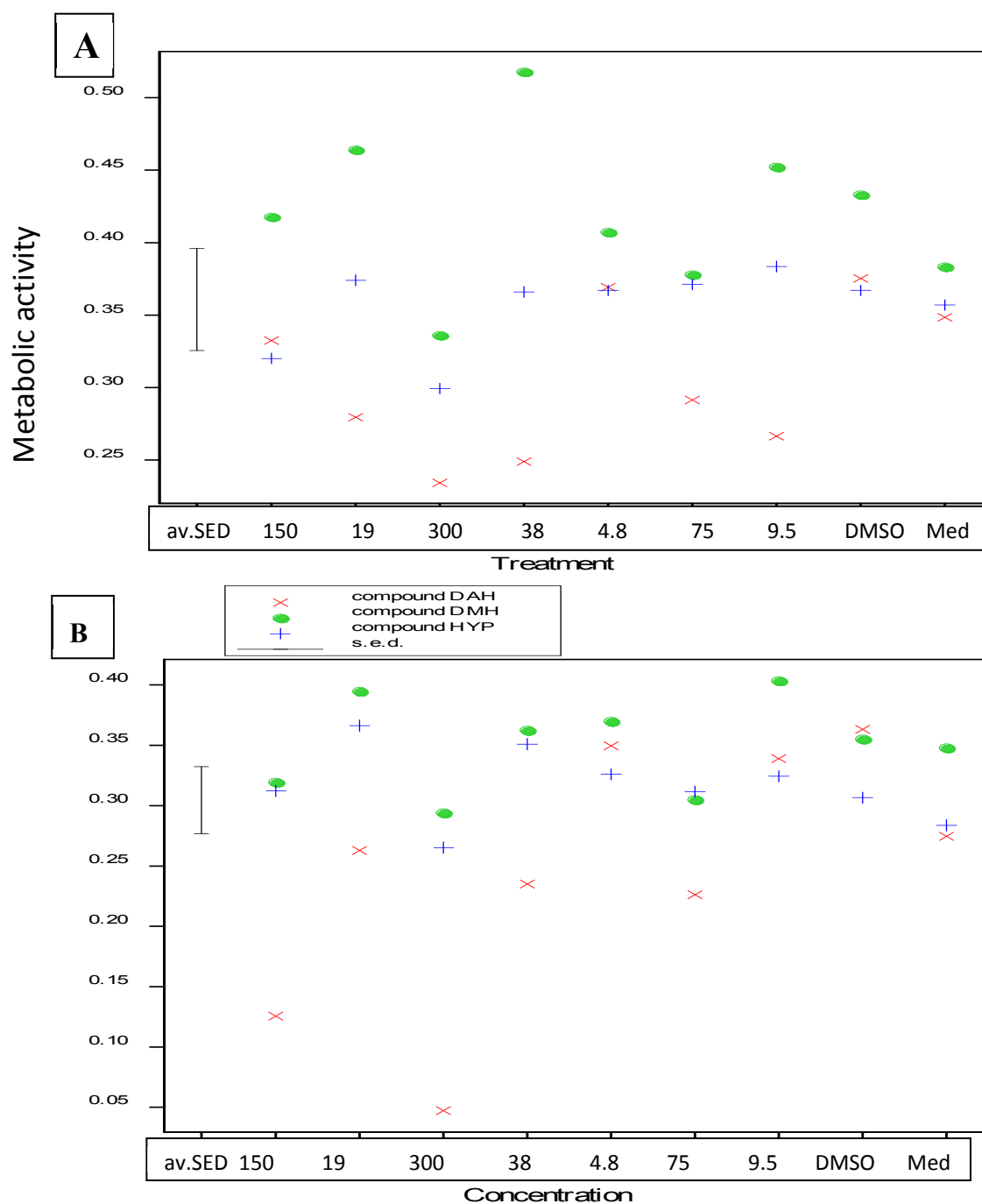


Figure 3.9: Mean plot of the mean metabolic activity induced by various concentrations (μM) of compounds tested on the MCF10A and MCF10A-NeoT.

Mean plot of the metabolic activity (Y axis) of the two cell lines MCF10A (A) and MCF10A-NeoT (B) after treatment with the three test compounds (i.e. HYP - hypoxoside, DMH- dimethylhypoxoside and DAH- decaacetylhypoxoside) at different concentrations (X axis). The average standard error of the difference (av.SED) bar indicates that the concentration points outside of the bar are outside of the predicted error and, therefore, have a significant effect on the cells from those concentration points inside the bar. Med = medium control, DMSO = dimethyl sulfoxide. **NOTE:** As each batch or samples were run at different times and DMSO and media controls varied slightly, the same symbol as the compound type is used for the controls.

Visual inspection of the metabolic activity of the MCF10A-NeoT cell line, displayed as a bar graph plot, like the mean metabolic activity plot, seems also to suggest that the metabolic activity was decreased to a greater extent in the MCF10A-NeoT cell line than the activity of the MCF10A cells after treatment with DAH (Figure 3.8, compared to 3.9A and B).

As mentioned, the DMH on the other hand, seems to stimulate the metabolic activity of MCF10A, most significantly at 38 μM (Figure 3.8A and 3.9A), but also at most levels below this value, though not at 75-300 μM . A similar effect is seen in the MCF10A-NeoT cells at levels below 75 μM (Figure 3.8, 3.9B). The HYP seems to have little effect on the MCF10A cells (except at 300 μM) with the DAH depressing metabolic activity of MCF10A cell line significantly from the 9.5 μM to 300 μM range (Figure 3.9A) (though strangely not significantly at 150 μM (Figure 3.8A, 3.9A). At this stage, however, the question remained as to whether all such effects are significantly different with respect to one another as a measure of such significance was still lacking.

Looking at the overall effect of the three compounds on the MCF10A, as represented in the plot of the means, however, except for the DAH compound and DMH, the HYP compound does not seem to have significant effect in depressing metabolic activity over the test range (as most points fall in the range of the average SED bar i.e. not a very wide range of around 0.2-0.55) (Figure 3.9A). Some increase in metabolic activity, however, in both cell lines was, to some extent, seen in the case of HYP and DMH treatments (Fig 3.9A and B). The concentration of DAH, however, seems less important for depressing metabolic activity (of the MCF10A cells) than its intrinsic nature of the compound (Fig. 3.9 all values outside of av. SED). A program assessing and measuring relative effects of various concentrations would more directly indicate which concentrations cause the most significantly different and important effect, however.

In summary, looking at the effect of the three compounds on the premalignant MCF10A-NeoT cell line, the mean plot from GenStat, confirms that the DAH derivative has the more marked effect, markedly reducing the metabolic activity (Fig 3.8 and Table 3.2). This is validated by points outside the average standard error of the difference range bar plot (av. SED) in the plot of the mean. This indicates a major depression of the metabolic activity between 150 and 300 μM , in a range of 0.05-0.4 (Figure 3.9B), a very wide range of values. This indicates significant differences between different compounds, of different

concentrations, on the metabolic activity of MCF10A-NeoT cells. In the premalignant cell line (i.e. MCF10A-NeoT cells), the DAH compound seems have the most significant, selective metabolic effect, though the metabolic activity of the MCF10A cells is slightly affected. Therefore, the DAH compound may have possible applications as an anti-cancer drug and effects should be further explored.

After rejection of the null hypothesis, i.e. the statement that the treatments have no significant effect, and to check which results were significantly different relative to one another, both within specific treatment groups and between such groups, a multiple comparison test (or further post hoc test), was performed. This was completed to further expand the conclusions from the mean metabolic activity plot (Figure 3.9). Though there are a number of programs facilitating specialized multiple comparisons, the Duncan's multiple range test was chosen as it allows closer and more direct and accurate comparison of variables such as the effects of concentration and compound type. The mean plot (Figure 3.9) and the plot of the metabolic activity against metabolic activity (Figure 3.8), however, are necessary as the Duncan's gives no indication of whether the effects of compound type and concentration have stimulatory or depressing effects on metabolism.

As mentioned, the Duncan's multiparameter test is an analytical program for testing significant difference indicated by the assignment of a distinct letter to significantly different metabolic activity values. Looking at the effect of the three compound types on the metabolic activity, according to the Duncan's analysis, it is observed that all compound types affect the metabolic activity of the MCF10A cells significantly differently relative to one another, (Table 3.3, MCF10A compound type, indicated by "a", "b", "c" letters assigned for DAH, HYP and DMH, respectively). This confirms what is apparent from the graphical representation of the MTS values (Figure 3.8A).

When considering the effect of compound type alone, the metabolic activity of the MCF10A-NeoT cells it is seen to be not significantly different when treated with the HYP and DMH (Table 3.3, MCF10A-NeoT, Compound type, both being represented by "b"). The metabolic activity of the premalignant cells, after treatment with these two compounds are not significantly different to each other but significantly different from the metabolic effects induced by DAH compound (Table 3.3, MCF10A-NeoT compound type, DAH, HYP and DMH being assigned the letters "a", "b", "b", respectively). Analysis of this parameter alone is only part of the analysis necessary.

The analysis of the overall effect of concentration only on the two test cell lines showed that of all concentrations, only the 300 μM concentration had a significant effect on the MCF10A cell line relative to the DMSO control (Table 3.3, MCF10A, concentration, 300 μM represented by “a” and the DMSO control by “b”). For the MCF10A-NeoT cell line both the 150 and 300 μM concentrations had a significant effect relative to the DMSO control (Table 3.3, MCF10A-NeoT, concentration, 300 and 150 μM represented by “a” and “ab”, respectively, while the DMSO control was represented by “cd”).

From the final multiparameter Duncan’s analysis for both compound type and concentration, where the MCF10A-NeoT cells shows the greatest depression of the metabolic activity at 300 μM DAH with a gradual decrease in concentration-dependent depression from 150, 75, 38 – 19 μM DAH in metabolic plots (Figure 3.8B), the effects 300 and 150 μM DAH seem most significantly different from the DMSO control (Table 3.3, MCF10A-NeoT, Compound type.concentration, 300 and 150 μM DAH are represented by an “a” and “ab”, whereas the DMSO control is represented by “cdef”). Though the 150 μM DAH concentration produces results not significantly different to those of the 38, 75, 300 μM DAH (Table 3.3, MCF10A-NeoT, compound type.concentration, the 150 μM concentration represented by “ab”, and the 38, 75, 300 μM DAH represented by “bcd”, “bc” and “a”), results were significantly different to the 300 μM HYP and 19 μM DAH treatments (Table 3.3, MCF10A-NeoT, Compound type.concentration, the 300 μM HYP and 19 μM DAH concentrations both represented by “cde”). The 300 μM HYP and 19 μM DAH concentrations, in turn, however, were not significantly different from the DMSO control (Table 3.3, MCF10A-NeoT, compound type.concentration, the DMSO control represented by “cdef”). Therefore, only the 300 and 150 μM DAH produced significantly different effects on the MCF10A-NeoT, compared to the DMSO control (Table 3.3, MCF10A-NeoT, Compound type.concentration, 300 and 150 μM DAH giving “a” and “ab”, whereas the DMSO control is represented by “cdef”).

This appears to mean that, though the effect of the 150 μM DAH is not significantly different from the 300 μM DAH effect on the MCF10A-NeoT, for drug choice, the 300 and 150 μM DAH concentration should be chosen over lower concentrations as the lower concentrations of DAH and the 300 μM HYP would not be effective choices as they produce results not significantly different to the DMSO control.

Though from the ANOVA readout for the effect of concentration (Table 3.3, MCF10A-NeoT, Concentration), concentration differences seem not as important as the effect of compound type in the case of the MCF10A-NeoT cells (Table 3.3 MCF10A-NeoT, concentration, most giving similar not significantly different results), DAH would possibly be the compound of choice and 300 μ M or 150 μ M the level of choice for treatment of a premalignant breast epithelial cell mass, of a similar phenotype to that represented by the current premalignant breast cancer model used in this study. The selection of either concentration of DAH, however, probably depends on what concentration is best tolerated by the “normal” MCF10A cell line.

On the MCF10A cells, though the 300 μ M DAH compound seems visually to have a significantly different effect relative to the other two compounds and the DMSO control (Figure 3.8A and 3.9A). The Duncan’s evaluation of the effect of concentration and compound type showed that the 300 μ M concentration of DAH had no significant effect in decreasing the metabolic activity of the MCF10A cell line relative to the DMSO control (Table 3.3, MCF10A, Compound type.concentration, revealed by “a” and “abcdef” for 300 μ M DAH and DMSO control, respectively). This was also true for any other compound types except the 150, 9.5, 19 and 38 μ M DMH concentrations (Table 3.3, MCF10A, Compound type.concentration all other compound types giving “a” and a combination of other letters, whereas the DMH concentrations had no “a” and the DMSO control, “abcdef”). In the MCF10A cells most concentrations of DMH, except the 300 μ M concentration, produced a significantly different effect from the 300 μ M DAH, as is evident from inspection of Figure 3.8A. The DMH compound seems to stimulate metabolic activity over most concentrations, relative to other compounds, whereas the 300 μ M DAH has an overall depressing effect on metabolism (Figure 3.8A). This difference was shown to be not a significant result, however, as the various DMH concentrations do not produce an effect significantly different from the DMSO control (Table 3.3, MCF10A, Compound_type.concentration, the DMSO control represented by “cdef” and “abcdef” and various DMH concentrations being represented by a combination of these letters). This means that essentially all levels of test compounds were well tolerated by the MCF10A cells, as the Duncan’s analysis becomes more reliable when more parameters are included. The results seen when considering only concentration effects, i.e. that the 300 μ M concentrations had significant effect may, therefore, be disregarded (i.e. results from Table 3.3 concentration, where 300 μ M concentrations are assigned an “a” and the DMSO control “b”). This means the DAH shows overall selective cytotoxicity for the

MCF10A-NeoT relative to the MCF10A cells and is possibly the overall drug of choice as, for the treatment of Ras related premalignant breast cancer, no compound really emerges as having a greater effect than the 150 and 300 μ M level of DAH according to the MTS assay.

At this stage, however, the question remains: is the MTS assay monitoring metabolic activity related to cell death and increased or decreased proliferation? To address these questions further staining and flow cytometry methods for assessing viability and confirmatory total and basic viability cell counts were performed.

Table 3.3: Duncan's multiple range test.

MCF10A (controls in boxes)

Compound type

	Mean		
DAH	0.3051	a	*
HYP	0.3562	b	*
DMH	0.4210	c	*

Concentration

	Mean		
300 μ M	0.2899	a	*
75 μ M	0.3469	ab	
150 μ M	0.3568	ab	
Med contrl	0.3629	ab	
9.5 μ M	0.3674	ab	
19 μ M	0.3725	ab	
38 μ M	0.3776	ab	
4.8 μ M	0.3812	ab	
DMSO contrl	0.3918	b	*

Not significantly different from a*, b* and to each other

Compound_type.Concentration

	Mean		
DAH 300 μ M	0.2343	a	*
DAH 38 μ M	0.2489	ab	
DAH 9.5 μ M	0.2664	abc	
DAH 19 μ M	0.2796	abcd	
DAH 75 μ M	0.2915	abcde	
HYP 300 μ M	0.2993	abcde	
HYP 150 μ M	0.3202	abcde	
DAH 150 μ M	0.3324	abcde	
DMH 300 μ M	0.3360	abcde	
DAH Med contrl	0.3484	abcdef	
HYP Med contrl	0.3570	abcdef	
HYP 38 μ M	0.3660	abcdef	
HYP DMSO contrl	0.3671	abcdef	
HYP 4.8 μ M	0.3671	abcdef	
DAH 4.8 μ M	0.3693	abcdef	
HYP 75 μ M	0.3713	abcdef	
HYP 19 μ M	0.3741	abcdef	
DAH DMSO contrl	0.3753	abcdef	
DMH 75 μ M	0.3780	abcdef	
DMH Med contrl	0.3833	abcdef	
HYP 9.5 μ M	0.3836	abcdef	
DMH 4.8 μ M	0.4073	abcdef	
DMH 150 μ M	0.4177	bcdef	
DMH DMSO contrl	0.4330	cdef	
DMH 9.5 μ M	0.4523	def	
DMH 19 μ M	0.4640	ef	
DMH 38 μ M	0.5178	f	*

significantly different to f* but not to each other

not significantly different to a* and to each other

bcdef \Rightarrow significantly different to a* but not to the values on the bracket above and below

significantly different to a* and ab but not to each other

also significantly different to abc

MCF10A-NeoT (controls in boxes)

Compound_type

	Mean	
DAH	0.2470	a *
HYP	0.3163	b
DMH	0.3502	b

} significantly different to a* but not to each other

Concentration

	Mean	
300 µM	0.2022	a *
150 µM	0.2523	ab *
75 µM	0.2809	bc *
Med contrl	0.3020	bcd
38 µM	0.3162	bcd
19 µM	0.3413	cd
DMSO contrl	0.3416	cd
4.8 µM	0.3485	cd
9.5 µM	0.3556	d *

} significantly different to a* but not to each other

} significantly different to a* and ab* but not to each other

Compound_type.Concentration

	Mean	
DAH 300 µM	0.0472	a *
DAH 150 µM	0.1256	ab *
DAH 75 µM	0.2262	bc *
DAH 38 µM	0.2351	bcd *
DAH 19 µM	0.2629	cde
HYP 300 µM	0.2652	cde
DAH Med Contrl	0.2745	cdef
HYP Med Contrl	0.2836	cdef
DMH 300 µM	0.2941	cdef
DMH 75 µM	0.3050	cdef
HYP DMSO contrl	0.3066	cdef
HYP 75 µM	0.3115	cdef
HYP 150 µM	0.3121	cdef
DMH 150 µM	0.3194	cdef
HYP 9.5 µM	0.3243	cdef
HYP 4.8 µM	0.3260	cdef
DAH 9.5 µM	0.3390	cdef
DMH Med Contrl	0.3479	cdef
DAH 4.8 µM	0.3495	cdef
HYP 38 µM	0.3510	cdef
DMH DMSO contrl	0.3552	cdef
DMH 38 µM	0.3625	cdef
DAH DMSO contrl	0.3631	cdef
HYP 19 µM	0.3664	def
DMH 4.8 µM	0.3698	def
DMH 19 µM	0.3947	ef ***
DMH 9.5 µM	0.4035	f ***

} significantly different to ef*** and f*** but not to each other

} significantly different to a* and f* but not to each other

} significantly different to a* and ab* but not to each other

} significantly different to a*, ab* and bc but not to each other

3.4.2 The influence of hypoxoside and its derivatives on cell death of MCF-10A and MCF-10A-NeoT cell lines using AO/PI staining

The fluorescence microscopy results of AO (cells staining green and indicating all cells) and PI staining performed for the assessment of induction of apoptosis or cell death (those stained red revealing dead and dying cells) in normal and premalignant cells are summarized in Table 3.4 below.

Table 3.4: Cell death indicated by PI staining in the two cell lines seen after treatment with hypoxoside and derivatives.

Concentration (μM)	cell death rate	
	10 A	NT
DMSO Control	-	-
Media Control	-	-
Cyclohexamine	++++	+++
4.8 HYP	-	+++
19 HYP	-	+++
38 HYP	-	+++
75 HYP	-	+++
150 HYP	-	+++
300 HYP	-	+++
4.8 DMH	-	+
19 DMH	-	+
38 DMH	-	++
75 DMH	-	++
150DMH	-	++
300DMH	-	+++
4.8 DAH	-	+++
19 DAH	-	+++
38 DAH	-	+++
75 DAH	-	+++
150DAH	-	+++
300DAH	+	+++

+ early apoptotic, ++ apoptotic, +++ possibly necrotic. Black-HYP, green-DMH, red-DAH, MCF10A = 10A and MCF10A-NeoT = NT.

3.4.2.1 Cell death assessment of MCF10A cell line through AO/PI staining

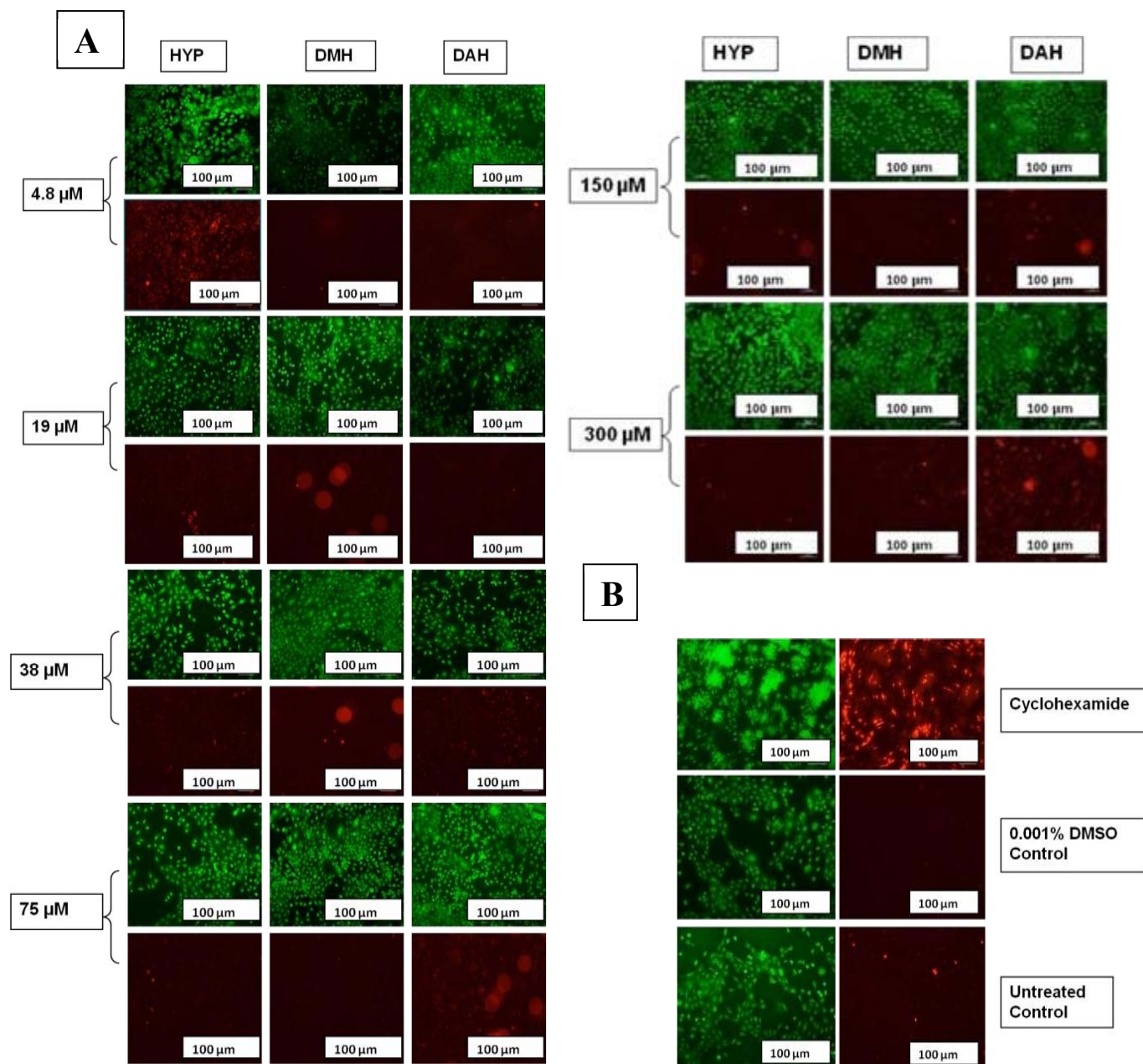


Figure 3.10: Effect of various concentrations of hypoxoside and its derivatives on MCF-10A assessed using AO/PI staining.

The MCF10A cells were treated with the three compounds overnight and then treated with acridine orange and propidium iodide. The effect of the compounds was analysed with fluorescence microscopy. The AO stained viable cells green and PI stained dead cells red. (A) AO/PI staining with the three different compounds treated MCF10A cells. (B) AO/PI staining with cyclohexamide, 0.001% DMSO and medium treated MCF10A cells and these were treated as positive, negative and zero controls, respectively.

3.4.2.2 Cell death assessment of MCF10A-NeoT cell line through AO/PI staining

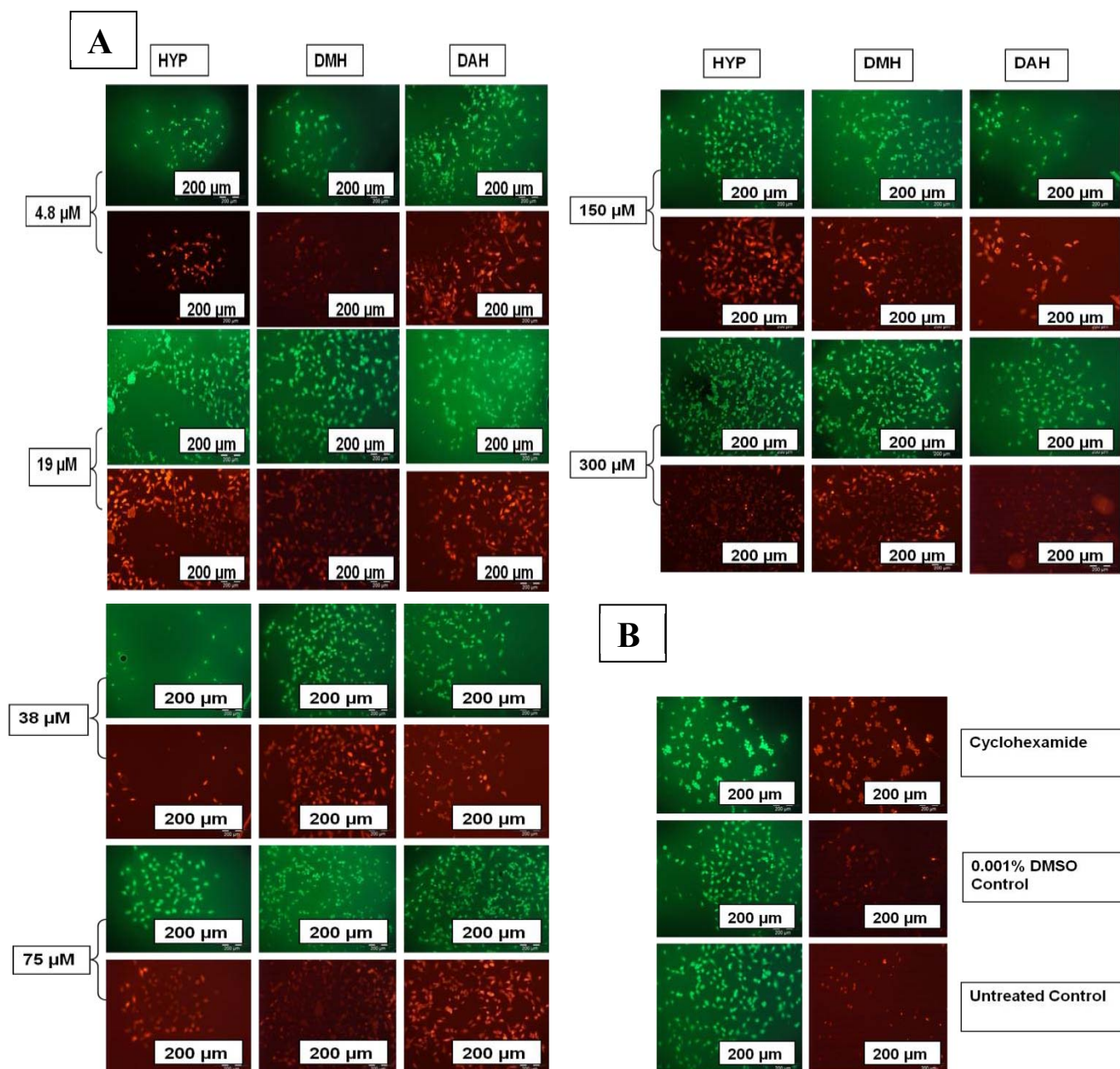


Figure 3.11: Effect of various concentrations of hypoxoside and its derivatives on MCF10A-NeoT assessed using AO/PI staining.

The MCF10A-NeoT cells were treated with the three compounds overnight and then treated with a 1:1 mixture of acridine orange and propidium iodide. The effect of the compounds was analysed with fluorescence microscopy. The AO stained viable cells green and PI stained dead cells red. (A) AO/PI staining with three different compounds treated MCF10A-NeoT cells. (B) AO/PI staining with cyclohexamide, 0.001% DMSO and medium treated MCF10A-NeoT cells and these were treated as positive, negative and zero controls, respectively.

The staining technique used, optimized specifically for the use with the current cell lines, seems to indicate selective induction of cell death in the MCF10A-NeoT (NT) cells by all compounds (Table 3.3 and Figure 3.10 and 3.11). This only partially seems to agree with the Duncan's analysis (Table 3.3).

As mentioned earlier, AO binds to DNA and RNA in both living and dead cells and PI binds DNA and RNA but is excluded from viable cells. AO staining, therefore, indicates the total number of cells present and PI staining indicates that in these cells there is no significant induction of cell death in the normal control MCF10A (10A) cell line, except at a 300 μM DAH (Figure 3.10A). This agrees with the Duncan's analysis and appears to indicate that the DAH, HYP and DMH compounds are not toxic to the normal control MCF10A cells at all of the test concentrations. The amount of cell death induced by the highest concentration of DAH was slight and not as significant as that of the positive control (cyclohexamine) (Figure 3.10) and all levels of DAH were similarly well tolerated. This seems to agree with the plots of the MTS and mean metabolic activity (Figure 3.8 and 3.9) and possibly indicates that the DAH and all other compounds are well tolerated by the normal breast epithelial cells (assessed using the MCF10A cell line).

The stained premalignant (MCF10A-NeoT) cell line samples, on the other hand, appeared to show cell death from even the lowest concentration of HYP (Figure 3.11A). Significant induction of cell death indicated by bright red staining of the cells seems to start at a concentration of 4.8 μM HYP and DAH, and at 38 μM DMH (Figure 3.11A), a result not well reflected in the HYP and only vaguely reflected in DMH and DAH, in the MTS results (Figure 3.8, 3.9 and Table 3.3 of the Duncan's multiple range test).

The control MCF10A cells show positive induction of cell death with cyclohexamide treatment whereas the DMSO-treated cells do not show significant staining, indicating that staining seems to accurately reflect the non-viability and viability of cells, respectively (Figure 3.10B). The MCF10A-NeoT cells seem to exhibit some resistance to induction of cell death with cyclohexamide treatment (the positive control) (Figure 3.11B). Propidium iodide staining, however, seems to indicate that the test system accurately reflects the presence of live and dead cells in the MCF10A-NeoT cells also and that all compounds show selective activity against the *ras* transfected premalignant cell line (Figure 3.11A). To resolve slight

discrepancies in the toxicity levels indicated by the MTS and staining assays, flow cytometry checks using PI staining and cell counts were performed.

It should be noted, at this stage that possibly the staining results may most accurately reflect cell death as the MTS assay may give a result more susceptible to error from the changes in cell number (as the MTS assay is highly susceptible to such influences). *In situ* staining, as performed above, may be more reliable than flow cytometry, though both use PI as an indicator of cell death, as cells require trypsinizing, washing and using centrifugation prior to analysis. Both methods use live cells (vital staining on a slide and flow cytometry on live cells) it was suspected that the slide staining method may deliver superior results as the flow cytometry results may be affected by loss of dead cells during the many manipulations, especially centrifugation.

3.4.3 Cell death assessment of the MCF10A and MCF10A-NeoT cell lines by Flow Cytometry and PI staining.

As the MTS results on lower concentrations of HYP did not show much selective cytotoxicity, only the effects of the 150 and 300 μM levels of HYP were assessed, but for the DAH and DMH compounds, four concentration levels (i.e. 4.8, 19, 75 and 300 μM) were assessed. Effects on cell numbers were assessed using the concentration of PI previously optimized in our laboratory for the cell lines used, except that only PI staining was performed as we found annexin V staining did not work well on our adherent cells.

Compared to the DMSO control, HYP and DMH seem to show slight effects on the MCF10A cell line % cell death (Table 3.5). The DAH derivative shows induction of low levels of cell death at lower concentrations, in the MCF10A cell line but as the concentration increases the induction of cell death increasing marginally up to 150 μM and then decreases at 300 μM . The percentage of dead cells relative to controls, however, seems low possibly due to some stimulatory effect of the compound or less dead cells during cell preparation (especially centrifugation). Significance was not assessed due to low number of tests performed $n=2$, in triplicate (Table 3.4) and the preliminary range-find nature of the assessment of this novel method to our laboratory. These results seem to partially mirror the results from the MTS assay, however (Figure 3.8A, 3.8B and Table 3.3) indicating low toxicity of all compounds to the MCF10A cells.

Table 3.5: Flow cytometric determination of % live and dead cells in the two test cell lines post treatment.

Standard Concentrations of the compounds(μ M)	Name of the compound	MCF10A Cell line		MCF10A-NeoT Cell line	
		% live cells	% dead cell	% live cells	% dead cells
0	DMSO Control	95.64	4.36	90.72	9.28
0	Medium Control	94.32	5.68	93.13	6.87
0	Cyclohexamine Control	32.40	67.60	76.40	23.60
4.8	Hypoxoside				
	Dimethylhypoxoside	96.87	3.13	96.88	5.12
	Decaacetylhypoxoside	97	2.71	96.39	5.61
19	Hypoxoside				
	Dimethylhypoxoside	98.72	2.28	94.17	5.83
	Decaacetylhypoxoside	95.47	4.53	92.37	7.63
75	Hypoxoside				
	Dimethylhypoxoside	99.18	1.82	94.44	5.56
	Decaacetylhypoxoside	96.54	3.46	93.55	6.45
150	Hypoxoside	94.63	6.36	94.83	5.17
	Dimethylhypoxoside				
	Decaacetylhypoxoside				
300	Hypoxoside	96.88	3.35	93.49	6.51
	Dimethylhypoxoside	99.72	1.28	91.23	8.77
	Decaacetylhypoxoside	97.03	2.97	79.10	20.90

The MCF10A-NeoT cells seem to show only minimal compound concentration-dependent increase in the cell death, except with the DAH derivative showing the highest % induction of cell death at 300 μ M (20.9%). The DMH derivative, on the other hand, shows a % cell death of 8.77% and finally HYP, a 6.51% cell death. The % cell death induced by HYP and DMH (i.e. 6.51 and 8.77, respectively) are possibly not significantly different from the negative controls % cell death values i.e. DMSO control (9.28%) and media control (6.87%) (Table 3.5), results largely confirmed by the MTS graphical and Duncan's analysis (Figure 3.8 A and B and Table 3.3), though these do not directly measure cell death. Therefore, the flow

cytometric results show no significant induction of cell death in either cell line, except with the DAH treatment at 300 μ M in the MCF10-NeoT cells, with a % cell death induced being comparable with that of the positive control (cyclohexamine, 23.6%). Flow cytometry, using the method of single staining a cell preparation seems to need optimization or seems to be less sensitive than the optimized staining and MTS assay methods.

3.4.4 Trypan blue hemocytometric cell count.

As some treatments seem to have stimulatory effects (Figure 3.8), cell numbers of the treated and untreated cells were further assessed using the trypan exclusion method. This allows assessment of cell death, and, by manual counting, using a hemocytometer chamber the total number of cells.

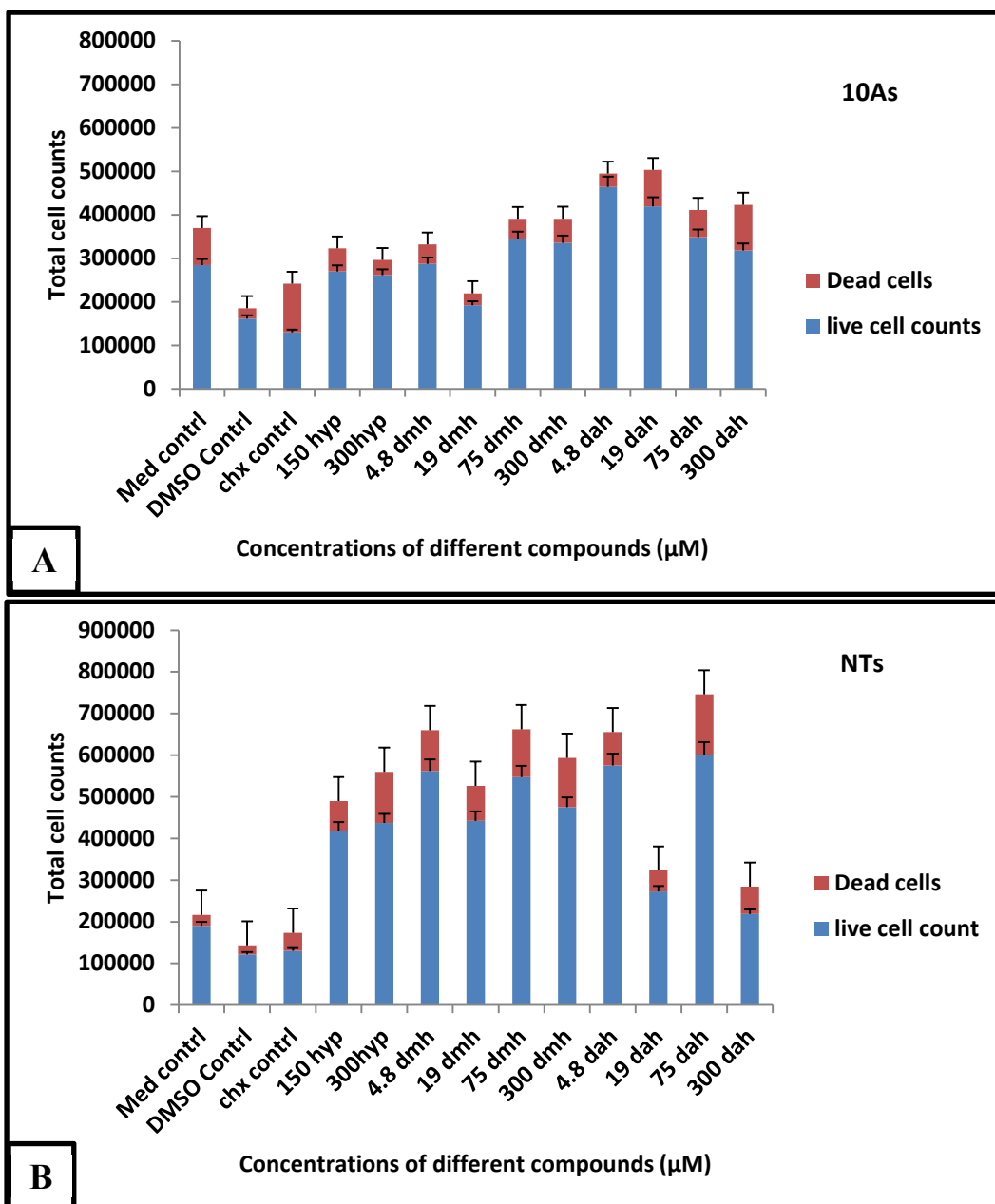


Figure 3.12: Total cell counts and the percentage dead cells (trypan blue stained) after treatment with different hypoxoside compounds.

The MCF10A (A) and MCF10A-NeoT (B) cells were seeded in 25 ml TI flasks and allowed to grow overnight. These cells were treated overnight with the three hypoxoside compounds at different concentrations as indicated in the graph. The cells were trypsinized, stained with trypan blue (dead cell blue), and the live (unstained) and dead cells were counted using hemocytometer in duplicate, n=2. Total live and dead cell counts were plotted in a stacked column showing the dead cells at the top red bar and the live on the bottom blue column.

When the total number of cells (uncorrected) were counted post treatment with the different compounds and the cells that stained blue (dead cells i.e. late apoptotic or necrotic) were recorded as a % to reflect % cell death of total counts (Figure 3.12) results indicate that most

of compounds seem to stimulate an increase in cell numbers relative to the DMSO control group for both cell lines (MCF10A and MCF10A-NeoT), with the malignant cell line showing the greatest stimulation of proliferation with induction of very little cell death (Figure 3.12). In the MCF10A-NeoT treatment with the 19 and 300 μM concentrations of DAH, seems to show the greatest induction of cell death (evidenced by reduced cell numbers and relative % dead cells as indicated by trypan blue staining) (Figure 3.12B NT).

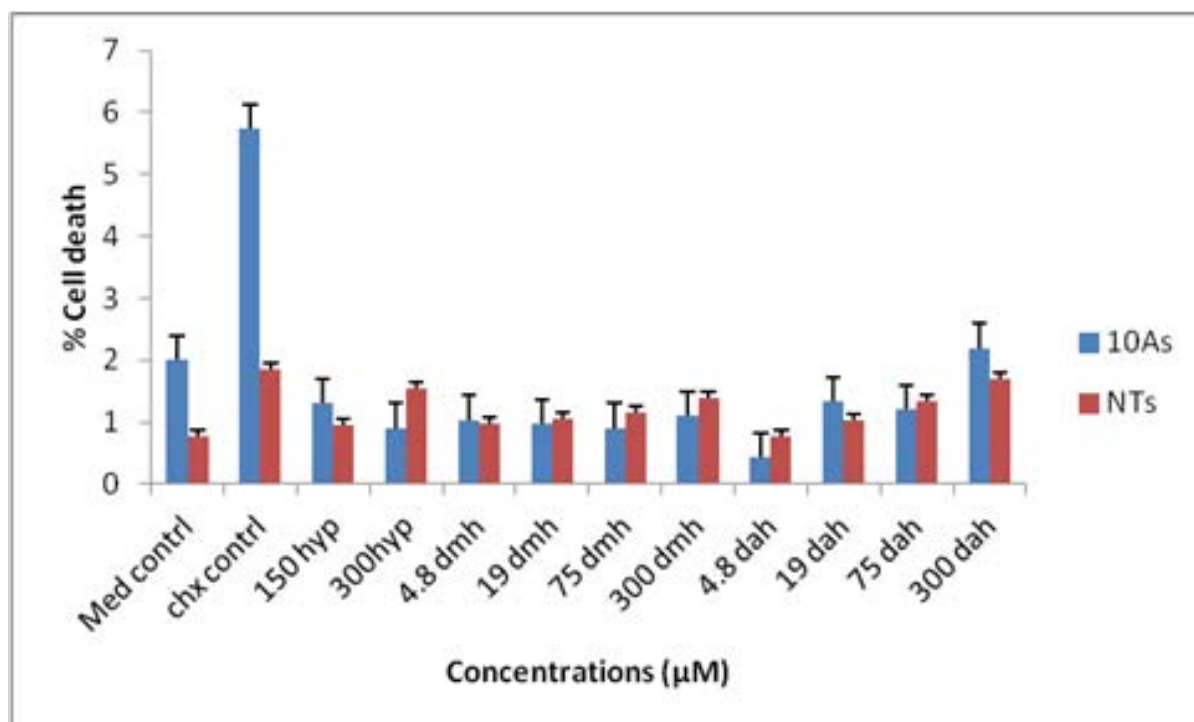


Figure 3.1 3: Cell death after treatment with three hypoxoside compounds assessed using cell counts with trypan blue staining.

Cells were seeded and allowed to grow overnight and subsequently treated with the three hypoxoside test compounds overnight. To assess cell death after treatment with various concentrations of HYP, DMH or DAH, the cells were stained with trypan blue, which passes through the membrane of the dead cells and is excluded by the membrane of the live cells. The % dead cells (blue stained cells), expressed as a % of total cell counts, was calculated for both cell lines using hemocytometer and corrected for the DMSO-induced cell death seen in the control (i.e. by subtraction of % dead cells on the DMSO control).

Surprisingly, the 75 μM concentration seems to kill proportionately about the same number of cells as the 150 μM concentration but it also seems to give rise to the greatest stimulation of cell proliferation in the MCF10-NeoT cells, implying a non-linear response (Figure 3.12). The trypan blue exclusion method reveals that all the compounds do not have a major effect of inducing cell death, however (Figure 3.13). Instead most show growth stimulatory effect on both cell lines, with the greatest effect on MCF10A-NeoT cells (Figure 3.12). As in the

case of the flow cytometry method, cell numbers and % cell death are only determined after trypsinization, washing and using centrifugation (a point at which especially dead cells may be lost).

When looking at the portion of dead cells relative to the total cell count for each concentration or the various compounds (i.e. % cell death or dead cells expressed as a % of the total cell number for each treatment group), it seems there are no major compound-specific or concentration-specific effects observed for induction of cell death in the MCF10A (Figure 3.13), with most except the 300 μM concentration, apparently depressing the relative percentage cell death in the MCF10A. This does not seem to be due to proliferation-promoting activity, as seen with treatment of MCF10A-NeoT cells with most compounds (Figure 3.12, as evident in increased cell numbers in MCF10A-NeoT cells) as the compounds seem to have a lower proliferation-promoting effect on the MCF10A cells (Figure 3.10A and 3.12A). This seems to support the Duncan's test conclusion on the metabolic activity for the MCF10A but contradicts PI staining results and the results of the trypan blue staining due to a lower sensitivity of the two methods for detection of cell death. Despite the apparent low sensitivity of trypan blue for detecting cell death, the HYP is seen to have a slight concentration-dependent effect of increasing cell death in the MCF10A-NeoT cells relative to the DMSO control, as do the DMH and DAH (Figure 3.12 and 3.13). This seems to agree with the supravital PI staining results for induction of cell death (Figure 3.11B).

In the MCF10A cells, the DAH derivative also has only a slight concentration-dependent effect especially at 300 μM (Figure 3.13). The overall effect of the three compounds in inducing cell death does not seem to be significantly different according to the trypan blue staining test except that the total cell counts in the MCF10A-NeoT cells seem significantly depressed at 19 μM (and possibly 150 μM which was not tested) and the 300 μM DAH (Figure 3.12).

Comparing % cell death determined using trypan blue staining for dead cells and total cell counts and the flow cytometry results, the HYP, DMH and even DAH produced similar trends, by either method, at all concentrations (relative to the control) on the MCF10A cells (Table 3.6).

Table 3.6: Comparison of the PI Flow cytometric test with the Trypan blue test results

Concentration (μM)	% Cell Death			
	Flow Cytometer		Trypan Blue	
	10 A	NT	10 A	NT
DMSO Control	4.36	9.28	15	18
Media Control	5.68	6.87	30	14
Cyclohexamine	67.6	23.6	86	33.5
150 HYP	6.36	5.17	19.5	17
300 HYP	3.35	6.51	13.5	28
4.8 DMH	3.13	5.12	15.5	17.5
19 DMH	2.28	5.83	14.5	19
75 DMH	1.82	5.56	13.5	21
300 DMH	1.28	8.77	16.5	25
4.8 DAH	2.71	5.61	6.5	14
19 DAH	4.53	7.73	20	18.5
75 DAH	3.46	6.45	18	24
300 DAH	2.97	20.9	33	30.5

Similar results are seen in the MCF10A-NeoT cells, with % cell death at all concentrations relative to the controls not significantly affected except at the 300 μM DAH treatment level for both cell lines where cell death increases (Figure 3.13 and Table 3.6). Though the 150 μM level DAH was not assessed, this result would be anticipated to be similar to what was seen in the Duncan's analysis of the MTS values and with the 300 μM concentrations.

From the flow cytometry cytotoxicity test results, one may conclude that the three hypoxoside compounds have no significant or selective effect on cell death in both cell lines, except for the 300 μM DAH compound on the MCF10A-NeoT cells (Table 3.5). Trypan blue staining seem to indicate a slightly more selective induction of cell death in the MCF10A-NeoT cells after treatment with all compounds and the 300 μM DAH concentration relative to the media control (Figure 3.12, 3.13 and Table 3.5). This agrees with the AO/PI supravital staining result trend, though the trypan blue staining method does not seem to be as sensitive. Some selective cytotoxicity on the MCF10A-NeoT cells seems to be observed, especially with the 300 μM HYP, 300 μM DMH and 300 μM DAH using trypan blue (Table 3.6). These results seem to mirror trends in the graphical representation of the MTS results (Figure 3.8).

3.5 CONCLUSION

In the current range-find experiment for the assessment of the effect of 3 compounds (i.e. HYP, DMH and DAH) on the normal MCF10A cell line and its VAL-12 c-Ha-*ras* derivative, the MTS metabolic activity assay results, together with the Duncan's multiple range test analysis, indicates statistically that the DAH compound, at a concentration of 150 and 300 μM , and none of the other compounds, have an overall rigorously statistically validated selective effect on the metabolic activity of the premalignant test breast epithelial cell line (with no major effect on the normal MCF-10A breast epithelial cells).

After performing this study, the simultaneous post treatment assessment of cell count, and a Duncan's multiple range test analysis of MTS metabolic assay results, is considered essential. Though the MTS assay proved a useful indicator of metabolic activity, visual inspection of the graphical representation of results, without Duncan's analysis of results and without cell counts, would seem to indicate that any level of DAH and any higher concentration of HYP and DMH would be an optimal choice for treatment of Ha-*ras*-related breast epithelial cell malignancies. Though this is also indicated by the supravital adherent cell staining technique using PI (Zamai *et al.*, 2001), this course of action is not supported by the Duncan's analysis, nor cell counts (which indicate that all compounds support premalignant cell proliferation, especially at lower concentrations).

Surprisingly, though flow cytometry has been pronounced (above) to lack sensitivity, it too supports the fact that only the 300 μM DAH (and possibly the 150 μM DAH, if it had been assessed by flow cytometry), would be suitable for the selective therapeutic application in the treatment of premalignant and possibly malignant breast cancers.

Only with multiple range analysis of the MTS results was the 150 and 300 μM range unequivocally advocated. Without the simultaneous assessment of cell numbers, further trials (including clinical trials) using other hypoxoside compounds at various levels may be attempted without being aware that the hypoxoside derivatives, including the DAH derivative, at levels below about a 150 μM limit, may have the undesirable effect of inducing proliferation of premalignant (cancer) cells. Total cell counts and, though insensitive, the Trypan blue staining method, and the Duncan's multiple range analysis, seem essential co-analytical control measures important for supporting conclusions drawn using the MTS assay.

The supravital staining method used was useful in confirming the lack of toxicity of the HYP and its derivatives, on the normal breast epithelial cell line, and may indicate the incipient death of the premalignant cell line, post treatment with all hypoxoside compounds, at all levels, as indicated by results of supravital adherent cell staining (being highly sensitive). Such staining results may portend a massive cell death event which may manifest itself if the 24 hour test exposure time were extended. The exposure time should, therefore, be extended and another method besides the PI staining method should be investigated to validate induction of cell death. The more long term outcome of exposure to the test compounds, should be investigated.

If the current conclusions are supported by such further investigations and additional tests for the induction of cell death, the trypan blue method, together with the MTS assay, total cell counts and the Duncan's analysis of MTS results and a 24 hour exposure to test compounds, seems to constitute an optimal system for drug screening.

CHAPTER 4

GENERAL DISCUSSION, CONCLUSION AND FUTURE WORK.

4.1 GENERAL DISCUSSION

Naturally available substances are important in everyday life. These substances are derived from various sources which include micro-organisms, marine creatures, animals and plants. The natural products are used in different fields of endeavor, such as in pharmaceuticals as drugs, and in agriculture as pesticides to manage insects and other pests. These may be associated with fewer risks compared to the synthetic products that are generally less biodegradable. They may be used in the food industry, in beauty industries in perfumes and body lotions and in other industries involved in producing synthetic products from bioactive components. The use of natural products requires the isolation and identification of active components and knowledge of their structure. Such information can be used to assist in the derivatization and hence synthesis of natural compounds with increased activity for specific purposes.

The efficacy of rooperol for the treatment of cancer is controversial as there has been little success seen in clinical trials (Albrecht *et al.*, 1995a; Albrecht *et al.*, 1995b; Boukes, 2008; Boukes *et al.*, 2010; Boukes and Van de Venter, 2011). For this reason, in the current study, derivatives of hypoxoside that may have greater activity against premalignant (and hopefully malignant) breast cancers were investigated. Few studies have been carried out on the role of hypoxoside or rooperol *per se* (Smit *et al.*, 1995) and no studies have been performed on the DAH and DMH derivatives previously synthesized by Bettolo *et al.* (1982), i.e. the derivatives chosen for the current investigation. Pure hypoxoside and the DAH and DMH derivatives were prepared and analyzed for the selective cytotoxicity on the normal (MCF10A) and premalignant cell lines (MCF10A-NeoT).

The problem with such a study is that a wide variety of methods are available for assessing the selective toxicity and induction of the safe form of cell death (or apoptosis) by such compounds. Due to time constraints, only four different methods could be assessed in the current study (i.e. (i) the MTS assay for the monitoring of effects on metabolic activity, (ii) AO/PI supravital staining of adherent cells, and fluorescence microscopy, (iii) supravital

staining with PI for flow cytometric determination of % cell death, and (iv) the trypan blue staining methods for checking the assessment of % cell death using a hemocytometer and total cell count).

The term apoptosis is used to describe a number of physiological, biochemical and molecular changes exhibited by a cell that is about to die in a programmed way (as mention in Chapter 1) (Darizynkiewicz *et al.*, 1992). The induction of apoptosis is usually the goal when testing an anticancer drug and there are a variety of methods used to assess the characteristic changes. The most consistent target for analyzing the induction of apoptosis is an examination of the membrane integrity or induction of permeability in the membrane of the target cell, a disrupted membrane being a feature of apoptotic cells. Therefore, fluorophores/dyes such as PI and DAPI, that are not usually able to enter inside non-apoptotic cells and stain the nucleus due to their intact nature, are used (Van England *et al.*, 1996).

Unfortunately, the different dyes used in assessing apoptosis or programmed cell death or cell viability are used at a variety of different concentrations and with a variety of different exposure times. Choice of protocol is difficult even if a common key dye used in this context, is selected. Supravital staining gave rise to results that could not be well reconciled with the an overall interpretation of the results of the current study.

Widely differing PI procedures are used in staining cells for either flow cytometry or fluorescence microscopy for cell death assessment. A review article by Darzynkiewicz *et al.* (1992), for example, gave the final concentration of PI to be used for supravital staining as 13 $\mu\text{g/ml}$, with cells being stained for 30 minutes after harvesting (Darizynkiewicz *et al.*, 1992). Longer exposure to allow PI to efficiently enter apoptotic cells and stain the nucleus was mentioned to be more desirable.

For this reason, the Zamai *et al.* (2001) protocol using supravital staining of cells (i.e. without fixation) and a higher concentration of PI (50 $\mu\text{g/ml}$) for 30 minutes was considered. Increasing the incubation time (to 4 h) and staining with higher concentrations (i.e. 50 $\mu\text{g/ml}$) of PI was also claimed to be necessary for staining apoptotic cells efficiently (Zamai *et al.*, 2001), but 30 min was deemed acceptable.

In another study on the anticancer activity of a certain compound, using supravital MCF7 cell line and AO and PI staining at much lower levels for much shorter periods was advised. Concentrations of AO and PI used were 1 µg/ml and 12 µM concentrations, respectively, with only 5 minutes exposure time used for AO staining and these measures gave reproducible results (Visagie and Joubert, 2011). Another study using a lower concentration of dyes and shorter exposure time involved Hoechst (HO) staining optimal at 20 µM for 20 minutes at 37°C, AO optimal at 0.67 nM at 37°C for 10 minutes and PI optimal at 3 nM for 5 minutes at 37°C (Foglieni *et al.*, 2001). This study outlined the importance of optimising the staining procedure for the specific cell line one is using. In this study cells were fixed prior to staining (assessment of cell death) and it was reckoned that the discrepancy of the result was due to that (Foglieni *et al.*, 2001). It was, decided to use the method of Zamai *et al.*, 2001, however, as the method was claimed to facilitate detection of living (PI negative), apoptotic (PI dim) and necrotic cells (PI bright) and also used supravital cells as in the current study (Zamai *et al.*, 2001). The subsequent apparent observed over-sensitivity of the detection of cell death and the lack of sensitivity of flow cytometric assay, however, were disappointing and need re-investigation. Results may, however, be explained as follows:

Early studies of flow cytometry-based PI assays and PI staining of adherent cells included an RNase treatment step, due to the fact that PI does not only bind DNA but any double stranded nucleic acid, such as RNA. A RNase pre-treatment step was, therefore, included to reduce the number of falsely PI-stained cells (Rieger *et al.*, 2010). This step was omitted in the current study, as over 99% of published data generated with PI staining have been generated without pre-treating cells with RNase. Increased production of proteins induced in the Ras-activated MCF10A-NeoT cells, however, may result in increased cellular mRNA, relative to that found in MCF10A cells and induced false positive staining for apparent cell death (PI positive staining). A lack in RNase pre-treatment, may, therefore, have resulted in the unanticipated positive PI staining pattern seen in the *ras*-transfected cells in the current study. The effect of RNase pre-treatment of MCF10A and MCF10A-NeoT cells, prior to staining should, therefore, be investigated. Supravital AO/PI staining has also been reported to only give reproducible results only when AO is applied to live cells before PI (Foglieni *et al.*, 2001). In the current study, both dyes were applied simultaneously and this might also have influenced fluorescence microscopy staining results, producing false positive results.

The flow cytometry assay results, using PI staining for detection of cell death, also did not confirm fluorescence microscopy results. If the positive results seen, post-treatment, on staining of adherent cells was “real”, this discrepancy in results may be due to the different staining protocols used or due to the fact that flow cytometric assays may give false negative results, if apoptotic cells stain weakly. These cells may subsequently be erroneously classified as viable cells if the detection threshold (sensitivity) of the flow cytometer is set too high (Darizynkiewicz *et al.*, 1992). This may also account for the apparent low detection of apoptotic cells in the current study.

When considering the supravital staining results, the possibility exists that the PI may react more avidly with the MCF10A-NeoT cells than the MCF10A cells, due to distinct intrinsic characteristics of the transformed cell and its membrane. The concentration of PI and length of time required for staining may need to be individually optimized for each cell line due to such differences, and differences in the cytoplasmic pH of the MCF10A-NeoT cells (unpublished results) which may also influence the intensity of PI staining. Control results seem to discount this theory, however, as both positive and negative controls deliver distinctive positive and negative results. The final concentration of the AO and PI dye used in supravital staining was 5 µg/ml per dye which is much less than is recommended by Zamai *et al.* (2001) (50 µg/ml), but the low concentrations gave more than adequate positive PI staining results and good positive and negative staining results for controls.

For flow cytometric studies, a similar problem was encountered. PI labeling was used at 5 µg/ml concentration and the exposure time was 45 minutes. Annexin V together with PI staining is often used to differentiate between live, apoptotic and necrotic cells, based on cell membrane integrity and the binding of annexin V to phosphatidylserine. Phosphatidylserine is usually present on the inner surface of intact, viable cells, but is present on the outer surface of apoptotic cells (Rieger *et al.*, 2010). It would have been most convenient if such a confirmatory staining procedure could have been used in the present study. Binding of annexin V, however, requires the presence of fairly high levels of calcium. This is usually added to the labeling buffer and, as with our cells, this often resulted in dislodgement and loss of adherent cells. For this reason, it has been recently reported that annexin V is only suitable for labelling non-adherent cell lines (Zamai *et al.*, 2001) and the annexin V method was not considered for this study.

Cells were also stained supravitaly to avoid the negative effect of fixation on the cell membrane. The low level of detection of cell death using the flow cytometric PI staining method may be due to the low concentration of PI used, or the length of exposure to PI, however, compared to the one recommended by Zamai *et al.*, (2001) for efficient assessment of apoptosis (i.e. 50 µg/ml for 4 h). The method used was, however, previously optimized for the cell lines used in this study as positive and negative controls seemed to indicate that, for detection of live and apoptotic cells, the system was working optimally in the flow cytometry as in the supravital staining methods. For this reason it seemed that differences in staining protocols used for these two analyses should not be of concern.

At the commencement of the study, supravital staining for fluorescence microscopy using stains with AO and PI seemed to be the most convenient, direct and reliable methods to use as no fixation step was employed and no dislodging of the adherent cells and subsequent manipulation was required (Coder, 1997). This would obviate any loss of specific cell populations during centrifugation procedures necessary for cell preparation for flow cytometry, trypan blue staining and cell counts. Centrifugation is potentially a great problem as damaged or apoptotic cells more easily aggregate and may be removed as clumps that will not re-suspend after centrifugation.

The MTS assay too was considered an optimal choice of technique, as here too there was no dislodgement of cells which may cause disruption of the cell compartmentalization and loss of damaged cells by aggregation (Coder, 1997). This method also detects metabolic activity related to viability, so represented a complementary method to validate the metabolic related results. These two methods were, therefore, considered the most important methods for use in the current study.

When looking at the proliferation assays graphs for the optimization of MCF10A and MCF10A-NeoT cell numbers to be used in the MTS assay, to check the linearity and sensitivity of both cell lines, the graph produced for the MCF10A-NeoT cells clearly shows that the two cell lines react differently with the MTS tetrazolium salt. The normal (MCF10A) cell line results showed a greater sensitivity to cell number. This surprisingly was not the case with the premalignant (MCF10A-NeoT) cell line, where a lower response to changes in cell numbers was observed. This may be explained by the Warburg metabolism of the cancer cells, and the possible decreased conversion of MTS tetrazolium salt by the MCF10A-NeoT

cells, due to an altered metabolism of the premalignant cells. In spite of this, the MTS assay results revealed the marked selective proliferation of cells with most treatments but depression of the metabolic activity in the MCF10A-NeoT with DAH treatment. This showed the most significant ($p < 0.001$) depression of metabolic activity compared to the MCF10A or any other test compound.

The MTS assay is a widely used method, widely assumed to assess the level of cell death induced when it actually tests effects on metabolic activity. Such a parameter may be only vaguely associated with cell number. While the MTS assay is normally known to test cell viability, this is not factually accurate, because cells can be metabolically depressed without necessarily dying. Cells may also be depressed metabolically for some time and later recover fully. Assessment of cell counts is, therefore, essential as the MTS assay is also affected by cell number. This became startlingly clear in the current study, where, without associated cell counts, metabolic depression may have been taken to mean that cells were dying with treatment, where, in fact cell proliferation was being induced. This is a startling novel finding of this study.

The MTS assay, on the other hand, is a convenient assay being simple, quick, and inexpensive and more importantly, it gives a measure of cell viability without disturbing cells in culture i.e. without the requirement for damaging trypsinization and other procedures which may introduce errors (Huang *et al.*, 2004). This assay can give fairly early stage indication of incipient cell death, but it is really important to interpret results using powerful multiparameter programs such as the ANOVA post hoc Duncan's multiple range analysis and at least a cell count. Without the Duncan's analysis and cell counts, the MTS assay results are difficult to accurately interpret.

Where PI staining for indication of cell death proved problematic, the crude and simple trypan blue viability staining method, using hemocytometer total and trypan blue stained cell counts, for a rough assessment of % cell death, proved almost adequate. The trypan blue assay reflected similar results as those seen with the PI flow cytometric assay i.e. no significant killing of the normal cell line and only a marginal concentration-dependent low level of killing of the abnormal cell line at low levels of DAH. More significant killing, however, was seen at 150 and 300 μM levels of DAH. The effect of treatments in increasing

proliferation of normal, and, more, markedly the abnormal cell line, was, however, surprising. This appears to mean that, even with treatment with the DAH compound that shows selective toxicity in the premalignant cells, the concentration of DAH needs to be approximately 150 μM or more to be effective in controlling premalignant cell proliferation.

The aim of the current study was to:

- Isolate and purify hypoxoside from the *Hypoxis hemerocallidea*, through extraction of corms with ethanol and further isolation with HPCL pre-packed reverse phase column – this was achieved.
- Prepare two derivatives from pure hypoxoside through methylation and acetylation, resulting in a dimethyl and a decaacetyl derivative, respectively - this was achieved.
- Confirm the purity of hypoxoside and the derivative using NMR spectroscopy and HR-MS - this was achieved.
- Establish an inexpensive, rapid, high-throughput method for the preliminary assessment of the selective effects and cytotoxicity of the prepared compounds. This was assessed using cell counts, metabolic assessment (MTS assay) and imaging using flow cytometry and fluorescence microscopy, using dyes (especially supravital staining with propidium iodide claimed to be useful in distinguishing live from early apoptotic and late apoptotic/necrotic cells). It is now considered that this has been achieved. The system that seems to work well is the use of the Trypan blue and total cell counts, together with the MTS assay, and the Duncan's analysis of the 24 hour exposure MTS results of the test cell lines. This seems to constitute an optimal system for drug screening.

4.2 CONCLUSION

The preliminary data collected, suggests that one may not make valid conclusions on assessment of cytotoxicity with only the metabolic activity test (MTS assay) without performing the Duncan's multiple range test on the MTS results and cell counts with trypan blue staining for cell death.

Analysis of chloroform extracts of corms of various *Hypoxis* species and cancer cell toxicity studies showed that *H. hemerocallidea* extracts had the highest concentration of hypoxoside compared to other species (Boukes *et al.*, 2008), but had the lowest anticancer activity (Boukes *et al.*, 2011). Such extracts, however, were impure, containing various sterols and sterolins. This suggests that hypoxoside/rooperol activity has a synergic effect with other unknown compounds such as sterols and sterolins present in impure test extracts (Boukes *et al.*, 2011).

Our data on purified hypoxoside, however, suggests that purified HYP from *H. hemerocallidea* (converted to rooperol by deglycosylation, as indicated in Figure 1.2) has a protective and proliferation-stimulating effect in both normal and premalignant breast epithelial cells. The DMH and DAH derivatives represent methyl and acetyl derivatives of both the sugar groups and the 3' and 3'' hydroxyl groups on the hypoxoside molecule (Figure 2.3). Just as the hypoxoside is converted to the aglycone *in vivo* to produce rooperol, the DMH derivative would be anticipated to be similarly deglycosylated to yield the 3',3''-dimethyl derivative of rooperol. This conclusion seems supported by the fact that the methyl derivative (DMH compound) seems to have a similar protective and proliferation-inducing effect, like rooperol.

The acetyl derivative, DAH, on the other hand, is substantially less polar than HYP and DMH. Although it can be envisaged that DAH is eventually metabolized to rooperol by the action of esterase and glucosidase enzymes, this may be a slower process. This would explain the seemingly significant, selective effect of the acetyl derivative, at a concentration of 150 and 300 μM , on the premalignant breast epithelial test cell model. This compound may, therefore, have similar action on other Ras-related malignancies and this possibility should be further explored.

4.3 FUTURE STUDIES

- For all cell death assessment procedures carried out in the current study, the treatment exposure period of the tested drugs should be increased to better observe their long term effects on the cancer cell model used. Tests should also be extended to other cell lines of other cell types.

- In the AO/PI staining procedure, the two dyes should not be applied simultaneously- the AO should be applied first and then PI, as the simultaneous application has been reported to give erroneous results.
- The flow cytometric PI staining procedure can be improved by coupling the PI with another dye, which may better detect apoptotic cells, as the PI “dim-staining” apoptotic cells may be erroneously miss-classified apoptotic cells as viable in flow cytometric analyses.
- As rooperol has been reported to have a strong antioxidant activity, the antioxidant activity of the derivatives (i.e. DMH and DAH) prepared in the current study should be further investigated.
- The mode of action of the DAH in it’s selective toxicity to the premalignant cancer cell model used should be investigated.

REFEENCES

- ABDULLAH, H., PIHIE, A. H. L., HOHMANN, J. & MOLNAR, J. 2010. A natural compound from *Hydnophytum formicarium* induces apoptosis of MCF-7 cells via up-regulation of Bax. *Cancer Cell International*, 10, 1-6.
- ALBERTS, B., JOHNSON, A., LEWIS, J., RAFF, M., ROBERTS, K. & WALTER, P. 2002. *Molecular biology of the cell*, New York, Garland.
- ALBRECHT, C. F., KRUGER, P. B., SMIT, B. J., FREESTONE, M., GOUWS, L., MILLER, R. & VAN JAARSVELD, P. P. 1995a. The pharmacokinetic behaviour of hypoxoside taken orally by patients with lung cancer in a phase I trial. *South African Medical Journal*, 85, 861-865.
- ALBRECHT, C. F., THERON, E. J. & KRUGER, P. B. 1995b. Morphological characterisation of the cell-growth inhibitory activity of rooperol and pharmacokinetic aspects of hypoxoside as an oral prodrug for cancer therapy. *South African Medical Journal*, 85, 853-860.
- ARMITAGE, P. & COLTON, T. 2005. *Encyclopedia of Biostatistics*, John Wiley & Sons.
- ARNDT, F., NOLLER, C. R. & LIEBERMAN, S. 1935. Nitrosomethylurea. *Organic Syntheses*, 15, 48.
- BARRETT, N. A., RAHMAN, O. M., FERNANDEZ, J. M., PARSONS, M. W., XING, W., AUSTEN, K. F. & KANAOKA, Y. 2011. Dectin-2 mediates Th2 immunity through the generation of cysteinyl leukotrienes. *J Exp Med*, 208, 593-604.
- BASKIĆ, D., POPOVIĆ, S., RISTIĆ, P. & ARSENIJEVIĆ, N. N. 2006. Analysis of cycloheximide-induced apoptosis in human leukocytes: Fluorescence microscopy using annexin V/propidium iodide versus acridin orange/ethidium bromide. *Cell Biology International*, 30, 924-932.
- BASOLO, F., ELLIOTT, J., TAIT, L., QIN CHEN, X., MALONEY, T., RUSSO, I. H., MOMIKI, P. S., CAAMANO, J., KLEIN-SZANTO, A. J. P., KOSZALKA, M. & RUSSO, J. 1991. Transformation of human breast epithelial cells by c-Ha-ras oncogene. *Molecular Carcinogenesis*, 4, 25-35.
- BELLO, B., FADAHUN, O., KIELKOWSKI, D. & NELSON, G. 2011. Trends in lung cancer mortality in South Africa: 1995-2006. *BMC Public Health*, 11, 1-5.
- BENJAMINI, Y. 2010. Simultaneous and selective inference: Current successes and future challenges. *Biometrical Journal*, 52, 708-721.

- BERTHO, Á. L., SANTIAGO, M. A. & COUTINHO, S. G. 2000. Flow cytometry in the study of cell death. *Memorias do Instituto Oswaldo Cruz*, 95, 429-433.
- BETTOLO, G. B. M., PATAMIA, M., NICOLETTI, M., GALEFFI, C. & MESSANA, I. 1982. Research on African medicinal plants. 2. Hypoxoside, a new glycoside of uncommon structure from *Hypoxis obtusa* Busch. *Tetrahedron*, 38, 1683-1687.
- BEWICK, V., CHEEK, L. & BALL, J. 2004. Statistics review 9: One-way analysis of variance. *Cell Cycle*, 8, 130-136.
- BLUFF, J. E., BROWN, N. J., REED, M. W. R. & STATON, C. A. 2008. Tissue factor, angiogenesis and tumour progression. *Breast cancer research*, 10.
- BOUKES, G. J. 2008. *Comparison of in vitro anticancer and immune stimulating effect of three Hypoxis spp.* MSc, Nelson Mandela Metropolitan University.
- BOUKES, G. J., DANIELS, B. B., ALBRECHT, C. F. & VAN DE VENTER, M. 2010. Cell survival or apoptosis: rooperol's role as anticancer agent. *Oncology Research*, 18, 365-376.
- BOUKES, G. J. & VAN DE VENTER, M. 2011. Cytotoxicity and mechanism(s) of action of *Hypoxis* spp. (African potato) against HeLa, HT-29 and MCF-7 cancer cell lines. *Journal of Medicinal Plants Research*, 5, 2766-2774.
- BOUKES, G. J., VAN DE VENTER, M. & OOSTTHUIZEN, V. 2008. Quantative and qualitative analysis of sterols/sterolins and hypoxoside contents in the three *Hypoxis* (African potato) ssp. *African Journal of biotechnology*, 7, 1624-1629.
- BOUKES, G. J. & VENTER, M. 2012. Rooperol as an antioxidant and its role in the innate immune system: an *in vitro* study. *Journal of Ethnopharmacology*, 144, 692-699.
- BRADBURY, D. A., SIMMONS, T. D., SLATER, K. J. & CROUCH, S. P. M. 2000. Measurement of the ADP:ATP ratio in human leukaemic cell lines can be used as an indicator of cell viability, necrosis and apoptosis. *Journal of Immunological Methods*, 240, 79-92.
- BRADBURY, S. & EVENNETT, P. 1996. *Fluorescence microscopy, Contrast Techniques in Light Microscopy*, Oxford, United Kingdom BIOS Scientific Publishers, Ltd.
- BRAY, F., MCCARRON, P. & PARKIN, D. M. 2004. The changing global patterns of female breast cancer incidence and mortality. *Breast Cancer Research*, 6, 229-239.
- BUNGER, C. M., JAHNKE, A., STANGE, J., DE VOS, P. & HOPT, U. T. 2002. MTS Colorimetric Assay in Combination with a Live-Dead Assay for Testing Encapsulated L929 Fibroblast in Alginate Poly-L-Lysine Microcapsules In Vitro. *International Society for Artificial Organs*, 26, 111-116.

- CALAF, G., ZHANG, P. L., ALVARADO, M. V., ESTRADA, S. & RUSSO, J. 1995. c-Ha-ras enhances the neoplastic transformation of human breast epithelial cells treated with chemical carcinogens. *International Journal of Oncology*, 6, 5-11.
- CANCER FACTS AND FIGURES. 2009. American Cancer Society. Available: <http://www.cancer.org/acs/groups/content/@nho/documents/document/500809webpdf.pdf>. Accessed [22 March 2010].
- CAO, X. G., LI, X. X., BAO, Y. Z., XING, N. Z. & CHEN, Y. 2007. Responses of Human Lens Epithelial Cells to Quercetin and DMSO. *Investigative Ophthalmology & Visual Science*, 48.
- CHIN, Y. W., BALUNAS, M. J., CHAI, H. B. & KINGHORN, A. D. 2006. Drug discovery from natural sources. *AAPS Journal*, 8, 239-253.
- CODER, D. M. 1997. Assessment of Cell Viability. *Current Protocols in Cytochemistry*, 9.2.1-9.2.14.
- COHEN, G. M. 1997. Caspases: The executioners of apoptosis. *Biochemical Journal*, 326, 1-16.
- COOPER, G. M. 1993. *The Cancer Book.*, London, Jones and Bartlett Publishers International.
- CRAGG, G. M. & NEWMAN, D. J. 2003. Plants as a source of anti-cancer and anti-HIV agents. *Annals of Applied Biology* 143, 127-133.
- CRAGG, G. M. & NEWMAN, D. J. 2005. Plants as a source of anti-cancer agents. *Journal of Ethnopharmacology*, 100, 72-79.
- CRAWFORD, K. W., BITTMAN, R., CHUN, J., BYUN, H. S. & BOWEN, W. D. 2003. Novel ceramide analogues display selctive cytotoxicity in drug-resistant tumor cell lines compared to normal epithelial cells. *Cellular and Molecular Biology*, 49, 1017-1023.
- DACIE, J. V. & LEWIS, S. M. 1970. *Practical haematology*, 104 Gloucester Place, London, J. & A. Churchill Ltd.
- DANZIGER, K. & SIMONSEN, J. 2011. What Are the Different Types of Breast Cancer. *Breast and Ovarian Cancer*.
- DARIZYNKIEWICZ, Z., BRUNO, S., DEL BINO, S., GORCZYCA, W., HOTZ, M. A., LASSOTA, P. & TRAGANOS, F. 1992. Features of Apoptotic Cells Measured by Flow Cytometry. *Cytometry*, 13, 795-808.

- DARZYNKIEWICZ, Z., BRUNO, S., DEL BINO, G., GORCZYCA, W., HOTZ, M. A., LASSOTA, P. & TRAGANOS, F. 1992. Features of apoptotic cells measured by flow cytometry. *Cytometry*, 13, 795-808.
- DARZYNKIEWICZ, Z., JUAN, G., LI, X., GORCZYCA, W., MURAKAMI, T. & TRAGANOS, F. 1997. Cytometry in cell necrobiology: Analysis of apoptosis and accidental cell death (necrosis). *Cytometry*, 27, 1-20.
- DECLERCQ, W., VANDEN BERGHE, T. & VANDENABEELE, P. 2009. RIP Kinases at the crossroads of cell death and survival. *Cell*, 138, 229-232.
- DREWES, S. E., ELLIOT, E., KHAN, F., DHLAMINI, J. T. B. & GCUMISA, M. S. S. 2008. *Hypoxis hemerocallidea* - Not merely a cure for benign prostate hyperplasia. *Journal of Ethnopharmacology*, 119, 593-598.
- DREWES, S. E., HALL, A. J., LEARMONTH, R. A. & UPFOLD, U. J. 1984. Isolation of hypoxoside from *Hypoxis rooperi* and synthesis of (E)-1,5-bis(3',4'-dimethoxyphenyl)pent-4-en-1-yne. *Phytochemistry*, 23, 1313-1316.
- DREWES, S. E. & KHAN, F. 2004. The African potato (*Hypoxis hemerocallidea*): A chemical-historical perspective. *South African Journal of Science*, 100, 425-430.
- DREWES, S. E. & LIEBENBERG, R. W. 1987. *Rooperol and its derivatives*. United States Patent patent application 740,969.
- DUNCAN, D. B. 1955. Multiple range and multiple F tests. *Biometrics*, 11, 1-42.
- EKERMANS, G., SAKLOFSKE, D. H., AUSTIN, E. & STOUGH, C. 2010. Measurement invariance and differential item functioning of the Bar-On EQ-i: S measure over Canadian, Scottish, South African and Australian samples. *Personality and Individual Differences*, 50, 286-290.
- ELMORE, S. 2007. Apoptosis: A review of programmed cell death. *Toxicologic Pathology*, 35, 495-516.
- FADEEL, B. & ORRENIUS, S. 2005. Apoptosis: a basic biological phenomenon with wide-ranging implications in human disease. *Journal of Internal Medicine*, 258, 479-517.
- FAN, T., HAN, L., CONG, R. & LIANG, J. 2005. Caspase Family Proteases and Apoptosis. *Institute of Biochemistry and Cell Biology*, 37, 719-727.
- FOGLIENI, C., MEONI, C. & DAVALLI, A. M. 2001. Fluorescence dyes for cell viability: an application on prefixed conditions. *Histochemistry Cell Biology*, 115, 223-229.
- GAVRILESCU, L. C. & DENKERS, E. Y. 2003. Apoptosis and the balance of homeostatic and pathologic responses to protozoan infection. *Infection and Immunity*, 71, 6109-6115.

- GHOSH, M., THAPLIYAL, M. & GURUMURTHI, K. 2009. *Anticancer compounds of plant origin.*, New Hampshire, Science Publishers.
- GOLOVANCHIKOV, A. B. & POPOV, M. V. 1998. Extraction of active components from medicinal plants in an electric field. *Khimiko-Farmatsevticheskii Zhurnal*, 32, 31-33.
- HANAHAN, D. & WEINBERG, R. A. 2000. The hallmarks of cancer. *Cell*, 100, 57-70.
- HANNON, M. J. 2007. Metal-based anticancer drugs: From a past anchored in platinum post-genomic future and biology. *Pure and Applied Chemistry*, 79, 2243-2261.
- HAUPT, S., BERGER, M., GOLDBERG, Z. & HAUPT, Y. 2003. Apoptosis - the p53 network. *Journal of Cell Science*, 116, 4077-4085.
- HENDERSON, J. F. 1969. Variation in Selective Toxicity: Causes and Consequences. *Cancer Research*, 29, 2404-2406.
- HERMAN, B. 1998. *Fluorescence microscopy*, United Kingdom, Bios Scientific Publishers
- HUANG, K. T., CHEN, Y. H. & WALKER, A. M. 2004. Inaccuracies in MTS assays: major distorting effects of medium, serum albumin, and fatty acids. *BoiTechniques*, 37, 406-412.
- HUTCHINGS, A., SCOTT, A. L., LEWIS, G. & CUNNINGHAM, A. 1996. *Zulu Medicinal Plants*, Pinetown, University of Natal Press.
- IVANOV, E. V., SHVYREV, M. V., ARTEMOVA, M. A. & MININA, S. A. 2006. Extraction under vacuum-oscillation boiling conditions. *Pharmaceutical Chemistry Journal*, 40, 39-43.
- JEMAL, A., BRAY, F., CENTER, M. M., FERLAY, J., WARD, E. & FORMAN, D. 2011. Global Cancer Statistics. *Ca-a Cancer Journal for Clinicians*, 61, 69-90.
- JONNALAGADDA, S. B., KINDNESS, A., KUBAYI, S. & CELE, M. N. 2008. Macro, minor and toxic elemental uptake and distribution in Hypoxis hemerocallidea, "the African Potato"--an edible medicinal plant. *Journal of Environmental Science and Health, Part B*, 43, 271-80.
- KERRY, J. F. R., WYLLIE, A. H. & CURIE, A. R. 1972. Apoptosis: Basic Biological Phenomenon with Wide Ranging Implications in Tissue Kinetics. *British Journal of Cancer*, 26, 239-258.
- KIM, I. Y. 2007. Type I Collagem-induced Pro-MMP-2 activation is Differentially Regulated by H-Ras and N-Ras in Human Breast Epithelial Cells. *Journal of Biochemistry and Molecular Biology*, 40, 825-831.
- KOLS, A. 2002. Breast Cancer: Increasing Incidence, Limited Options. *PATH*, 19, 1-8.

- KRUGER, P. B., ALBRECHT, C. F., LIEBENBERG, R. W. & VAN JAARVELD, P. P. 1994. Studies on hypoxoside and rooperol analogues from *Hypoxis rooperi* and *Hypoxis latifolia* and their biotransformation in man by using high-performance liquid chromatography with in-line sorption enrichment and diode-array detection. *Journal of Chromatography B Biomedical Sciences and Applications*, 662, 71-78.
- KRYSKO, D. V., BERGHE, T. V., PATHOENS, E., D'HERDE, K. & VANDENABEELE, P. 2008. Methods for Distinguishing Apoptotic from Necrotic Cells and Measuring their Clearance. *Methods of Enzymology*, 442, 307-339.
- LANGDON, S. P. 2004. Basic principles of cancer cell culture. *Methods Mol Med*, 88, 3-15.
- LAPORTA, O., FUNES, L., GARZON, M. T., VILLALAIN, J. & MICOL, V. 2007a. Role of membranes on the antibacterial and anti-inflammatory activities of the bioactive compounds from *Hypoxis rooperi* corm extract. *Archives of Biochemistry and Biophysics*, 467, 119-131.
- LAPORTA, O., PEREZ-FONS, L., MALLAVIA, R., CATURLA, N. & MICOL, V. 2007b. Isolation, characterization and antioxidant capacity assessment of the bioactive compounds derived from *Hypoxis rooperi* corm extract (African potato). *Food Chemistry*, 101, 1425-1437.
- LEIST, M. & NICOTERA, P. 1997. The shape of cell death. *Biochemical and Biophysical Research Communications*, 236, 1-9.
- LI, Y., YANG, X., MA, C., QIAO, J. & ZHANG, C. 2008. Necroptosis contributes to the NMDA-induced excitotoxicity in rat's cultured cortical neurons. *Neuroscience Letters*, 447, 120-123.
- LICHTMAN, J. W. & CONCHELLO, J. A. 2005. Fluorescence microscopy. *Nature Methods*, 2, 910 - 919.
- LUTTMAN, W., BRATKE, K., KUPPER, M. & MYRTEK, D. 2006. *Immunology*, London, UK, Elsevier Inc.
- MA, X. & YU, H. 2006. Global burden of cancer. *The Yale Journal of Biology and Medicine*, 79, 85-94.
- MALICH, G., MARKOVIC, B. & WINDER, C. 1997. The sensitivity and specificity of the MTS tetrazolium assay for detecting the in vitro cytotoxicity of 20 chemicals using human cell lines. *Toxicology*, 124, 179-192.
- MARTINEZ, M. M., REIF, R. D. & PAPPAS, D. 2010. Detection of apoptosis: A review of conventional and novel techniques. *Analytical Methods*, 2, 996-1004.

- MATATIELE, P. R. 2008. Scientific letters: Breast cancer profiles of women presenting with newly diagnosed breast cancer at Universitas Hospital (Bloemfontein, South Africa). *South African Family Practice Journal*, 50.
- MILLER, F. R., SOULE, H. D., TAIT, L., PAULEY, R. J., WOLMAN, S. R., DAWSON, P. J. & HEPPNER, G. H. 1993. Xenograft model of progressive human proliferative breast disease. *Journal of the Nation Cancer Institute*, 85, 1725-1731.
- MILLER, R. J. 1981. *Simultaneous Statistical Inferences*, New York, Springer Verlag.
- MILLS, E., FOSTER, B. C., VAN HEESWIJK, R., PHILLIPS, E., WILSON, K., LEONARD, B., KOSUGE, K. & KANFER, I. 2005. Impact of African herbal medicines on antiretroviral metabolism. *Aids*, 19, 95-7.
- MOON, A., KIM, M. S., KIM, T. G., KIM, S. H., KIM, H. E., CHEN, Y. Q. & KIM, H. R. C. 2000. H-ras, but not N-ras, induces an invasive phenotype in human breast epithelial cells: A role for MMP-2 in the H-ras-induced invasive phenotype. *International Journal of Cancer*, 85, 176-181.
- MULHOLLAND, D. A. & DREWES, S. E. 2004. Global phytochemistry: indigenous medicinal chemistry on track in southern Africa. *Phytochemistry*, 65, 769-782.
- NAGY, M. A. 2011. HIF-1 is the Commander of Gateway to Cancer. *Cancer Science and Therapy*, 3, 35-40.
- NAIR, V. D., DAIRAM, A., AGBONON, A., ARNASON, J. T., FOSTER, B. C. & KANFER, I. 2007. Investigation of the antioxidant activity of African potato (*Hypoxis hemerocallidea*). *Journal of Agricultural and Food Chemistry* 55, 1707-11.
- NAIR, V. D. & KANFER, I. 2006. High-performance liquid chromatographic method for the quantitative determination of Hypoxoside in African potato (*Hypoxis hemerocallidea*) and in commercial products containing the plant material and/or its extracts. *J Agric Food Chem*, 54, 2816-21.
- NEWMAN, D. J. & CRAGG, G. M. 2012. Natural Products As Sources of New Drugs over the 30 Years from 1981 to 2010. *J. Nat. Prod*, 75, 311-335.
- NICHOLSON, D. W. 1999. Caspase structure, proteolytic substrates, and function during apoptotic cell death. *Cell Death and Differentiation*, 6, 1028-1042.
- NIKON 2000-2012. Microscopy U: The source for microscopic education.
- NIRMALA, M. J., SAMUNDEESWARI, A. & SANKAR, P. D. 2011. Natural plant resources in anti-cancer therapy-A review *Research in Plant Biology* 1, 01-14.

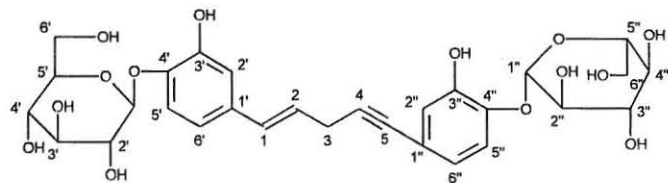
- O'TOOLE, S. A., SHEPPARD, B. L., MCGUINNESS, E. P. J., GLEESON, N. C., YONEDA, M. & BONNA, J. 2003. The MTS assay as an indicator of chemosensitivity/resistance in malignant gynaecological tumours. *Cancer detection and prevention*, 27, 47-54.
- OJEWOLE, J. A. 2006. Antinociceptive, anti-inflammatory and antidiabetic properties of *Hypoxis hemerocallidea* Fisch. & C.A. Mey. (Hypoxidaceae) corm ['African Potato'] aqueous extract in mice and rats. *Journal of Ethnopharmacology*, 103, 126-34.
- OJEWOLE, J. A. 2008. Anticonvulsant activity of *Hypoxis hemerocallidea* Fisch. & C. A. Mey. (Hypoxidaceae) corm ('African potato') aqueous extract in mice. *Phytother Res*, 22, 91-6.
- OJEWOLE, J. A., KAMADYAAPA, D. R. & MUSABAYANE, C. T. 2006. Some in vitro and in vivo cardiovascular effects of *Hypoxis hemerocallidea* Fisch & CA Mey (Hypoxidaceae) corm (African potato) aqueous extract in experimental animal models. *Cardiovasc J S Afr*, 17, 166-71.
- OLYMPUS 2012. Microscopy resource centre.
- ORMEROD, M. G. 1994. *Flow Cytometry*, Oxford, UK, Bios Scientific Publishers.
- OTA, I., LI, X.-Y., HU, Y. & WEISS, S. J. 2009. Induction of a MT1-MMP and MT2-MMP-dependent basement membrane transmigration program in cancer cells by Snail1. *Proceedings of the National Academy of Sciences*, 106, 20318-20323.
- OWIRA, P. M. & OJEWOLE, J. A. 2009. 'African potato' (*Hypoxis hemerocallidea* corm): a plant-medicine for modern and 21st century diseases of mankind? - a review. *Phytotherapy Research*, 23, 147-52.
- PEREIRA, W. O. & AMARANTE-MENDES, G. P. 2011. Apoptosis: A programme of cell death or cell disposal? *Scandinavian Journal of Immunology*, 73, 401-407.
- PETER, M. E. 2011. Programmed cell death: Apoptosis meets necrosis. *Nature*, 471, 310-312.
- PHELAN, M. C. 1996. Techniques for Mammalian Cell. *Current Protocols in Molecular Biology* A.3F.1-A.3F.14.
- PRATT, W. B., RUDDON, R. W., ENSMINGER, W. D. & MAYBAUM, J. 1994. *The Anticancer Drugs.*, New York, Oxford University Press.
- PROMEGA 2009. CellTiter 96 aqueous non-radioactive cell proliferation assay.
- RANPURA, V. 2011. Treatment-related mortality with bevacizumab in cancer patients: A meta-analysis *Jama-Journal of the American Medical Association*, 305, 2294-2294.

- RASTOGI, R. P., RICHA & SINHA, R. P. 2009. Apoptosis: molecular mechanisms and pathogenicity. *Experimental and Clinical Sciences, International Journal* 8, 155-181.
- RIEGER, A. M., HALL, B. E., LUONG, L. T., SCHANG, L. M. & BARREDA, D. R. 2010. Conventional apoptosis assays using propidium generate a significant number of false positive that prevent accurate assessment of cell death. *Journal of Immunological Methods*, 358, 81-92.
- RUSSO, J., TAIT, L. & RUSSO, I. H. 1991. Morphological expression of cell transformation induced by c-Ha-ras oncogene in human breast epithelial cells. *Journal of Cell Science*, 99, 453-463.
- SAMEJIMA, K. & EARNSHAW, W. C. 2005. Trashing the genome: the role of nucleases during apoptosis. *Nat Rev Mol Cell Biol*, 6, 677-688.
- SEMROCK. A unit of IDEX corporation.
Available: www.semrock.com/flowcytometry.aspx. Accessed [17 May 2011]
- SCHULER, M. & GREEN, D. R. 2001. Mechanisms of p53-dependent apoptosis. *Biochemical Society Transactions*, 29, 684-686.
- SHAPIRO, H. M. 2003. *Practical Flow Cytometry.*, Hoboken, New Jersey, John Wiley and Sons.
- SHOEB, M. 2006. Anticancer agents from medicinal plants. *Bangladesh Journal of Pharmacology*, 1, 35-41.
- SIMON, J. A., SZANKASI, P., NGUYEN, D. K., LUDLOW, C., DUNSTAN, H. M., ROBERTS, C. J., JENSEN, E. L., HARTWELL, L. H. & FRIEND, S. H. 2000. Differential Toxicities of Anticancer Agents among DNA Repair and Checkpoint Mutants of *Saccharomyces cerevisiae*1. *CANCER RESEARCH* 60, 328–333.
- SMIT, B. J., ALBRECHT, C. F., LIEBENBERG, R. W., KRUGER, P. B., FREESTONE, M., GOUWS, L., THERON, E., BOUIC, P. J., ETSEBETH, S. & VAN JAARSVELD, P. P. 1995. A phase I trial of hypoxoside as an oral prodrug for cancer therapy--absence of toxicity. *S Afr Med J*, 85, 865-70.
- SOULE, H. D., MALONEY, T. M., WOLMAN, S. R., PETERSON, W. D., BRENZ, J. R., MCGRATH, C. M., RUSSO, J., PAULEY, R. J., JONES, R. F. & BROOKS, S. E. 1990. Isolation and characterization of a spontaneously immortalized human breast epithelial cell line, MCF-10¹. *Cancer Research*, 50, 6075-6086.
- SPANDIDOS, D. A., SOURVINOS, G. & MIYAKIS, S. 1999. Transcriptional activation of the *ras* oncogenes and implications of *BRAC1* in the cell cycle regulation through *p53* checkpoint. *Gene Therapy and Molecular Biology*, 3, 373-378.

- STEPHAN, P. 2009. Ductal, Lobular, Inflammatory, and Paget's. *Types of Breast Cancer*.
- STROBER, W. 2001. Trypan Blue Exclusion Test of Cell Viability. *Current Protocols in Immunology*. John Wiley & Sons, Inc.
- SWEDLOW, J. R. 2003. Quantitative fluorescence microscopy and image deconvolution. *Methods in Cell Biology*, 72, 349-367.
- TAIT, L., SOULE, H. D. & RUSSO, J. 1990. Ultrastructural and Immunocytochemical characterization of an immortalized human breast epithelial cell line, MCF-10¹. *Cancer Research*, 50, 6087-6094.
- TELFORD, W. G., KOMORIYA, A. & PACKARD, B. Z. 2004. Multiparametric Analysis of Apoptosis by Flow and Image Cytometry. *Methods in Molecular Biology: Flow Cytometry Protocols*, 2, 141-159.
- TRAPANI, J. A. & SMYTH, M. J. 2002. Functional Significance of the Perforin/Granzyme Cell Death Pathway. *Nature Reviews Immunology*, 2, 735-747.
- TUMBURRINO, L., MARCHIANI, S., MANTOYA, M., MARINO, F. E., NATALI, I., CAMBI, M., FORTI, G., BALDI, E. & MURATORI, M. 2011. Mechanisms and clinical correlates of sperm DNA damage. *Asian Journal of Andrology*, 1-8.
- VAN DOOREN, B. T., BEEKHUIS, W. H. & PELS, E. 2004. Biocompatibility of trypan blue with human corneal cells. *Arch Ophthalmol*, 122, 736-42.
- VAN ENGLAND, M., RAMAEKERS, F. C. S., SCHUTTE, B. & REUTELINGSPERGER, C. P. M. 1996. A novel assay to measure loss of plasma membrane asymmetry during apoptosis of adherent cells in culture. *Cytometry*, 24, 131-139.
- VASKIVUO, T. 2002. Regulation of apoptosis in the female reproductive system. *Oulu University Library*.
- VERMS, I., HANAAN, C., STEFFENS-NAKKEN, H. & REUTELINGSPERGER, C. 1995. A novel assay for apoptosis Flow cytometric detection of phosphatidylserine early apoptotic cells using fluorescein labelled expression on Annexin V. *Journal of Immunological Methods*, 39, 39-51.
- VISAGIE, M. H. & JOUBERT, A. M. 2011. 2-Methoxyestradiol-bis-sulfamate induces apoptosis and autophagy in a tumorigenic breast epithelial cell line. *Molecular Cell Biochemistry*.
- WANG, K., LI, J., DEGTEREV, A., HSU, E., YUAN, J. & YUAN, C. 2007. Structure-activity relationship analysis of a novel necroptosis inhibitor, Necrostatin-5. *Bioorganic & Medicinal Chemistry Letters*, 17, 1455-1465.

- WANG, P., HENNING, S. M. & HEBER, D. 2010. Limitations of MTT and MTS-based assays for measurement of antiproliferative activity of green tea polyphenols. *Plos One*, 5.
- WHO. 2006. Cancer. Available: www.who.int/mediacentre/fs297/en/. Accessed [18 August 2011]
- YANG, L., MENG, L., ZANG, X., CHEN, Y., ZHU, G., LIU, H., XIONG, X., SEFAH, K. & TAN, W. 2011. Engineering Polymeric Aptamers for Selective Cytotoxicity. *American Chemical Society*, 133, 13380–13386.
- YASUHARA, S., ZHU, Y., MATSUI, T., TIPIRNENI, N., YASUHARA, Y., KANENI, M., ROSENZWEIG, A. & MARTYN, J. A. 2003. Comparison of Comet Assay, Electron Microscopy, and Flow Cytometry for Detection of Apoptosis. *The Journal of Histochemistry and Cytochemistry*., 51, 873-885.
- ZAMAI, L., CANONICO, B., LUCHETTI, F., FERRI, P., MELLONI, E., GUIDOTTI, L., CAPELLINI, L., CUTRONEO, G., VITALE, M. & PAPA, S. 2001. Suprafacial Exposure to Propidium Iodide Identifies Apoptosis on Adherent cells. *Cytometry*, 44, 57-64.
- ZIBULA, S. M. X. & OJEWOLE, J. A. O. 2000. Hypoglycaemic effects of *Hypoxis hemerocallidea* (Fisch and C.A. Mey.) corm 'african potato' methanolic extracts in rats. *Medical Journal of Islamic Academy of Sciences*, 13, 75-78.
- ZIENTEK-TARGOSZ, H., KUNNEV, D., HOWTHORN, L., VENKOV, M., MATSUI, S., CHENEY, R. T. & IONOV, Y. 2008. Transformation of MCF-10A cells by random mutagenesis with frameshift mutagen ICR191: A model for identifying candidate breast-tumor suppressors. *Molecular Cancer*, 7, 1-12.

APPENDIX A: NMR SPECTRA AND HR-MASS SPECTRA Plate 1: ¹H NMR of hypoxoside



Hypox in CD3OD

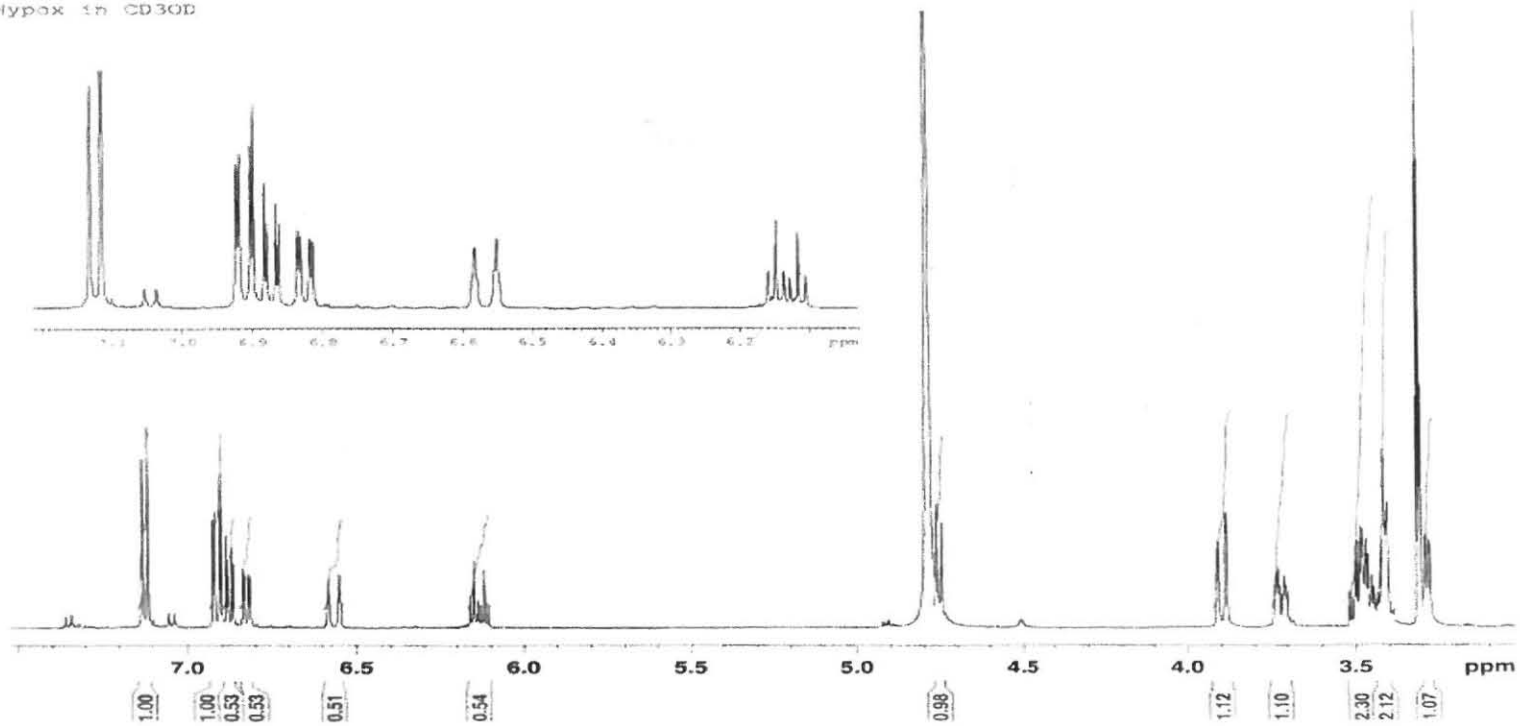


Plate 3: DEPT 135 spectrum of hypoxoside.

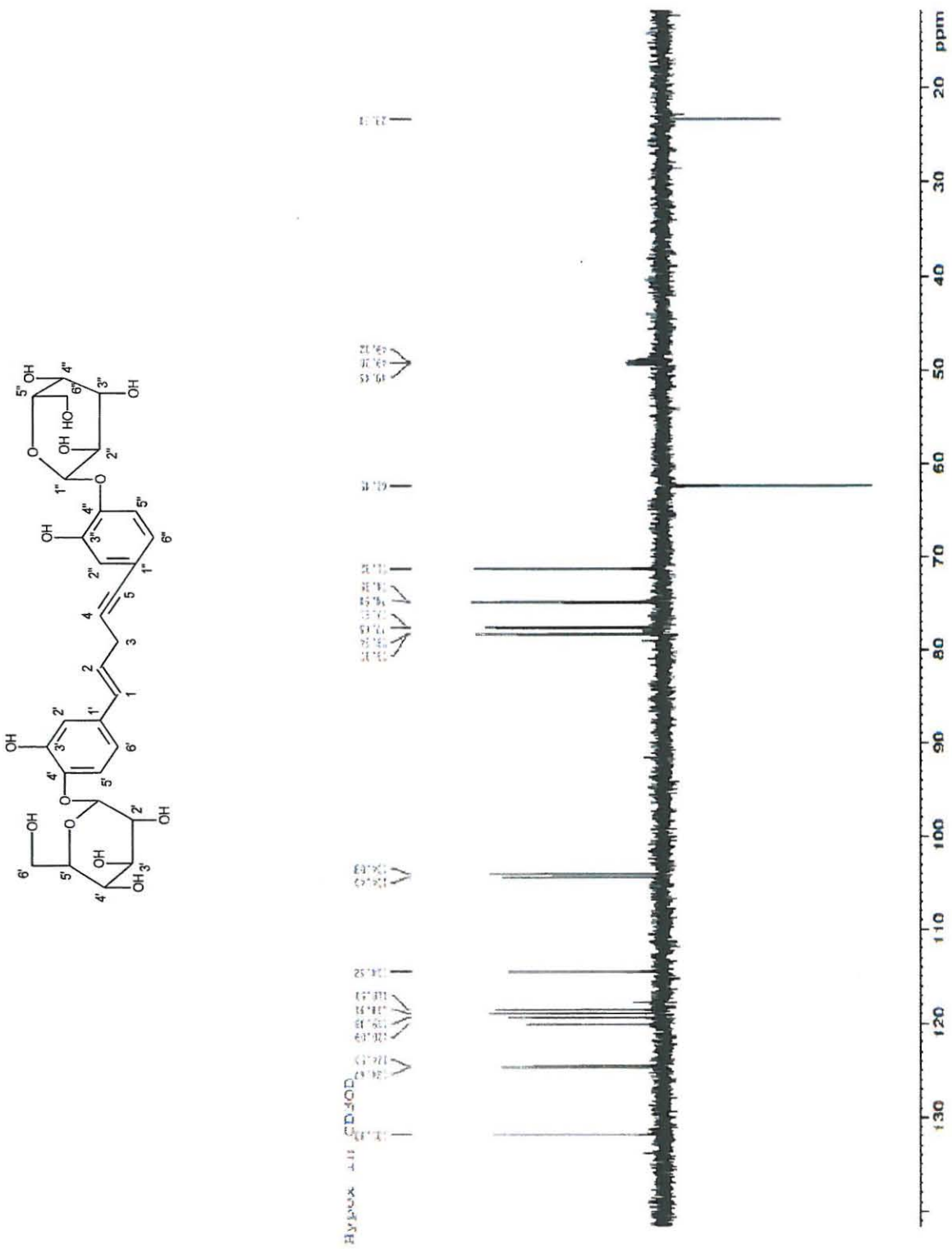


Plate 4: COSY 45 spectrum of hypoxoside

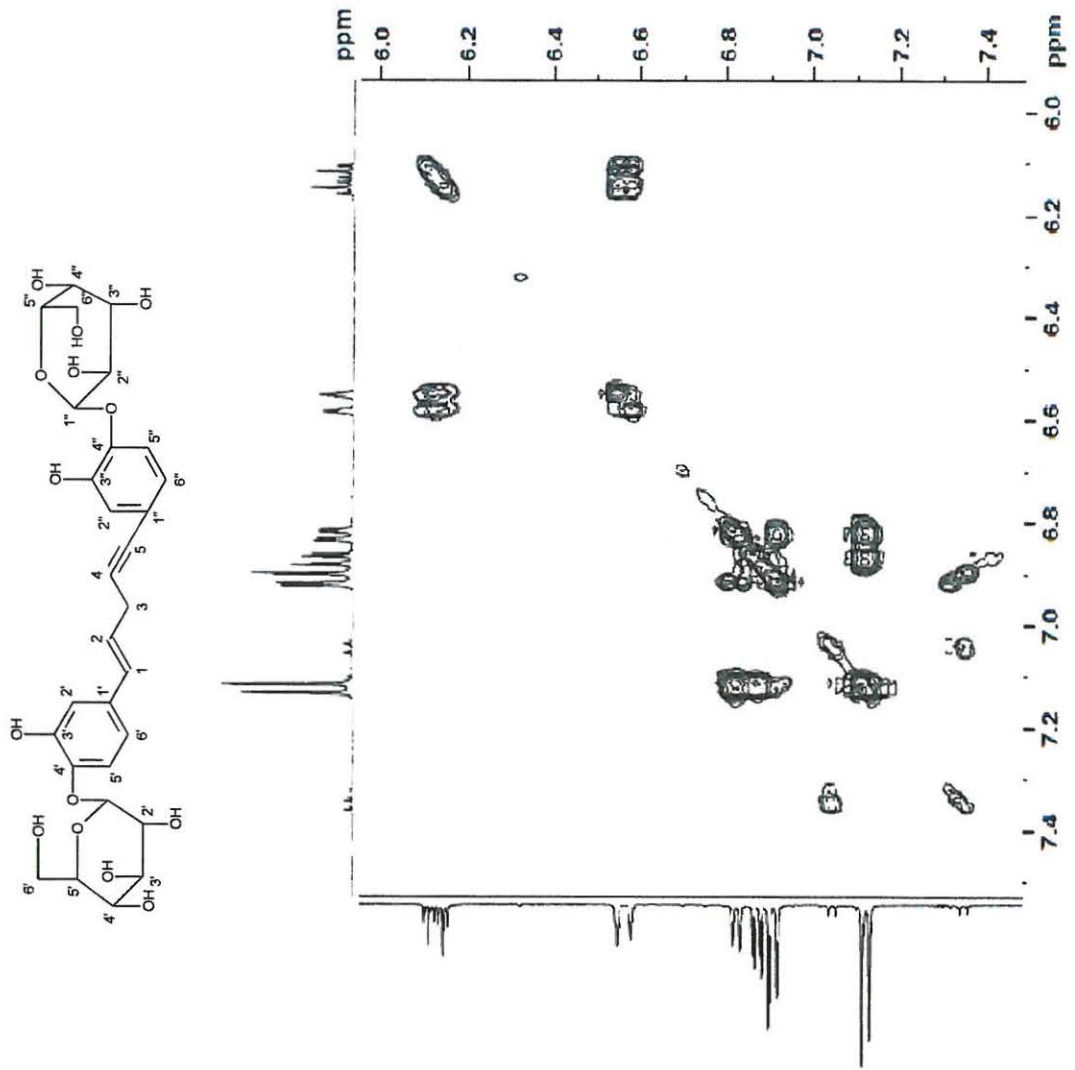
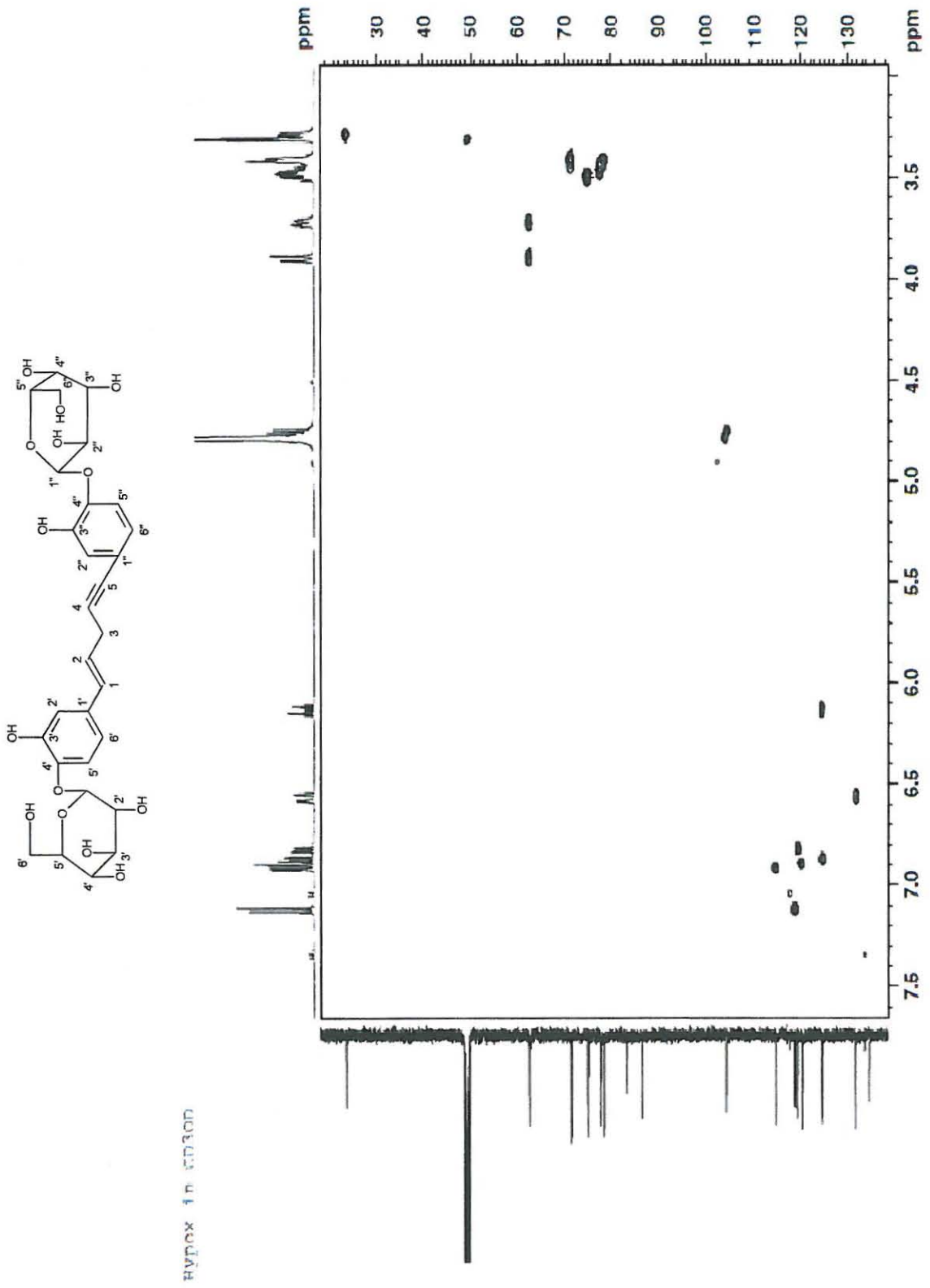
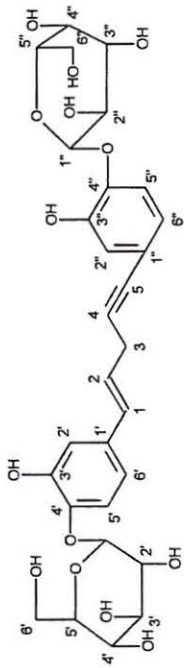


Plate 5: GHSQC spectrum of hypoxoside.



hypox in ethanol

Plate 6: GCOSY of hypoxoside.



HYPXOS in CDCl₃

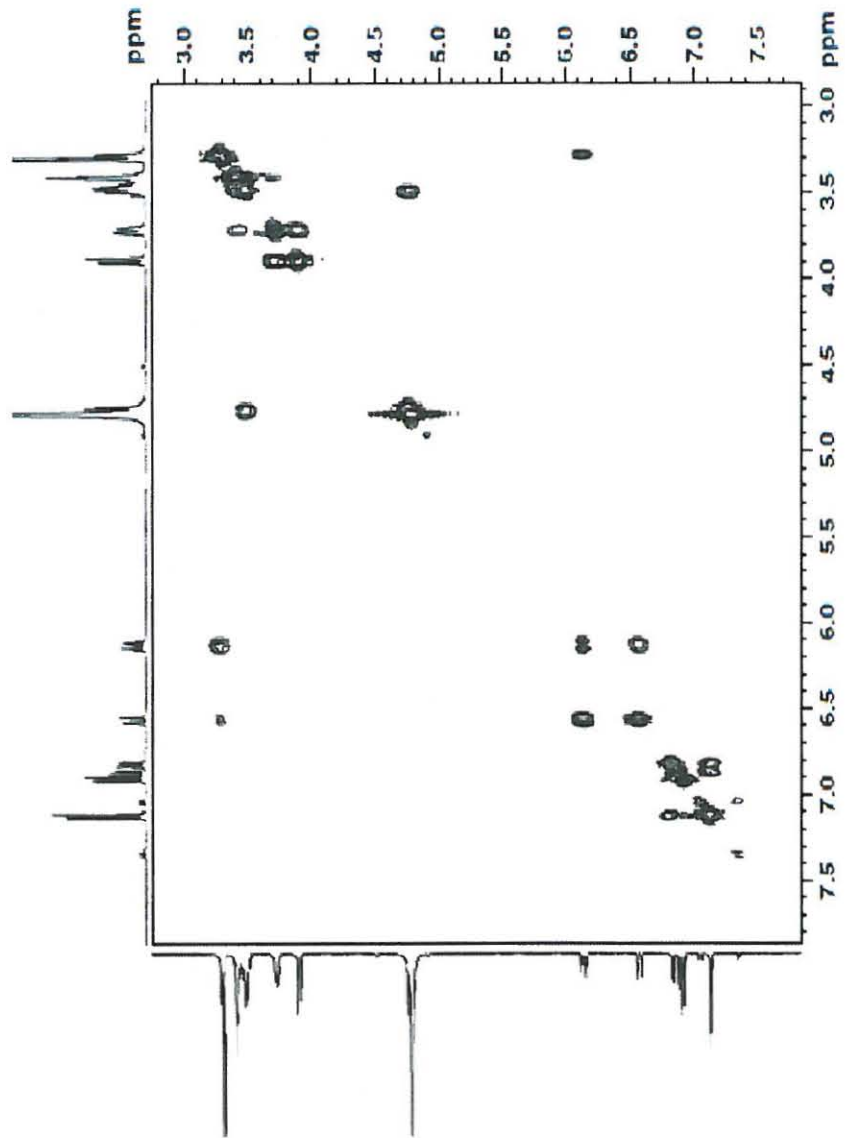
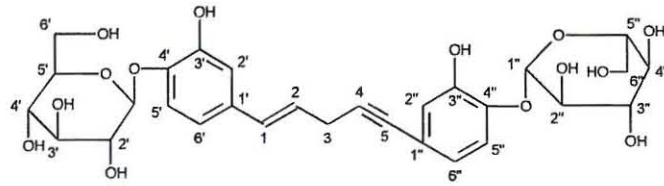


Plate 7: GHMBC spectrum of hypoxoside.



Hypox in CD3OD

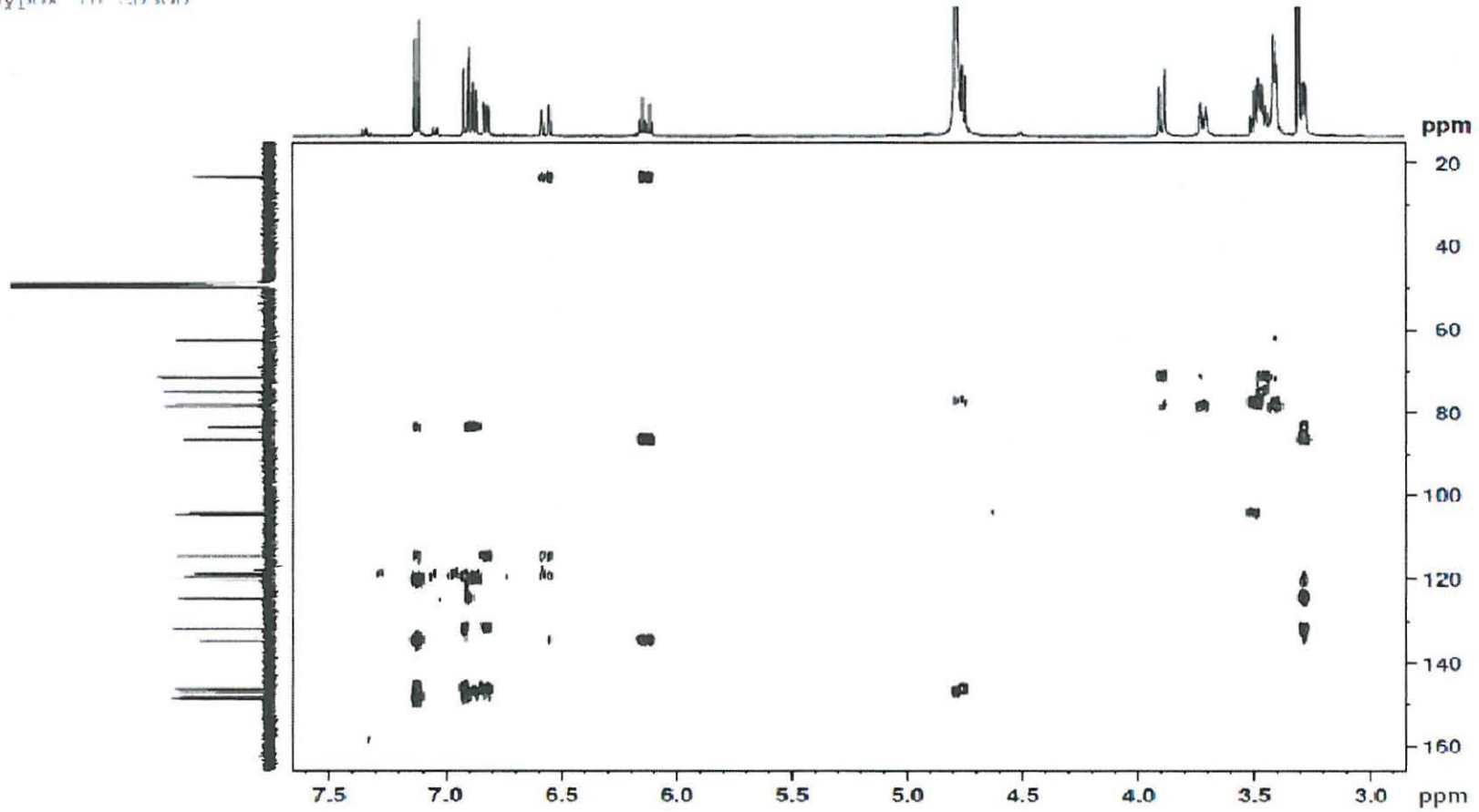


Plate 8: ^1H NMR of dimethylhypoxoside.

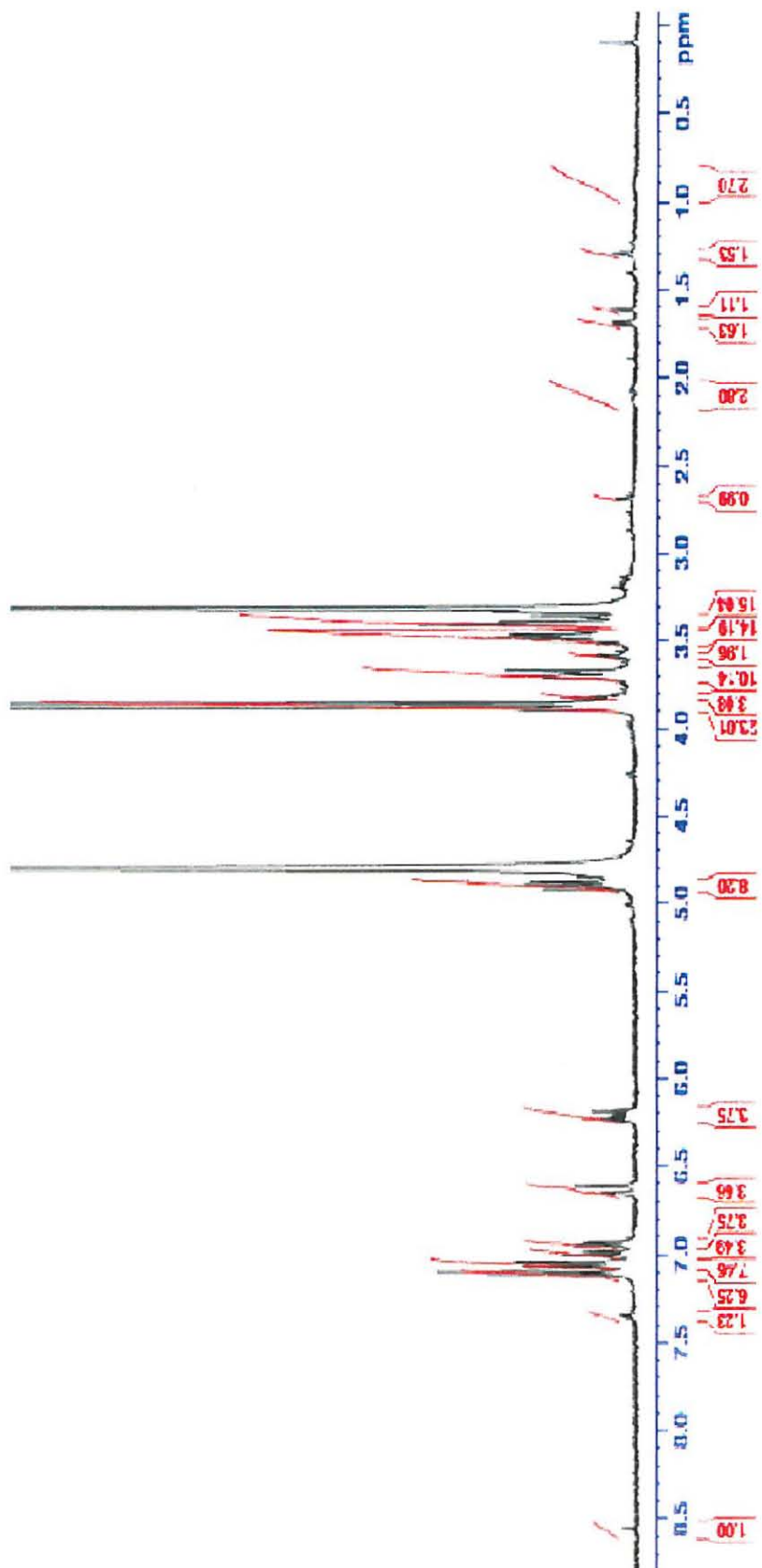
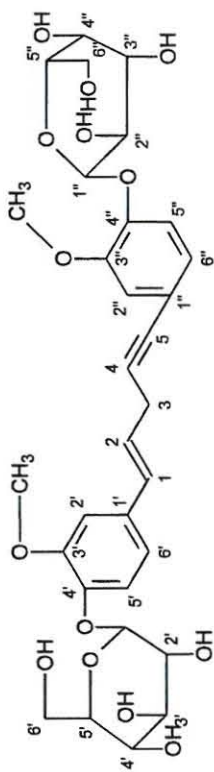
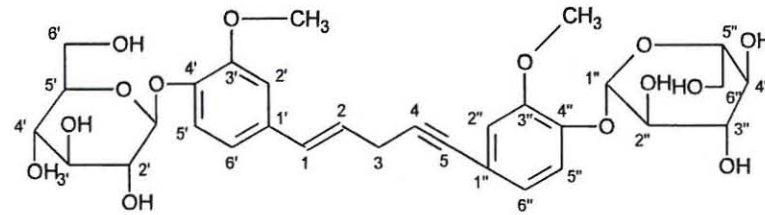


Plate 9: HR-MS of dimethylhypoxoside.



Single Mass Analysis

Tolerance = 4.0 PPM / DBE: min = -1.5, max = 50.0

Element prediction: Off

Number of isotope peaks used for i-FIT = 3

Monoisotopic Mass, Even Electron Ions

3 formula(e) evaluated with 1 results within limits (all results (up to 1000) for each mass)

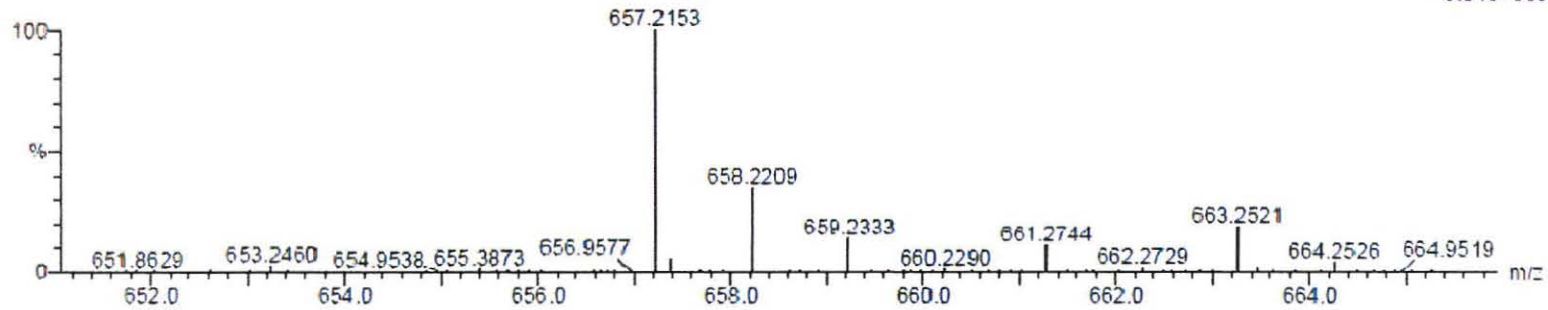
Elements Used:

C: 30-35 H: 35-40 O: 10-15 Na: 0-1

Prof. Drewes

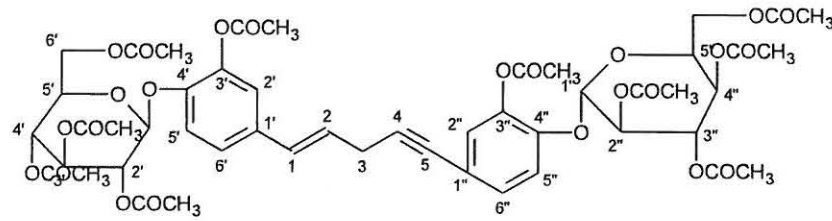
HYPOX Methoxy 20 (0.340)

TOF MS ES+
9.91e+003



Mass	Calc. Mass	mDa	DDM	DBE	i-FIT	i-FIT (Norm)	Formula
657.2153	657.2159	-0.6	-0.9	12.5	92.5	0.0	C31 H38 O14 Na

Plate 10: ^1H NMR of decaacetylhypoxoside.



DAH in CDCl₃

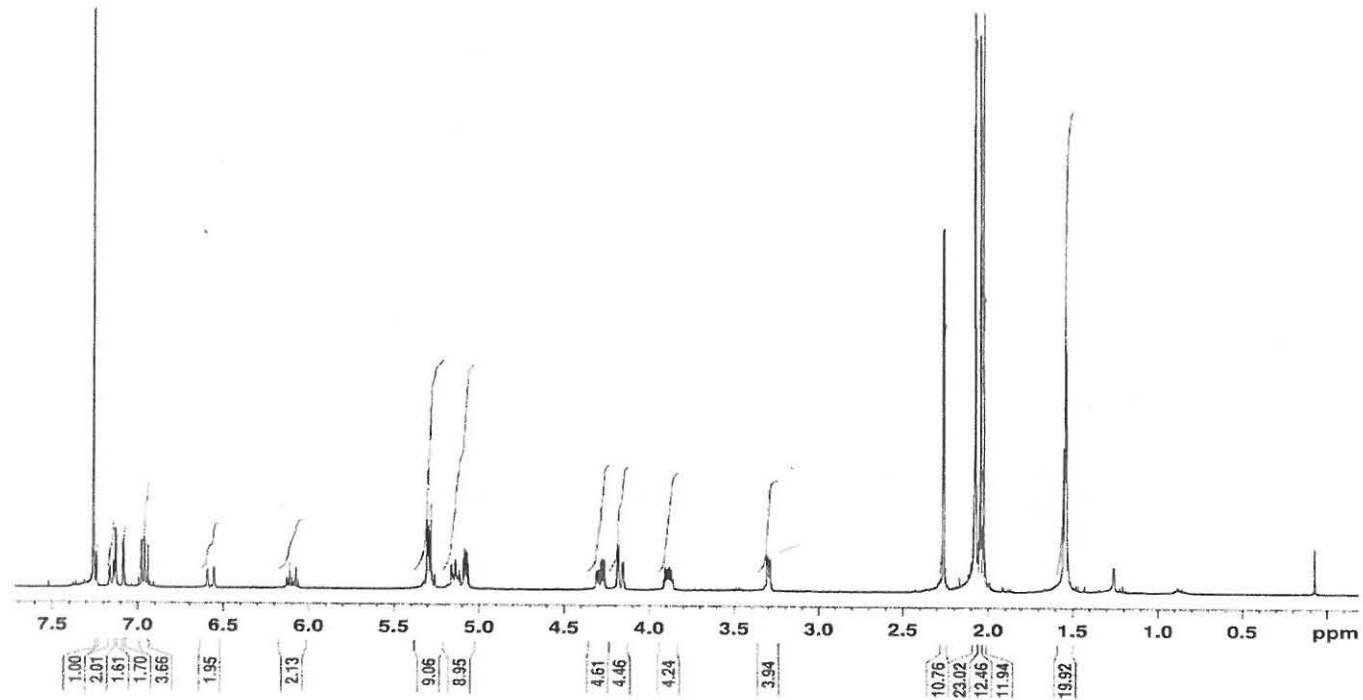
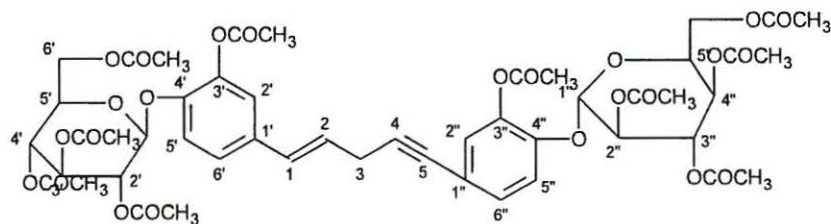


Plate 11: HR-MS of decaacetylhypoxoside.



Single Mass Analysis

Tolerance = 4.0 PPM / DBE: min = -1.5, max = 50.0

Element prediction: Off

Number of isotope peaks used for i-FIT = 3

Monoisotopic Mass, Even Electron Ions

2 formula(e) evaluated with 1 results within limits (all results (up to 1000) for each mass)

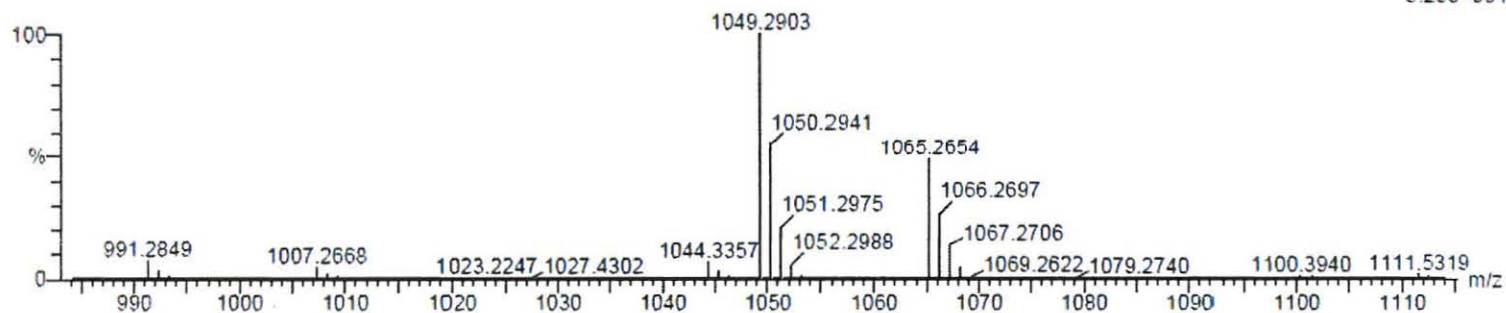
Elements Used:

C: 45-50 H: 50-55 O: 20-25 Na: 0-1

Prof. Drewes

HYPOX acetate 2 (0.017) Cm (1:60)

TOF MS ES+
5.25e+004



Minimum: -1.5
Maximum: 5.0 4.0 50.0

Mass	Calc. Mass	mDa	PPM	DBE	i-FIT	i-FIT (Norm)	Formula
1049.2903	1049.2903	0.0	0.0	22.5	320.7	0.0	C ₄₉ H ₅₄ O ₂₄ Na

APPENDIX B: FLOW CYTOMETRY RESULTS.

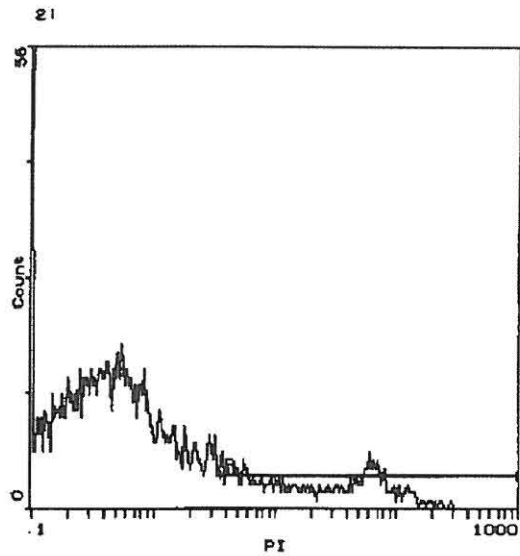
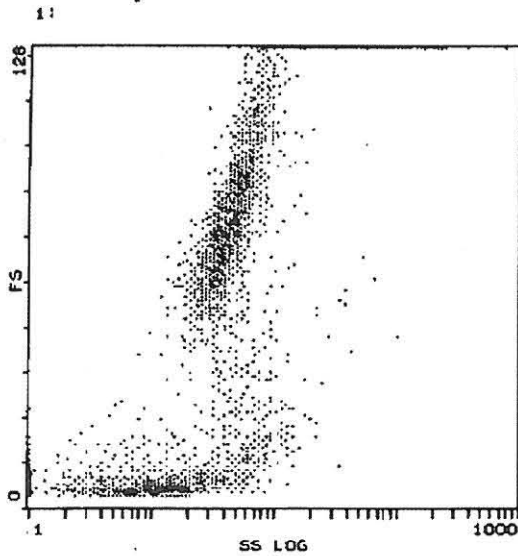
For abbreviation key-see end

A Beckman Coulter Epics XL-MCL

COULTER(R) EPICS(R) Listmode Replay Flow Cytometry Report
 C:\XLLMD\Z0012268.LMD, XL RAG18011, Run time protocol

OP ID: MJ722928

29Aug11 13:37:02
 PROPIDIUM IODIDE 2
 Z0012268
 med contrl nt
 120 seconds, 8179 events
 Stop Time: 120 secs



Stats: Not Normalized, Listgating: Disabled

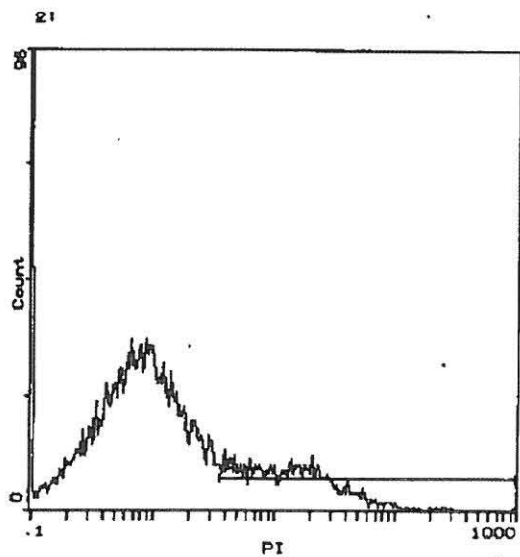
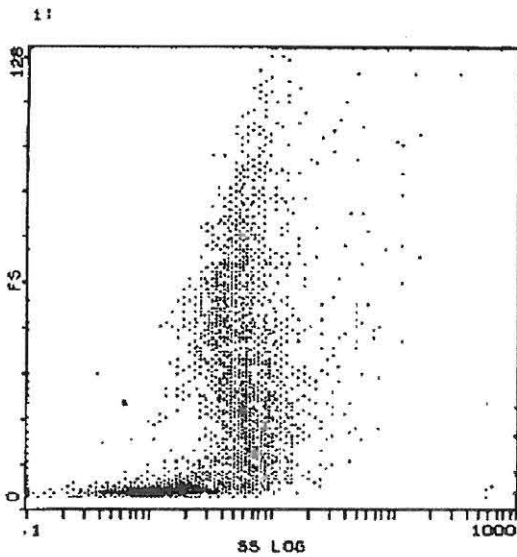
Hist	Region ID	%	Count	Mn X	Med X	PkPosX	PkCnt	HPCV	Min	Max
2	A B	14.3	1312	22.2	22.1	3.77	10	0.70	3.61	1024

B Beckman Coulter Epics XL-MCL

COULTER(R) EPICS(R) Listmode Replay Flow Cytometry Report
 C:\XLLMD\Z0012267.LMD, XL RAG18011, Run time protocol

OP ID: MJ722928

29Aug11 13:34:02
 PROPIDIUM IODIDE 2
 Z0012267
 chr contrl nto
 120 seconds, 10994 events
 Stop Time: 120 secs



Stats: Not Normalized, Listgating: Disabled

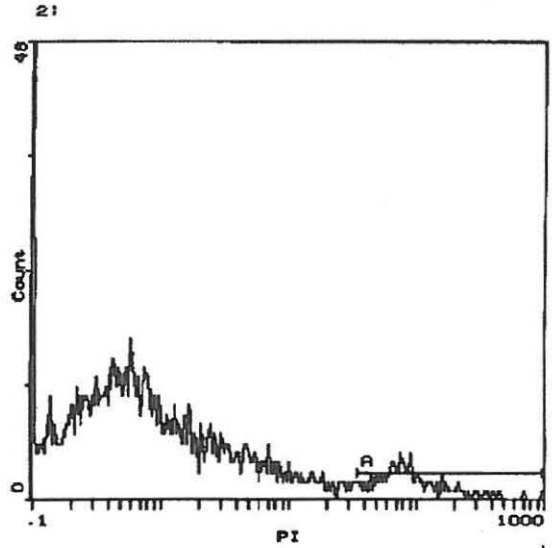
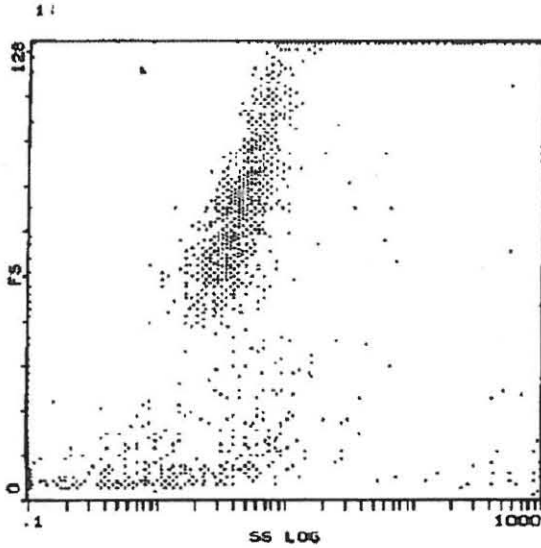
Hist	Region ID	%	Count	Mn X	Med X	PkPosX	PkCnt	HPCV	Min	Max
2	A B	23.4	2674	14.1	13.2	4.06	23	0.77	3.61	1024

C Beckman Coulter Epics XL-MCL

COULTER(R) EPICS(R) Listmode Replay Flow Cytometry Report
 C:\XL\LM\Z0012269.LMD, XL RAG19011, Run time protocol

OP ID: MJ722928

29Aug11 13:42:01
 PROPIDIUM IODIDE 2
 Z0012269
 150 hyp nt
 120 seconds, 6996 events
 Stop Time: 120 secs



Stats: Not Normalized, Listgating: Disabled

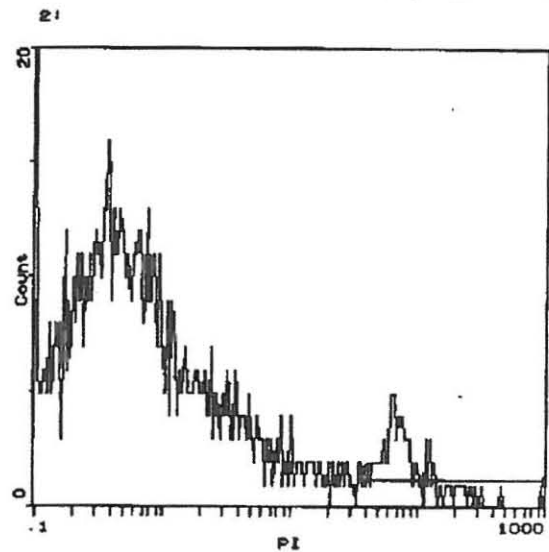
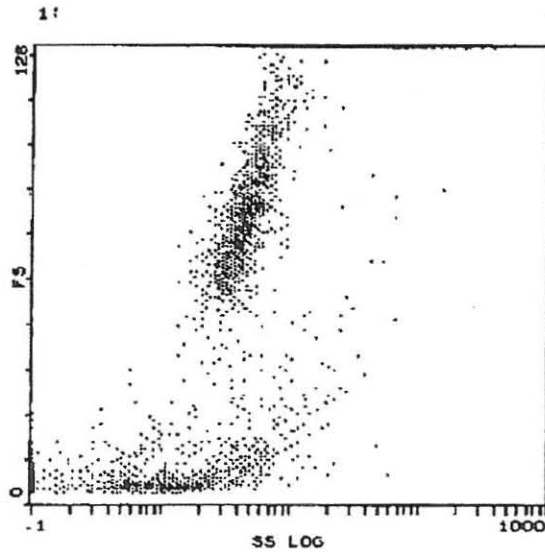
Hist	Region ID	%	Count	Min X	Mid X	PkPosX	PkCnt	HPCV	Min	Max
2	A B	6.97	488	101.0	87.8	81.0	7	0.91	35.4	1024

Beckman Coulter Epics XL-MCL

COULTER(R) EPICS(R) Listmode Replay Flow Cytometry Report
 C:\XL\LM\Z0012270.LMD, XL RAG18011, Run time protocol

OP ID: MJ722928

29Aug11 13:46:10
 PROPIDIUM IODIDE 2
 Z0012270
 300 hyp nt
 120 seconds, 6210 events
 Stop Time: 120 secs



Stats: Not Normalized, Listgating: Disabled

Hist	Region ID	%	Count	Min X	Mid X	PkPosX	PkCnt	HPCV	Min	Max
2	A B	6.51	404	86.9	75.1	63.0	7	1.60	35.4	1024

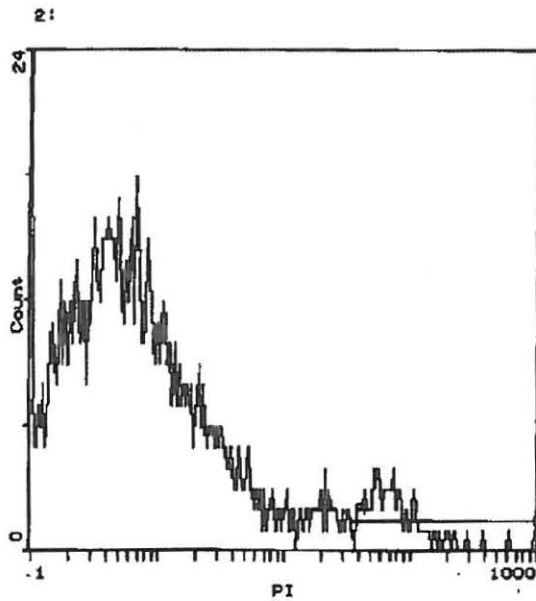
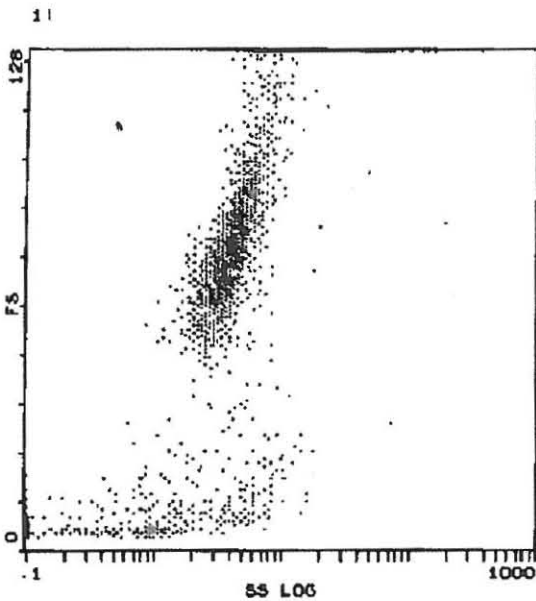
E

Beckman Coulter Epics XL-MCL

COULTER(R) EPICS(R) Listmode Replay Flow Cytometry Report
 C:\XL\LMD\20012271.LMD, XL RAG19011, Run time protocol

OP ID: MJ722928

29Aug11 13:48:41
 PROPIDIUM IODIDE 2
 Z0012271
 4.8 dmh nt
 120 seconds, 7088 events
 Stop Time: 120 secs



Stats: Not Normalized, Listgating: Disabled

Hist	Region ID	%	Count	Mn X	Md X	PkPosX	PkCnt	HPCV	Min	Max
2	A B	5.12	363	82.5	73.0	45.2	8	0.67	35.4	1024

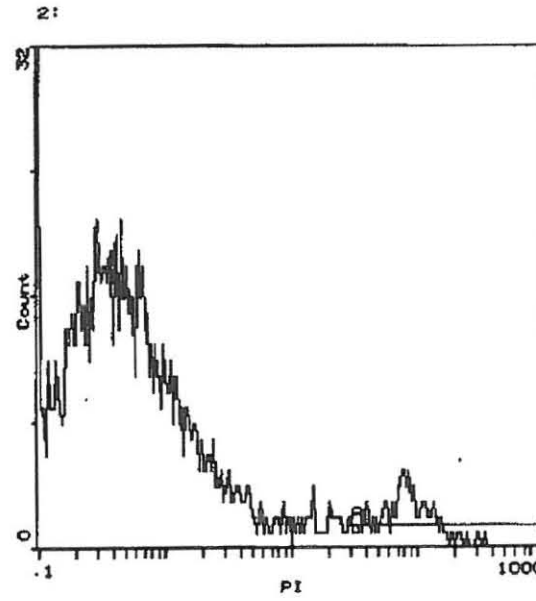
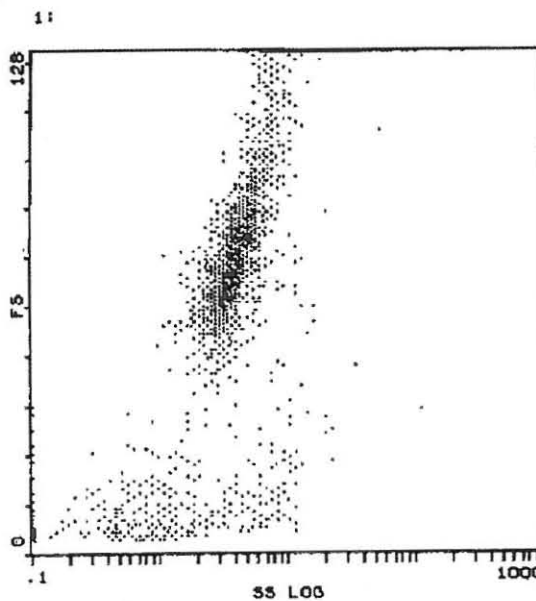
F

Beckman Coulter Epics XL-MCL

COULTER(R) EPICS(R) Listmode Replay Flow Cytometry Report
 C:\XL\LMD\20012272.LMD, XL RAG19011, Run time protocol

OP ID: MJ722928

29Aug11 13:51:37
 PROPIDIUM IODIDE 2
 Z0012272
 19 dmh nt
 120 seconds, 8432 events
 Stop Time: 120 secs



Stats: Not Normalized, Listgating: Disabled

Hist	Region ID	%	Count	Mn X	Md X	PkPosX	PkCnt	HPCV	Min	Max
2	A B	5.83	492	84.5	82.5	78.9	8	1.55	28.6	961.5

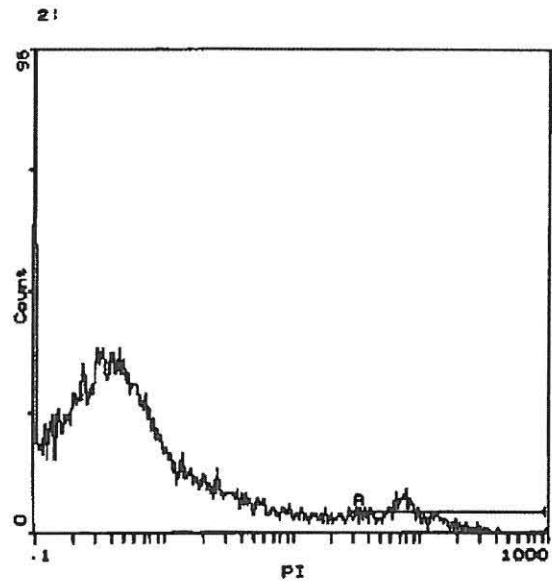
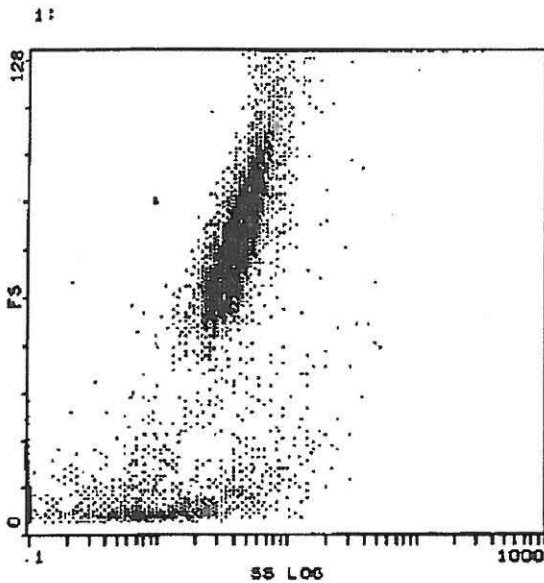
G

Beckman Coulter Epics XL-MCL

COULTER(R) EPICS(R) Listmode Replay Flow Cytometry Report
 C:\XL\LM\Z0012273.LMD, XL RAG19011, Run time protocol

29Aug11 13:54:11
 PROPIDIUM IODIDE 2
 Z0012273
 75 dmh nt
 120 seconds, 16312 events
 Stop Time: 120 secs

OP ID: MJ722928



Stats: Not Normalized, Listgating: Disabled

Hist	Region ID	%	Count	Mn X	Mid X	PkPosX	PkCnt	HPCV	Min	Max
2	A B	5.66	907	80.7	77.7	71.5	14	0.58	28.6	961.5

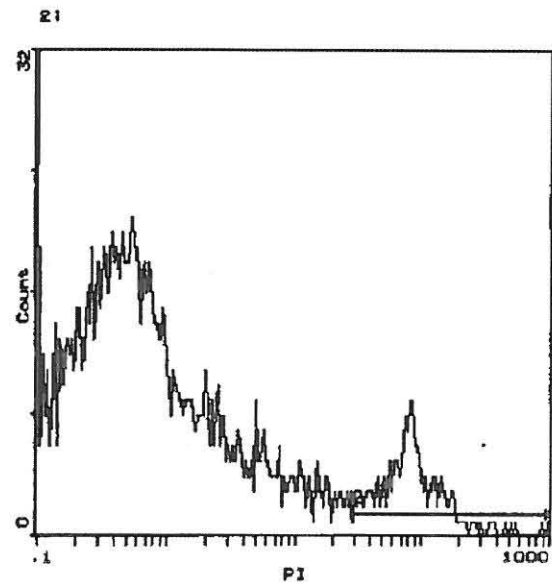
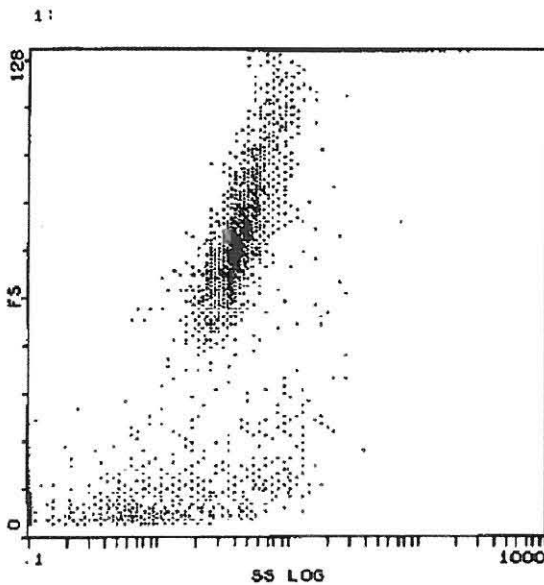
H

Beckman Coulter Epics XL-MCL

COULTER(R) EPICS(R) Listmode Replay Flow Cytometry Report
 C:\XL\LM\Z0012274.LMD, XL RAG19011, Run time protocol

29Aug11 13:56:50
 PROPIDIUM IODIDE 2
 Z0012274
 300 dmh nt
 120 seconds, 9769 events
 Stop Time: 120 secs

OP ID: MJ722928



Stats: Not Normalized, Listgating: Disabled

Hist	Region ID	%	Count	Mn X	Mid X	PkPosX	PkCnt	HPCV	Min	Max
2	A B	8.77	867	85.9	83.4	78.9	12	1.15	28.6	961.5

I Beckman Coulter Epics XL-MCL

COULTER(R) EPICS(R) Listmode Replay Flow Cytometry Report
 C:\XL\MD\Z0012275.LMD, XL RAG19011, Run time protocol

29Aug11 13:59:24

PROPIDIUM IODIDE 2

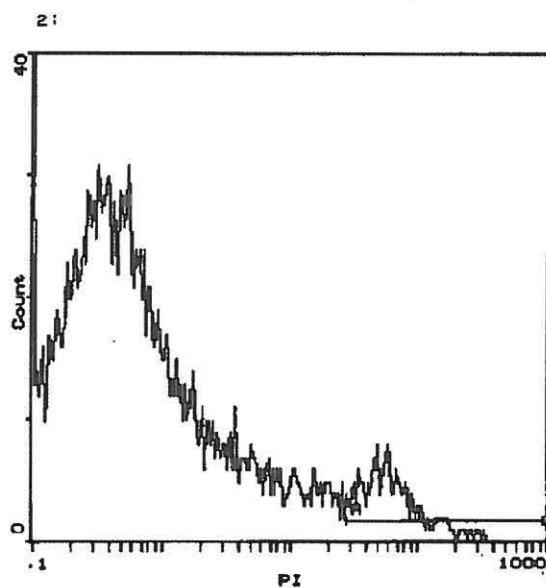
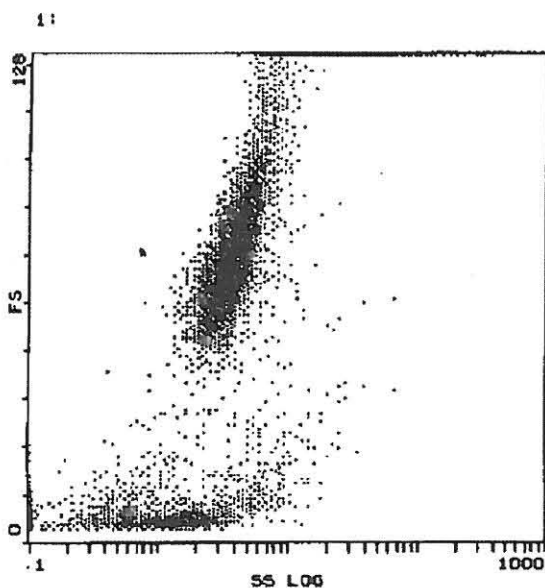
Z0012275

4.8 dah nt

OP ID: MJ722928

120 seconds, 14413 events

Stop Time: 120 secs



Stats: Not Normalized, Listgating: Disabled

Hist	Region ID	%	Count	Mn X	Md X	PkPosX	PkCnt	HPCV	Min	Max
2	A B	5.61	808	66.9	60.7	51.2	13	0.58	28.8	981.5

J Beckman Coulter Epics XL-MCL

COULTER(R) EPICS(R) Listmode Replay Flow Cytometry Report
 C:\XL\MD\Z0012276.LMD, XL RAG19011, Run time protocol

29Aug11 14:02:06

PROPIDIUM IODIDE 2

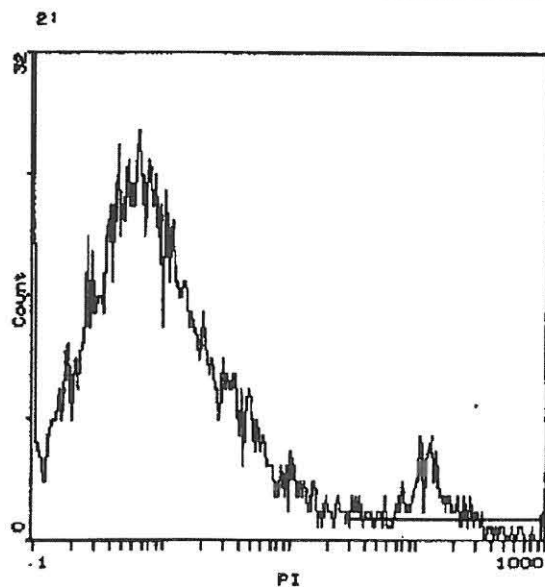
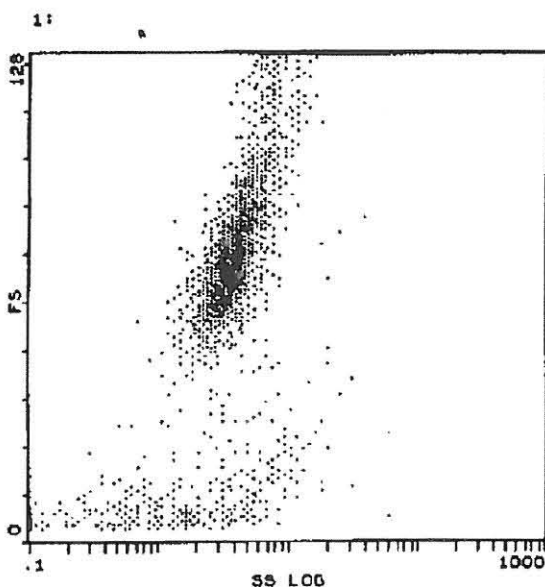
Z0012276

19 dah nt

OP ID: MJ722928

120 seconds, 9609 events

Stop Time: 120 secs



Stats: Not Normalized, Listgating: Disabled

Hist	Region ID	%	Count	Mn X	Md X	PkPosX	PkCnt	HPCV	Min	Max
2	A B	7.63	739	115.4	121.2	124.8	11	0.47	28.8	981.5

K

Beckman Coulter Epics XL-MCL

COULTER(R) EPICS(R) Listmode Replay Flow Cytometry Report
 C:\XL\LMD\Z0012277.LMD, XL RAG19011, Run time protocol

OP ID: MJ722928

28Aug11 14:04:36

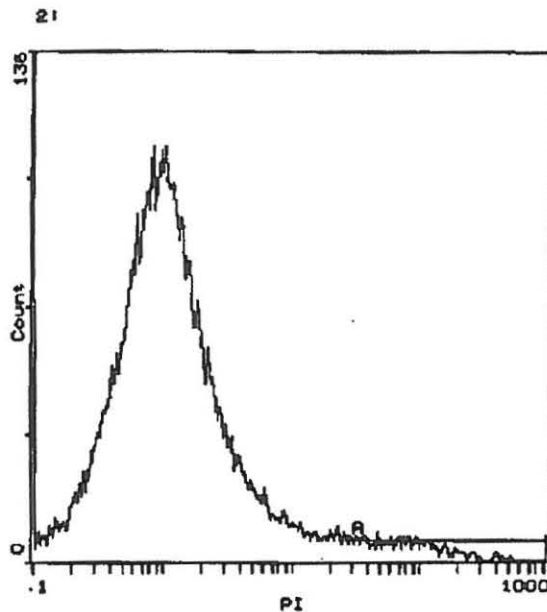
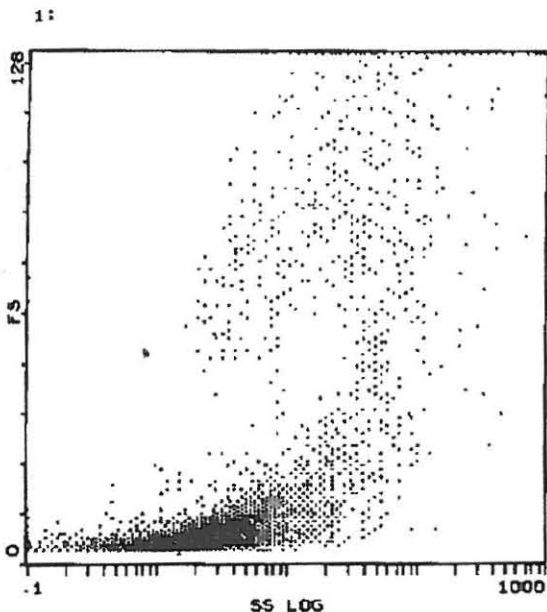
PROPIDIUM IODIDE 2

Z0012277

75 dah nt

120 seconds, 25414 events

Stop Time: 120 secs



Stats: Not Normalized, Listgating: Disabled

Hist	Region ID	%	Count	Mn X	Md X	PkPosX	PkCnt	HPCV	Min	Max
2	A B	5.17	1318	88.7	88.7	28.1	10	1.11	28.8	981.5

L

Beckman Coulter Epics XL-MCL

COULTER(R) EPICS(R) Listmode Replay Flow Cytometry Report
 C:\XL\LMD\Z0012264.LMD, XL RAG19011, Run time protocol

OP ID: MJ722928

28Aug11 12:17:37

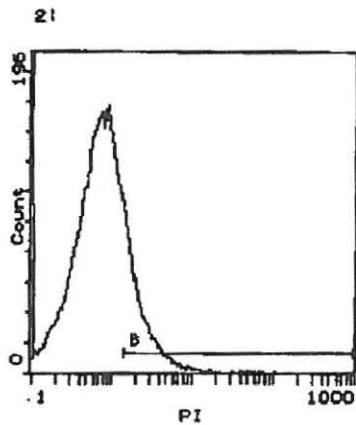
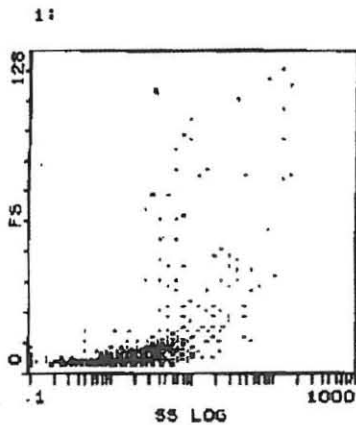
PROPIDIUM IODIDE 2

Z0012264

300 dah nt1

120 seconds, 33614 events

Stop Time: 120 secs



Stats: Not Normalized, Listgating: Disabled

Hist	Region ID	%	Count	Mn X	Md X	PkPosX	PkCnt	HPCV	Min	Max
2	B B	20.9	7021	2.82	2.21	1.51	110	71.35	1.47	1006

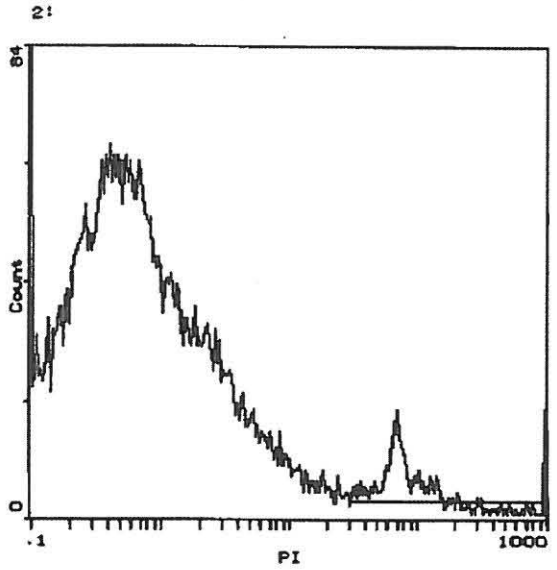
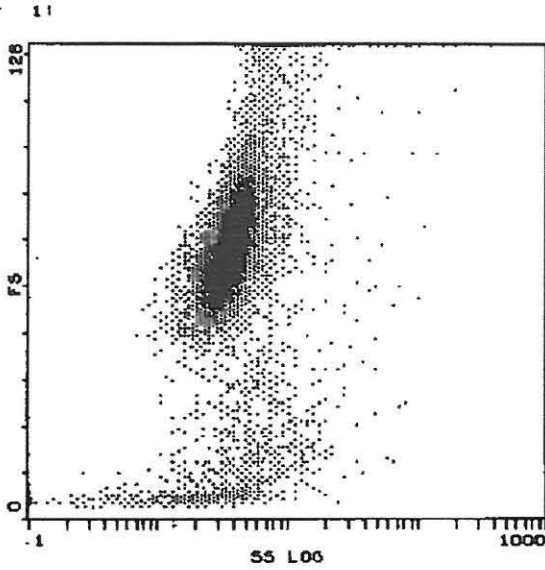
M

Beckman Coulter Epics XL-MCL

COULTER(R) EPICS(R) Listmode Replay Flow Cytometry Report
 C:\XL\MD\Z0012340.LMD, XL RAG19011, Run time protocol

OP ID: MJ722928

08Sep11 10:13:27
 PROPIDIUM IODIDE 2
 Z0012340
 med contrl 10a
 120 seconds, 31147 events
 Stop Time: 120 secs



Stats: Not Normalized, Listgating: Disabled

Hist	Region ID	%	Count	Mn X	Md X	PkPosX	PkCnt	HPCV	Min	Max
2	A B	5.68	1770	102.2	83.0	66.5	24	0.61	30.7	961.5

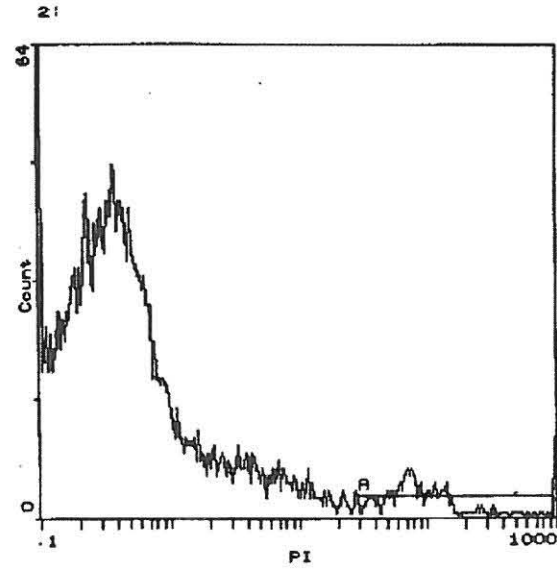
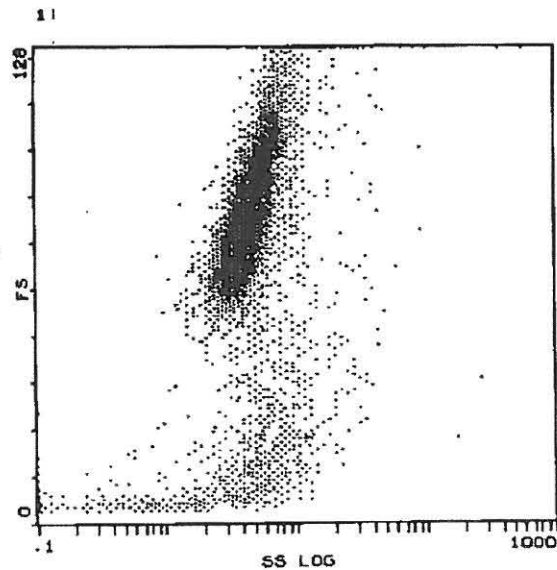
N

Beckman Coulter Epics XL-MCL

COULTER(R) EPICS(R) Listmode Replay Flow Cytometry Report
 C:\XL\MD\Z0012341.LMD, XL RAG19011, Run time protocol

OP ID: MJ722928

08Sep11 10:16:08
 PROPIDIUM IODIDE 2
 Z0012341
 dmeo contrl 10a
 120 seconds, 19238 events
 Stop Time: 120 secs



Stats: Not Normalized, Listgating: Disabled

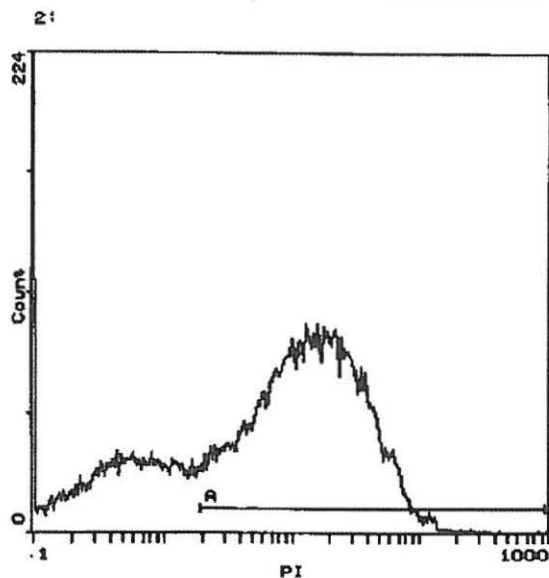
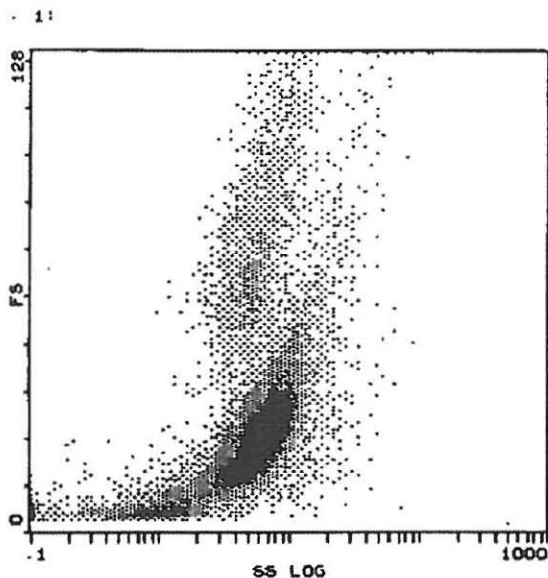
Hist	Region ID	%	Count	Mn X	Md X	PkPosX	PkCnt	HPCV	Min	Max
2	A B	4.36	839	98.0	84.1	80.3	11	0.61	27.5	961.5

O Beckman Coulter Epics XL-MCL

COULTER(R) EPICS(R) Listmode Replay Flow Cytometry Report
 C:\XL\MID\Z0012342.LMD, XL RAG19011, Run time protocol

OP ID: MJ722928

08Sep11 10:18:45
 PROPIDIUM IODIDE 2
 Z0012342
 chx contrl 10a
 120 seconds, 39738 events
 Stop Time: 120 secs



Stats: Not Normalized, Listgating: Disabled

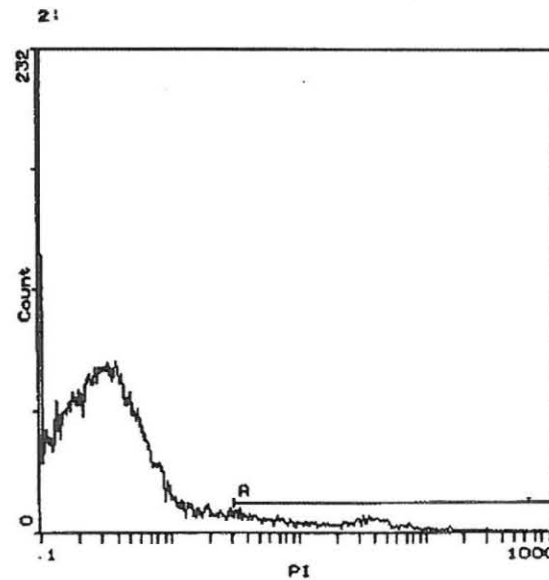
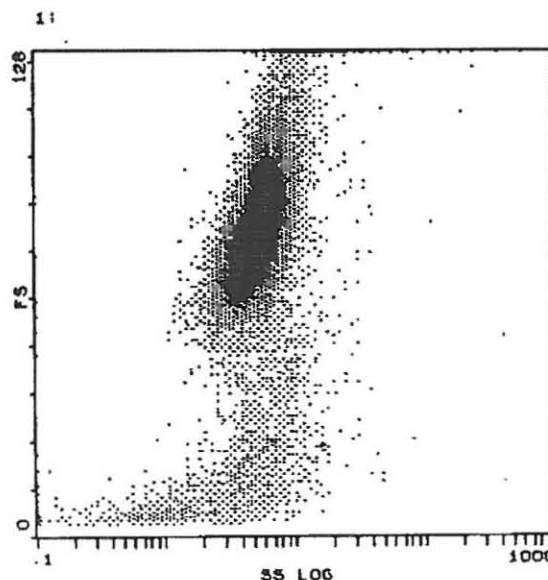
Hist	Region ID	%	Count	Mn X	Md X	PkPosX	PkCnt	HPCV	Min	Max
2	A B	67.8	29858	14.3	14.7	18.4	111	89.93	1.96	981.5

P Beckman Coulter Epics XL-MCL

COULTER(R) EPICS(R) Listmode Replay Flow Cytometry Report
 C:\XL\MID\Z0012343.LMD, XL RAG19011, Run time protocol

OP ID: MJ722928

08Sep11 10:21:28
 PROPIDIUM IODIDE 2
 Z0012343
 150 hyp 10a
 120 seconds, 35649 events
 Stop Time: 120 secs



Stats: Not Normalized, Listgating: Disabled

Hist	Region ID	%	Count	Mn X	Md X	PkPosX	PkCnt	HPCV	Min	Max
2	A B	6.36	2268	18.4	16.0	3.51	17	0.88	3.18	981.5

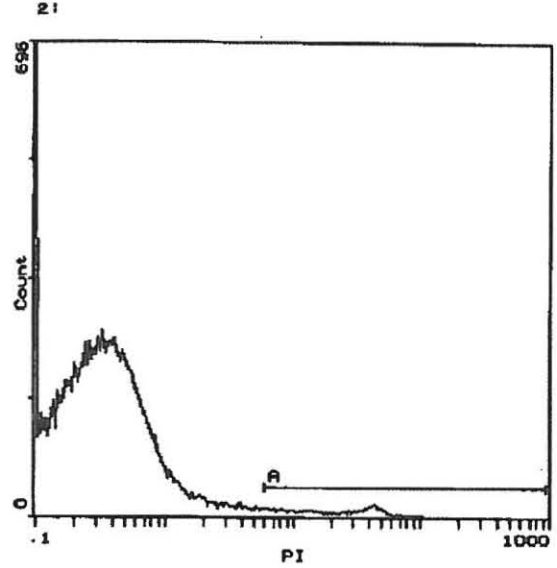
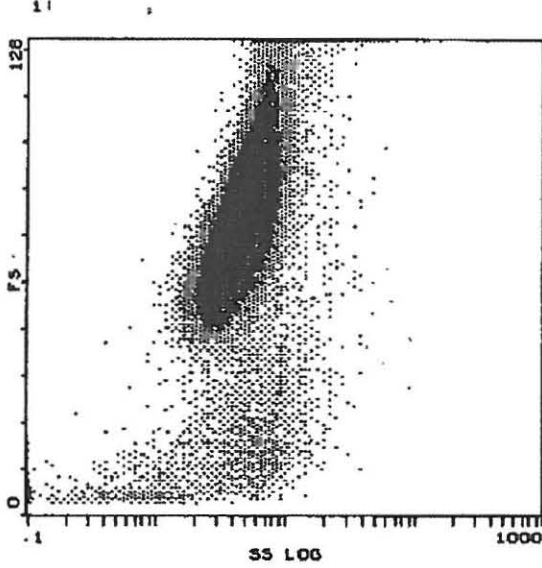
Beckman Coulter Epics XL-MCL

COULTER(R) EPICS(R) Listmode Replay Flow Cytometry Report
 C:\XLLMD\Z0012345.LMD, XL RAG19011, Run time protocol

OP ID: MJ722928

08Sep11 10:27:10
 PROPIDIUM IODIDE 2
 Z0012345

4.8 dmh 10a
 120 seconds, 107401 events
 Stop Time: 120 secs



Stats: Not Normalized, Listgating: Disabled

Hist	Region ID	%	Count	Mn X	Md X	PkPosX	PkCnt	HPCV	Min	Max
2	A B	3.13	3367	23.7	24.0	45.2	27	7.45	5.97	961.5

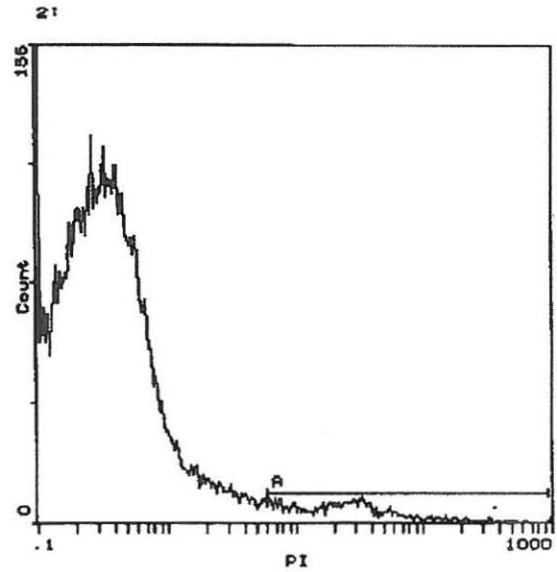
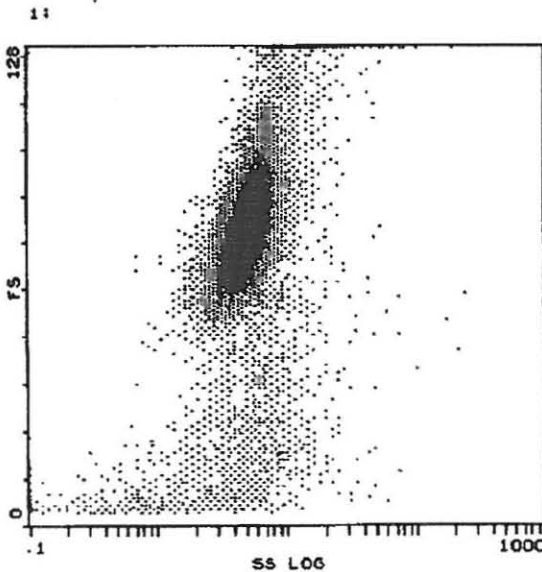
Beckman Coulter Epics XL-MCL

COULTER(R) EPICS(R) Listmode Replay Flow Cytometry Report
 C:\XLLMD\Z0012344.LMD, XL RAG19011, Run time protocol

OP ID: MJ722928

08Sep11 10:24:15
 PROPIDIUM IODIDE 2
 Z0012344

300 hyp 10a
 120 seconds, 52386 events
 Stop Time: 120 secs



Stats: Not Normalized, Listgating: Disabled

Hist	Region ID	%	Count	Mn X	Md X	PkPosX	PkCnt	HPCV	Min	Max
2	A B	3.35	1756	27.3	24.9	6.36	12	0.80	5.97	961.5

S

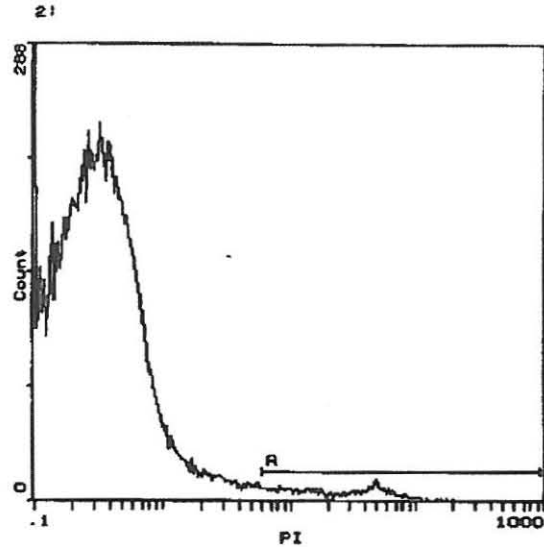
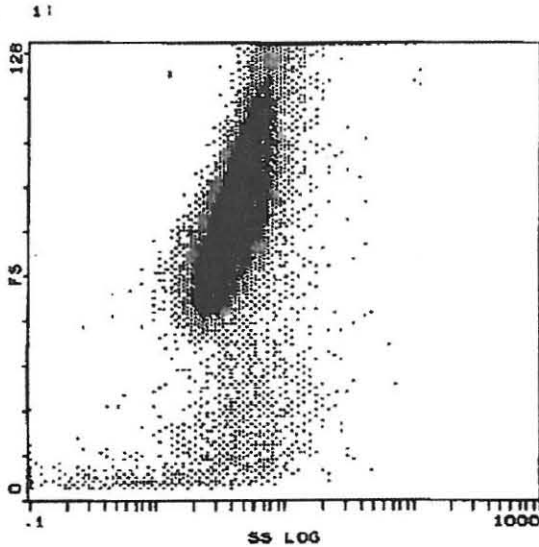
Beckman Coulter Epics XL-MCL

COULTER(R) EPICS(R) Listmode Replay Flow Cytometry Report
 C:\XL\LMD\20012346.LMD, XL RAG19011, Run time protocol

OP ID: MJ722928

08Sep11 10:29:44
 PROPIDIUM IODIDE 2
 Z0012346

19 dmh 10a
 120 seconds, 92969 events
 Stop Time: 120 secs



Stats: Not Normalized, Listgating: Disabled

Hist	Region ID	%	Count	Min X	Md X	PkPosX	PkCnt	HPCV	Min	Max
2	A B	2.28	2120	26.1	25.9	43.2	17	0.70	5.97	961.5

T

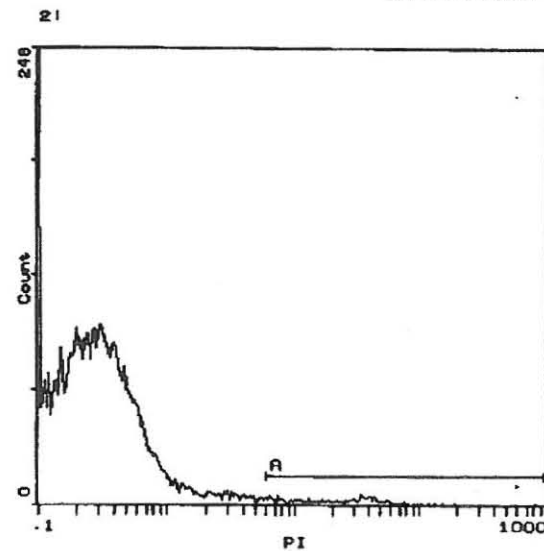
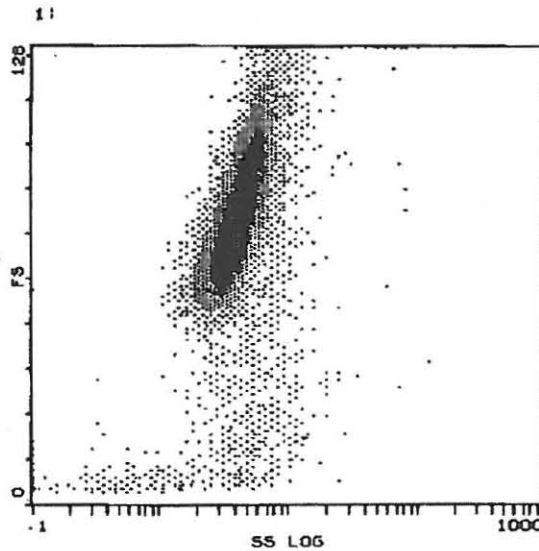
Beckman Coulter Epics XL-MCL

COULTER(R) EPICS(R) Listmode Replay Flow Cytometry Report
 C:\XL\LMD\20012347.LMD, XL RAG19011, Run time protocol

OP ID: MJ722928

08Sep11 10:32:29
 PROPIDIUM IODIDE 2
 Z0012347

75 dmh 10a
 120 seconds, 42458 events
 Stop Time: 120 secs



Stats: Not Normalized, Listgating: Disabled

Hist	Region ID	%	Count	Min X	Md X	PkPosX	PkCnt	HPCV	Min	Max
2	A B	1.82	772	23.3	24.9	35.4	10	0.85	5.97	961.5

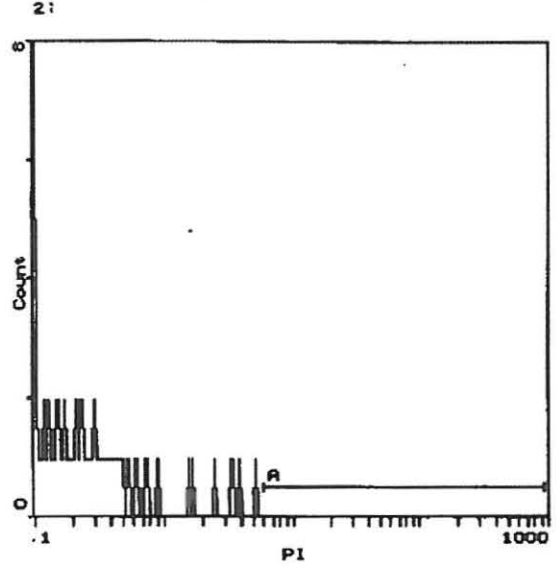
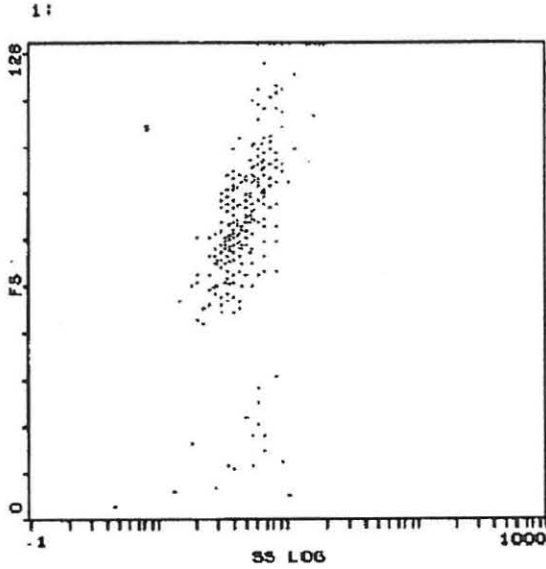
U

Beckman Coulter Epics XL-MCL

COULTER(R) EPICS(R) Listmode Replay Flow Cytometry Report
 C:\XL\LM\Z0012348.LMD, XL RAG19011, Run time protocol

OP ID: MJ722928

08Sep11 10:35:15
 PROPIDIUM IODIDE 2
 Z0012348
 300 dnm 10a
 120 seconds, 859 events
 Stop Time: 120 secs



Stats: Not Normalized, Listgating: Disabled

Hist	Region ID	%	Count	Mn X	Md X	PkPosX	PkCnt	HPCV	Min	Max
2	A B	1.28	11	14.6	13.9	6.53	1	0.38	5.97	961.5

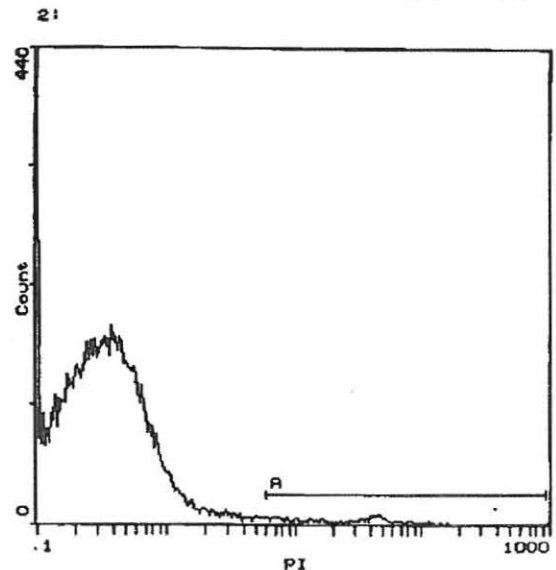
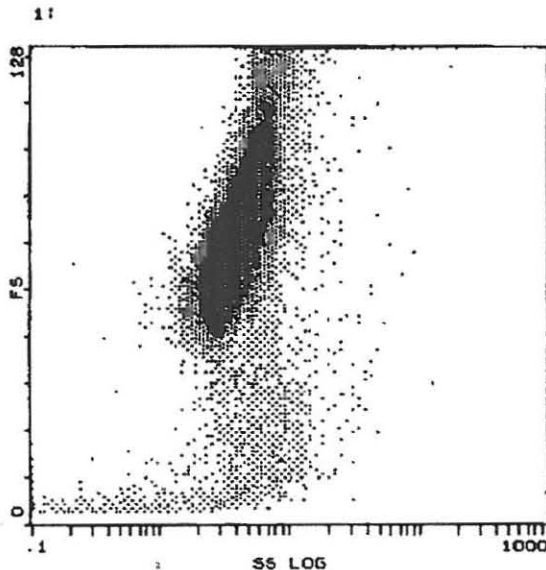
V

Beckman Coulter Epics XL-MCL

COULTER(R) EPICS(R) Listmode Replay Flow Cytometry Report
 C:\XL\LM\Z0012348.LMD, XL RAG19011, Run time protocol

OP ID: MJ722928

08Sep11 10:38:32
 PROPIDIUM IODIDE 2
 Z0012349
 4.8 dnm 10a
 120 seconds, 67836 events
 Stop Time: 120 secs



Stats: Not Normalized, Listgating: Disabled

Hist	Region ID	%	Count	Mn X	Md X	PkPosX	PkCnt	HPCV	Min	Max
2	A B	2.71	1841	29.2	30.3	48.4	19	0.74	5.97	961.5

W

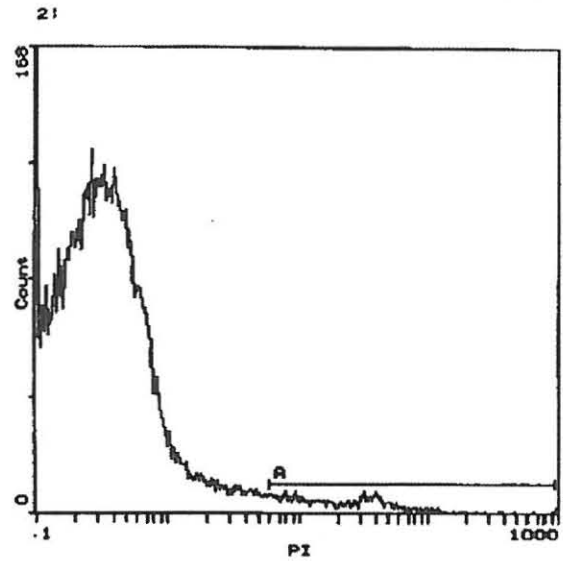
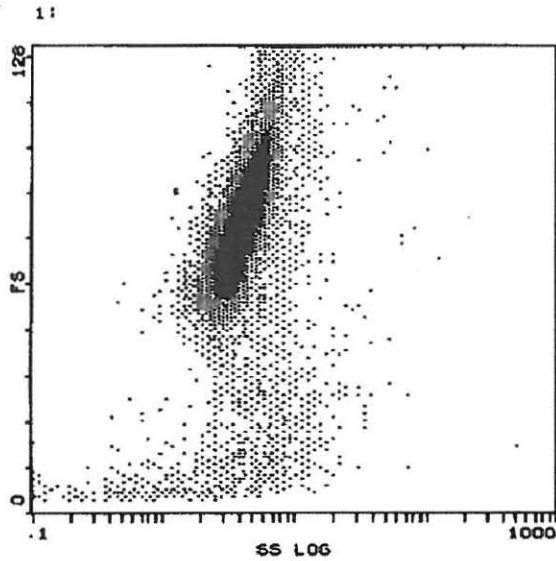
Beckman Coulter Epics XL-MCL

COULTER(R) EPICS(R) Listmode Replay Flow Cytometry Report
 C:\XL\LM\Z0012350.LMD, XL RAG19011, Run time protocol

OP ID: MJ722928

08Sep11 10:41:04
 PROPIDIUM IODIDE 2
 Z0012350

19 dah 10a
 120 seconds, 52110 events
 Stop Time: 120 secs



Stats: Not Normalized, Listgating: Disabled

Hist	Region ID	%	Count	Min X	Md X	PkPosX	PkCnt	HPCV	Min	Max
2	A B	2.68	1397	23.2	21.7	33.3	14	0.80	5.97	981.5

X

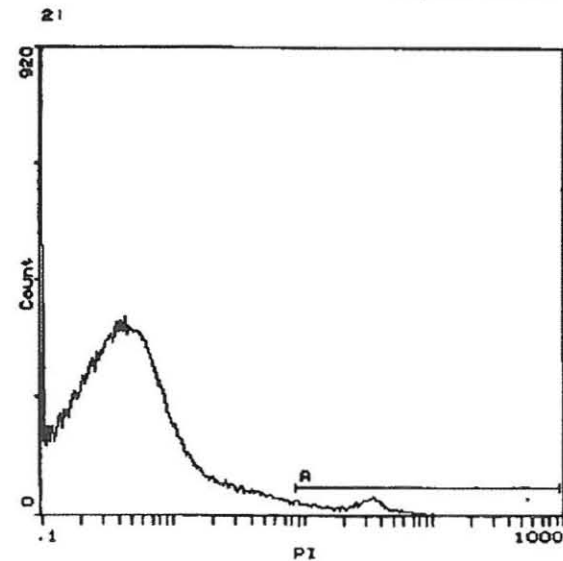
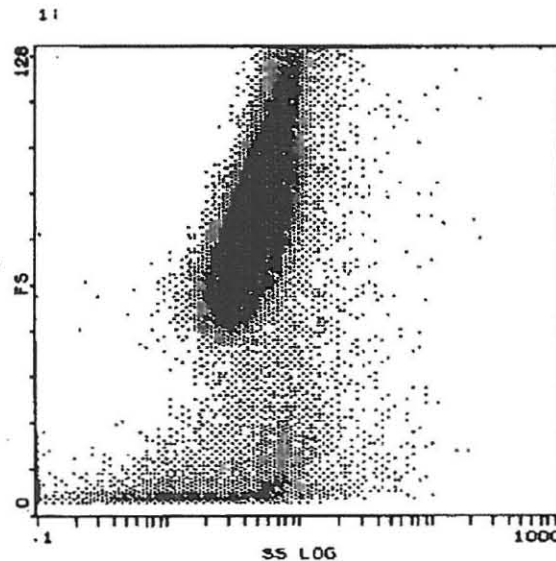
Beckman Coulter Epics XL-MCL

COULTER(R) EPICS(R) Listmode Replay Flow Cytometry Report
 C:\XL\LM\Z0012351.LMD, XL RAG19011, Run time protocol

OP ID: MJ722928

08Sep11 10:43:40
 PROPIDIUM IODIDE 2
 Z0012351

75 dah 10a
 120 seconds, 144345 events
 Stop Time: 120 secs



Stats: Not Normalized, Listgating: Disabled

Hist	Region ID	%	Count	Min X	Md X	PkPosX	PkCnt	HPCV	Min	Max
2	A B	3.46	4999	25.9	26.9	34.8	47	5.81	8.71	981.5

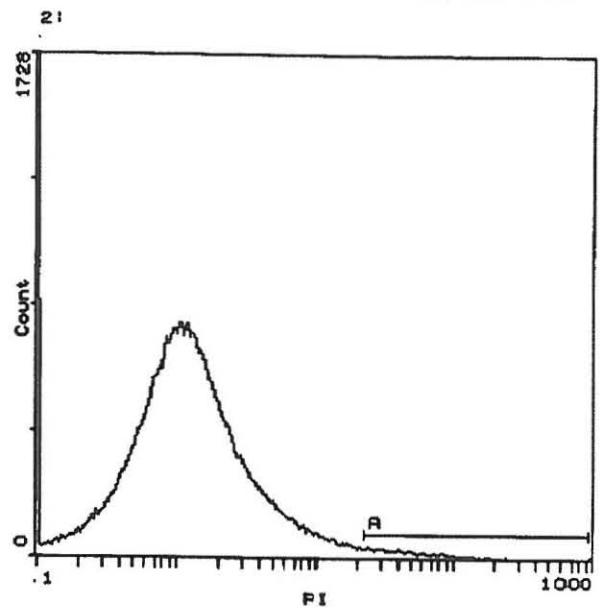
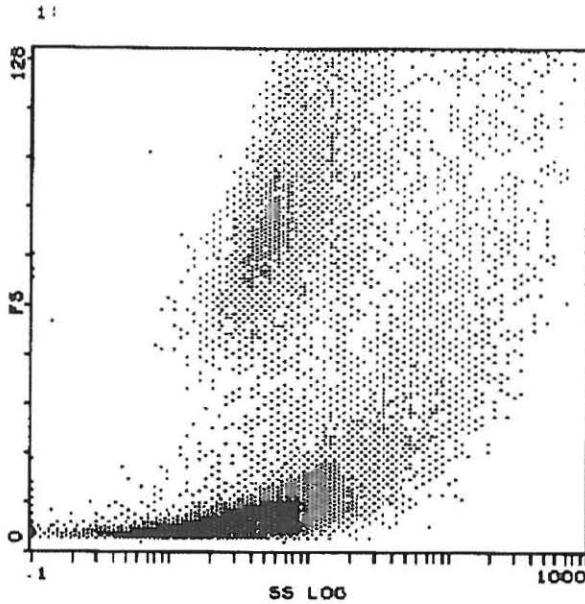
Y

Beckman Coulter Epics XL-MCL

COULTER(R) EPICS(R) Listmode Replay Flow Cytometry Report
 :XL1LMDZ0012352.LMD, XL RAG19011, Run time protocol

XP ID: MJ722928

08Sep11 10:46:43
 PROPIDIUM IODIDE 2
 Z0012352
 300 dah 10a
 120 seconds, 191329 events
 Stop Time: 120 secs



Stats: Not Normalized, Listgating: Disabled

Hist	Region ID	%	Count	Mn X	Mo X	PkPosX	PkCnt	HPCV	Min	Max
2	A B	2.97	5681	61.2	50.0	25.9	64	274.04	23.0	961.5

KEY FOR FLOW CYTOMETRY OUTPUTS

Sample code	Compound type	Concentration (µM)	Cell Type
A	chx contrl (cyclohexamide)	Positive control	nt (MCF10A-NeoT)
B	medium contrl (cell culture media)	Negative control 1	nt (MCF10A-NeoT)
C	hyp (hypoxoside)	150	nt (MCF10A-NeoT)
D	hyp (hypoxoside)	300	nt (MCF10A-NeoT)
E	dmh (dimethyl hypoxoside)	4.8	nt (MCF10A-NeoT)
F	dmh (dimethyl hypoxoside)	19	nt (MCF10A-NeoT)
G	dmh (dimethyl hypoxoside)	75	nt (MCF10A-NeoT)
H	dmh (dimethyl hypoxoside)	300	nt (MCF10A-NeoT)
I	dah (Decaacetyl hypoxoside)	4.8	nt (MCF10A-NeoT)
J	dah (Decaacetyl hypoxoside)	19	nt (MCF10A-NeoT)
K	dah (Decaacetyl hypoxoside)	75	nt (MCF10A-NeoT)
L	dah (Decaacetyl hypoxoside)	300	nt (MCF10A-NeoT)
M	medium contrl (cell culture media)	Negative control 1	10a (MCF10A)
N	dmsol contrl (DMSO control)	Negative control 2	10a (MCF10A)
O	chx contrl (cyclohexamide)	Positive control	10a (MCF10A)
P	hyp (hypoxoside)	150	10a (MCF10A)
Q	dmh (dimethyl hypoxoside)	4.8	10a (MCF10A)
R	hyp (hypoxoside)	300	10a (MCF10A)
S	dmh (dimethyl hypoxoside)	19	10a (MCF10A)
T	dmh (dimethyl hypoxoside)	75	10a (MCF10A)
U	dmh (dimethyl hypoxoside)	300	10a (MCF10A)
V	dah (Decaacetyl hypoxoside)	4.8	10a (MCF10A)
W	dah (Decaacetyl hypoxoside)	19	10a (MCF10A)
X	dah (Decaacetyl hypoxoside)	75	10a (MCF10A)
Y	dah (Decaacetyl hypoxoside)	300	10a (MCF10A)